

**DEVELOPMENT OF NOVEL EEG-BASED
METHODOLOGY FOR INVESTIGATION OF NEURAL
CORRELATES OF HUMAN DECEPTION**

Wang Yue

(B.S., Fudan University)

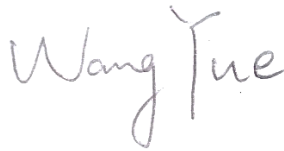
**A THESIS SUBMITTED
FOR THE DEGREE OF DOCTOR OF PHILOSOPHY
DEPARTMENT OF MECHANICAL ENGINEERING
NATIONAL UNIVERSITY OF SINGAPORE**

2014

DECLARATION

I hereby certify that the content of this thesis is my original work and it has been done and written by me in its entirety. I have duly acknowledged all the sources of information which have been used in this thesis.

This thesis has also not been submitted for any degree in any other university previously.



.....
Wang Yue

26 Dec 2014

ACKNOWLEDGMENTS

First of all, I would like to express my deepest gratitude to my supervisor, Professor Li Xiaoping, Director of the Neuroengineering Laboratories, for his gracious guidance, a global view of research, strong encouragement and detailed recommendations throughout the course of this research. His kind patience and encouragement always gave me great motivation and confidence in conquering the difficulties encountered in the study.

Great thanks should be given to Prof. Shu, who once mentored and guided me during my Phd course and selflessly devoted his time discussing with me.

I am also thankful to my awesome previous and current lab-mates, who have accompanied me throughout this wonderful Phd journey with their consistent and selfless supports, grateful thankfulness should be given to Dr. Ng Wu Chun, Dr. Yu Ke, Dr. Shao Shiyun, Dr. Fan Jie, Dr. Shen Kaiquan, Mr. Wu Tiecheng, Mr. Ng Khoon Siong, Mr. Rohit Tyagi, Mr. Li Zhe, Mr. Bui Ha Duc, Mr. Khoa Wei Long Geoffrey and Miss Ye Yan for their kind help, valuable suggestion, and gracious encouragement in my work.

Special acknowledgments are given to my dear parents. Their selfless love and unconditional support always supply me with endless positive energy to conquer all the challenges.

Last but not least, I am deeply grateful to the National University of Singapore for granting me the financial support, with which I can fully endeavor myself to my Phd research.

TABLE OF CONTENTS

Acknowledgments	i
Summary	vii
List of tables	ix
List of figures	xii
List of symbols	xvii
Acronyms	xviii
1 Introduction.....	1
1.1 The significance of deception to the society.....	1
1.2 Methodologies for studying deception.....	2
1.3 The objective of the thesis.....	5
1.4 Thesis outline.....	7
2 Literature review.....	9
2.1 Neurophysiology of EEG (electroencephalography).....	9
2.2 Brief history of EEG in practical application.....	11
2.3 Advantages and limitations of EEG as a neuro-diagnostic tool	12
2.4 EEG signal processing methods.....	15
2.4.1 EEG de-noising methods.....	16

2.4.2	Temporal EEG analysis (Event Related Potential - ERP).....	20
2.4.3	Spectral EEG analysis (Event Related Synchronization/De-synchronization- ERS/ERD).....	24
2.5	Inverse problem and source localization.....	25
2.5.1	Lead field theory.....	25
2.5.2	Inverse problem.....	26
2.5.3	Inverse model (source localization).....	27
2.6	Deception protocol/signal modalities and neural correlates of deception.....	29
2.6.1	Developed deception study protocols and signal modalities in literature.....	29
2.7	Specifying the research topics that merge the research gap.....	32
3	Experimental protocols established in this thesis.....	35
3.1	Deception tasks for experiment I and II.....	36
3.1.1	Experimental design and protocol.....	36
3.1.2	Instruction protocol.....	39
3.2	Deception task for experiment III.....	41
3.2.1	Stimuli.....	41
3.2.2	Instruction protocol.....	42
3.2.3	Experimental design.....	42
3.3	Participants.....	48
3.4	Data acquisition and pre-processing.....	48

4 Human electroencephalography-based source localization method to study various deception tasks.....	53
4.1 Introduction.....	54
4.2 Data analysis.....	57
4.3 Results.....	60
4.3.1 Behavioral data for experiment I and II.....	60
4.3.2 Source localization for experiment I and II.....	62
4.4 Discussion.....	71
4.4.1 Experiment stimuli control.....	71
4.4.2 Source localization in experiment I and experiment II.....	72
4.4.3 Comparison between the WE and the NE tasks.....	78
4.4.4 Comparison between the IL-IT and the SL-ST tasks.....	79
4.5 Concluding remarks.....	79
5 A human Electroencephalography network and connectivity based method to study instructed lying tasks.....	81
5.1 Introduction.....	82
5.2 Data analysis.....	84
5.3 Results.....	90
5.3.1 Network analysis.....	90
5.3.2 Connectivity analysis.....	96
5.3.3 Response time (correlation) analysis.....	97

5.4 Discussion.....	100
5.4.1 Network analysis.....	100
5.4.2 Connectivity analysis.....	109
5.4.3 Response time (correlation) analysis.....	110
5.5 Concluding remarks.....	111
6 Use judgmental feedbacks to study event-related electrical neural response by liars and innocents.....	113
6.1 Introduction.....	114
6.2 Data analysis.....	115
6.3 Results.....	117
6.3.1 Event related potentials (ERP).....	117
6.3.2 Independent component analysis (ICA) & ERP reconstruction.....	125
6.3.3 EEG Source localization (sLORETA) for PC-P400 and PC-N400.....	127
6.4 Discussion.....	131
6.5 Concluding remarks.....	140
7 Conclusions and recommendations.....	142
7.1 Conclusions.....	142
7.2 Recommendations for future deception researches and applications.....	145
Publications from the present study.....	147
Bibliography.....	149

Appendix.....172

SUMMARY

Deception is a prevalent phenomenon that can cause serious social and economic harm to the society by incurring huge social economic loss and safety threat to the society. It has been a keen interest throughout human history to detect lie due to its high stake to the society. Despite decades of researches in finding the neuronal mechanism of deception, this complex neuropsychology phenomenon remains obscure. Existing approaches suffer from various drawbacks for practical application. Among all the existing techniques, EEG is such a unique tool that offers low cost, high temporal resolution and appropriate spatial resolution for analyzing brain activity and has great promise to be applied in lie detection. However, the feasibility of EEG in lie detection is not fully recognized. The manifestation of deception in EEG signal is still largely unknown. Yet, it is of great value to design EEG-based experimental protocols and fully exploit advanced EEG analysis techniques to analyze the electrophysiological underlying of the dynamic brain activities associated with deception.

This thesis has contributed four novel EEG-based methodologies to investigate neural correlates of deception. Specifically, a feedback (stimulus) based and non-experiential knowledge test based protocols have been established; a source localization based, and a functional network/connectivity based methods have been proposed. None of these methodologies have been proposed or discussed in previous studies which makes them original and worth further investigation. Some interesting results have been achieved with the proposed investigation methodologies. Given the exciting results, these novel

methodologies have great promise to empower future lie detection technology and inspire the EEG community to invent / enhance closely related methods. These results enhance our belief that EEG is a promising tool to fill the gap of practical application with higher accuracy in the future.

LIST OF TABLES

Table 1 Spatial and temporal resolution of different neuro-diagnostic tools.....	14
Table 2 Number of trials per condition (spontaneous lying/truth-telling condition has a reported average number of trials since the real number of trial is dependent on the frequency of lying/truth-telling by the subject in the experiment, and they are constrained to be roughly the same).....	47
Table 3 Punishment and Duty values for the different items.....	47
Table 4 The sentences used in the doubtful feedbacks for instructed lying/truth-telling and spontaneous lying/truth-telling conditions respectively.....	47
Table 5 Detailed information on identified sources through frequency domain EEG source localization between the NE-IL and the NE-IT conditions.	69
Table 6 Detailed information on identified sources through frequency domain EEG source localization between the WE-IL and the WE-IT conditions.	70
Table 7 Detailed information on identified sources through frequency domain EEG source localization between the SL and the ST conditions.....	70
Table 8 Detailed information on identified sources through frequency domain EEG source localization between the ST and the IT conditions.	71
Table 9 Detailed information on identified sources through frequency domain EEG source localization between the SL and the IL conditions.	71
Table 10 Results from the dendrogram analysis; four groups of sources were found to be common to the WE-IL and the WE-IT conditions in the upper alpha band.	95
Table 11 Results from dendrogram analysis; four groups of sources were found to be common to the NE-IL and the NE-IT conditions in the upper alpha band.	95

Table 12 The difference in the intra- and inter-group connectivity among sub-networks in the upper alpha band between the WE-IL and the WE-IT conditions. The sources of groups A, B, C, D are depicted in Fig.24.....	96
Table 13 The difference in the intra- and inter-group connectivity among sub-networks in the upper alpha band between the NE-IL and the NE-IT conditions. The sources of groups A, B, C, and D are depicted in Fig.25.....	96
Table 14 Source level clustering coefficient increase in the upper alpha band in the WE-IL relative to the WE-IT condition (corrected $p < 0.05$).....	97
Table 15 Source level clustering coefficient increase in the upper alpha band in the NE-IL relative to the NE-IT condition (corrected $p < 0.05$).	97
Table 16 Time point and corresponding electrode sectors that show significant difference between the SL-check and the ST-check conditions.	120
Table 17 Time point and corresponding electrode sectors that show significant difference between the SL-trust and the ST-trust conditions.....	121
Table 18 Time point and corresponding electrode sectors that show significant difference between the ST-check and the ST-trust conditions.....	122
Table 19 Time point and corresponding electrode sectors that show significant difference between the SL-check and the SL-trust conditions.....	122
Table 20 Time point and corresponding electrode sectors that show significant difference between the IL-check and the IT-check conditions.	124
Table 21 Time point and corresponding electrode sectors that show significant difference between the IT-check and the IT-trust conditions.	124
Table 22 Coordinates, brodmann area, anatomical regions for nodes with biggest local source strength for the identified two major PCs in the instructed lying task.	128

Table 23 Coordinates, brodmann area, anatomical regions for nodes with biggest local source strength for the identified two major PCs in the spontaneous lying task. 129

LIST OF FIGURES

- Figure 1 The relationship between forward problem and inverse problem, the connection between them is source model and volume conductor model. 26
- Figure 2 The IL and IT conditions for both the WE and the NE tasks share the same schematic procedures: (I) fixation phase;(II) attending to auditory question; (III) answering phase; (IV) mentalization phase; (V) feedback phase, except that the visual images accompanying the auditory feedbacks were different in the two tasks to match the specific contexts. 39
- Figure 3 Timeline showing the different component and their sequence in a trial..... 45
- Figure 4 The structure of all the conditions involved in experiment III. 45
- Figure 5 Schematic demonstration of the timeline for a single trial in the experiment. The steps with dashed rectangular only appeared for trials that involve doubtful feedback which triggers further check on subject's response, after which a result announcement was delivered. The steps without dashed rectangular appeared for trials that involve only trustful feedback. The time spent on each step was listed below its corresponding step. 45
- Figure 6 The feedback stimuli used in the experiment. An example of (a).doubtful feedback and (b).trustful feedback in the instructed lying/truth-telling task (c). trustful feedback in the spontaneous lying/truth-telling task (d). the negative result feedback that indicates a punishment for detected lying in both the instructed and the spontaneous lying tasks. ... 46
- Figure 7 The item categories that the subjects would encounter in each block. The label '2' indicates that the subjects are carrying 2 units of one of the items at one time, and they can cheat by declaring '0' or '1', or tell the truth by declaring '2'; the label '×' instructs that the subjects are carrying 1 unit of one of the illegal items at one time, and the subjects have to cheat by declaring none; the label '√' instructs that the subjects are carrying 1 unit of one of the permitted items at one time, and the subjects have to tell the truth. 46
- Figure 8 Scenario showing experimental setting during the EEG recording..... 51

Figure 9 Topography showing the distribution of electric impedance across the whole head. The darker the blue color, the lower the impedance. Each electrode was guaranteed to have impedance below 20k Ohm. 51

Figure 10 Response time statistics for the IL and IT conditions in WE task and NE task (unit: ms). Paired t-test shows significantly longer response time ($p < 0.05$) for the IL condition compared to the IT condition in the WE task; significantly longer response time ($p < 0.05$) was also found for the IL condition compared to the IT condition in the NE task. 61

Figure 11 Response time statistics in IL task and SL task (unit: ms). Paired t-test shows significantly longer response time ($p < 0.05$) for the IL condition compared to the IT condition; there is no significant difference in response time found for the SL condition compared to the ST condition. 62

Figure 12 Frequency domain EEG source localization results indicate a significantly increased ERS (a) in the lower alpha band in left inferior frontal gyrus and insula as well as (b) in the upper alpha band in cuneus in the IL w.r.t the IT condition in the first 2s of the stimulus presence, significant voxels (corrected $p < 0.05$) are highlighted with yellow and are color-intensity coded with t-statistics. 63

Figure 13 EEG source localization in the frequency domain indicates increased ERS in delta band in multiple regions of the brain in the NE-IL w.r.t the NE-IT condition in the first 2s of the stimulus presence. (a). transverse view; (b). left sagittal view; (c). right sagittal view. Results also indicate increased ERS in the upper alpha band in multiple regions of the brain (d-f), significant voxels (corrected $p < 0.05$) highlighted with orange are color-intensity coded with t-statistics (d). left sagittal view; (e). right sagittal view; (f). transverse, sagittal and coronal cross-sectional views are presented in sequence. 64

Figure 14 (a)-(d) show quantified ERS/ERD results in the IL and IT conditions in the WE task (a-b) and in the NE task (c-d) respectively. Mean and standard deviation for the ERS value calculated for voxels that present significantly increased ERS in (a). lower alpha band, (b). upper alpha band, (c). delta band, (d). upper alpha band. 65

Figure 15 Frequency domain EEG source localization results indicate a significantly decreased ERS during the first 2s presence of the stimulus (a) in the lower alpha band in bilateral inferior parietal lobe, precentral gyrus, postcentral gyrus, precuneus, middle frontal gyrus and left insula as well as (b) in bilateral superior temporal gyrus in the SL

w.r.t the ST condition, significant voxels (corrected $p < 0.05$) are highlighted with blue and are color-intensity coded with t-statistics. 66

Figure 16 Frequency domain EEG source localization results indicate a significantly increased ERS during the last 2s presence of the stimulus in the lower alpha band in cuneus in the SL w.r.t the ST condition, significant voxels (corrected $p < 0.05$) are highlighted with yellow and are color-intensity coded with t-statistics. 66

Figure 17 (a)-(b) show quantified ERS/ERD results in the SL and ST conditions for the (a). first 2s and (b). last 2s of the stimulus presence, respectively. Mean and standard deviation for the ERS value calculated for voxels that present significantly (a).decreased ERS in lower alpha band, (b).increased ERS in upper alpha band. 67

Figure 18 Frequency domain EEG source localization results indicate a significantly increased ERS (a) in the upper alpha band in cuneus in the ST w.r.t the IT condition in the first 2s of the stimulus presence, significant voxels (corrected $p < 0.05$) are highlighted with yellow and are color-intensity coded with t-statistics. (b). shows quantified mean and standard deviation for the ERS/ERD results in the ST and the IT conditions for the first 2s of the stimulus presence calculated based on voxels that present significantly increased ERS in the upper alpha band. 67

Figure 19 Frequency domain EEG source localization results indicate a significantly decreased ERS (a) in the theta band in left and right frontal gyrus, left insula and precentral gyrus and right middle frontal gyrus as well as in the lower alpha band in (b). left inferior frontal gyrus and (c). left insula in the first 2s of the stimulus presence, significant voxels (corrected $p < 0.05$) are highlighted with blue and are color-intensity coded with t-statistics. 68

Figure 20 (a) and (b) show quantified ERS/ERD results in the SL and the IL conditions for the first 2s of the stimulus presence in the theta band and the lower alpha band, respectively. The mean and standard deviation for the ERS values were calculated for voxels that present significantly decreased ERS (a). in the theta band; (b) and in the lower alpha band. 69

Figure 21 The descriptive steps of analysis from input EEG raw signal to the output network. The major steps are EEG signals de-noising, inverse calculation for ROIs, group-wise paired connectivity computation, dendrogram analysis to cluster nodes into networks. 90

Figure 22 (A) and (B) represent the hierarchy structures based on the dendrogram analysis for the WE-IL and the WE-IT conditions, respectively. The x-axis: leaf number, each leaf represents a cluster of BAs. The y-axis: leaf distance calculated using average linkage clustering based on correlation distance. The yellow color indicates group A, the blue color indicates group B, the pink color indicates group C, and the green color indicates group D.
 91

Figure 23 (A) and (B) represent the hierarchy structures based on the dendrogram analysis for the NE-IL and the NE-IT conditions, respectively. The x-axis: leaf number, each leaf represents a cluster of BAs. The y-axis: leaf distance calculated using average linkage clustering based on correlation distance. The yellow color indicates group A, the blue color indicates group B, the pink color indicates group C, and the green color indicates group D.
 92

Figure 24 The corresponding cortical sources that functionally cluster into four sub-networks that are common for the WE-IL and the WE-IT conditions: (A), (B), (C) and (D) are hypothetical networks for executing higher-order function, comprehension/memory process processing, and speech perception, respectively. The dotted circle indicates a medial surface source, while the solid circle indicates a lateral surface source. The label for each anatomical region includes the Brodmann area name and the laterality information.
 92

Figure 25 The corresponding cortical sources that functionally cluster into the four sub-networks that are common for the NE-IL and the NE-IT conditions: (A), (B), (C) and (D) are hypothetical networks for executing higher-order function, comprehension/memory processing, and speech perception, respectively. The dotted circle indicates a medial surface source, while the solid circle indicates a lateral surface source. The label for each anatomical region includes the Brodmann area name and the laterality information..... 93

Figure 26 Significant positive correlations were found for between normalized event-related clustering coefficient (NERCC) and normalized response time (NRT) in the WE-IL and the WE-IT conditions. Marginally significant/Significant negative correlations were found for multiple regions between NERCC and NRT in the NE-IL and the NE-IT conditions..... 100

Figure 27 Across-subjects grand mean averaged ERP signals on example frontal electrode Fz and parietal-occipital electrodes POz and Oz in the IL, IT conditions (a,c,e) and in the SL, ST conditions (b,d,f)..... 119

Figure 28 The topographical scalp maps of the across-subject grand mean average voltage in the significant time window for the ‘check’ group in (a).instructed and (b).spontaneous lying/truth-telling task, and the corresponding condition differences. 120

Figure 29 Topography of the major PCs that contribute to the salient ERP signals in instructed/spontaneous tasks. (a) and (b) are major frontal components that contribute to the P400 and partially to the N500 components. (c) and (d) are major central-parietal components that contribute to the N400 and partially to the N500 components..... 127

Figure 30 Source localization results for the corresponding PCs identified through ICA-PCA analysis. Frontal sources mainly contribute to the P400 component for (a). the IL-IT conditions and (b). the SL-ST conditions. Central-parietal sources mainly contribute to the N400 component for (c).the IL-IT conditions and (d). the SL-ST conditions..... 128

Figure 31 Reconstructed ERP signals on example channels (i.e. Fz and POz) by major PCs. (a) and (b) show the reconstruction of the P400 and partially the N500 peak by its PCs in the IL-IT group and in the SL-ST group respectively. 131

Figure 32 Reconstructed ERP signals on example channels (i.e. Fz and POz) by major PCs. (a) and (b) show the reconstruction of the N400 and partially the N500 peak in the IL-IT group and in the SL-ST group respectively. 131

LIST OF SYMBOLS

$V_i(t)$	voltage potential measured at lead (i) at time t
$K_i(\mathbf{r})$	lead field at location \mathbf{r} with respect to lead (i)
$\mathbf{j}^p(\mathbf{r}, t)$	primary at location \mathbf{r} at time t
$K_i(\mathbf{r}_{j,m})$	lead field of dipole at $\mathbf{r}_{j,m}$ with respect to lead (i)
$\mathbf{J}_{i,m}$	dipole moment at $\mathbf{r}_{j,m}$
\mathbf{E}	Electrical field
\mathbf{B}	Magnetic induction
\mathbf{H}	Magnetic field
\mathbf{D}	Electric displacement field
μ	magnetic permittivity
μ_0	magnetic permittivity of free space
\mathbf{J}^p	dipole moment of primary current
C_i	clustering coefficient at brain region (i)
w_{il}	connectivity between brain region (i) and (l)
σ	conductivity
ϵ	electrical permittivity

ACRONYMS

EEG	Electroencephalography
MEG	Magnetoencephalography
EOG	Electrooculography
EMG	Electromyography
fMRI	Functional magnetic resonance imaging
fNIR	Functional near infra-red
sLORETA	Standardized Low-resolution brain Electromagnetic Tomography
IL	Instructed Lying
IT	Instructed Truth-telling
SL	Spontaneous Lying
ST	Spontaneous Truth-telling
WE	With Experience
NE	Non-experienced
ERP	Event Related Potential
ERS/ERD	Event Related Synchronization/Desynchronization
ICA	Independent Component Analysis
CCA	Canonical Correlation Analysis
PCA	Principle component analysis
GKT	Guilty Knowledge Test
BEM	Boundary Element Method
MRI	Magnetic Resonance Imaging

CT	Computed Tomography
PSP	Postsynaptic Potential
EPSP	Excitatory Postsynaptic Potentials
PET	Positron Emission Tomography
SPECT	Single Photon Emission Computed Tomography
MSST	Multistart Spatial and Temporal
ECD	Equivalent Current Dipole
ACC	Anterior Cingulate Cortex
ALE	Activation Likelihood Estimation
SDP	Stimulus Delivery Period
ISI	Inter-stimulus Interval
SNR	Signal-to-noise Ratio
DMN	Default Mode Network
BA	Broadmann Area
PLI	Phase-Lagged Index
PDC	Partial-Directed Coherence
LPS	Lagged-Phase Synchronization
PDC	Partial-Directed Coherence
GC	Granger Causality
ROI	Region of Interest
DLPFC	Dorsolateral Prefrontal Cortex
APFC	Anterior Prefrontal Cortex
IC	Independent Component

CHAPTER 1

INTRODUCTION

Lie detection, also termed as deception detection, can be traced to early researches in 1900s. This application is most commonly used by law enforcement which involves investigating suspects and screening out criminals. Due to the critical role of such application, there have been various technologies proposed for this purpose and the fundamental core is to use questioning technique combined with technology that records physiological signals to ascertain truth or falsehood in response. Despite over a century's research endeavors, there is no widely adopted accurate lie detector. The most widely used lie detector is polygraph, which has been tested useful in populations untrained in countermeasures, and can discriminate lying from truth telling at rates above chance, though below perfection (Council 2003). This accuracy indicates that there is still a large application gap between existing technologies and real-life need.

1.1 The significance of deception to the society

There is no universally accepted definition of 'lying'. A common feature shared by various definitions is that deception is associated with deliberately causing someone to believe something that is not true, especially for personal gain. Deception can cause serious social

and economic harm by incurring huge social economic loss and safety threat to society. On the economic level, the costs of job applicants' dishonesty and employee misconduct or tax evasion have been estimated to range from six to two hundred billion dollars per year in the United States alone. On the social environmental level, social interactions permeate with political lies, and criminal violation of law. Hence, deception is so prevalent in our daily life in this modern society that it is of primary importance to be studied, and improvement on the understanding of the cognitive neurobiology and the neuro-anatomy related to deception is indispensable. Practically, to counteract these detrimental deceptive events, lie detection has been used in criminal investigation, employee honesty pre-screening and forensic settings. However, the existing lie detectors are lack of sensitivity and specificity to deception and hence new methods based on new theories and methodologies need to be researched and proposed.

1.2 Methodologies for studying deception

There are several methods that have been attempted to detect lies, i.e. polygraph, fMRI (functional magnetic resonance imaging), personality screening, EEG (electroencephalography) /MEG (magnetoencephalography).

Currently, polygraph remains the most widely used lie detector in real-life scenarios. Polygraph test is also termed psychophysiological detection of deception (PDD) examination. It measures and records several physiological indices based on responses from the peripheral nervous system such as blood pressure, pulse, respiration, and skin conductivity while the suspect is asked to answer a series of questions (Saxe 1999,

Ganapati M. Tarase 2013). The belief of the underpinning usage of the polygraph is that a person with deception intention is scared of being detected, which entails mild to severe consequence of being detected. As such, the liars are normally more anxious and nervous when deceiving. Polygraphs measure arousal, meaning a person with deceptive activities tend to have higher arousal level (Vrij 2000, Bull 2006, Grubin 2010); nevertheless, this measurement of arousal level is inadequate. Since arousal can be caused by nervousness, fear, confusion, hypoglycemia, psychosis, depression, substance induced (nicotine, stimulants), substance withdrawal state (alcohol withdrawal) or other emotions. This arousal status is closely associated with symptoms such as increased blood pressure, heart rate, faster respiration. Therefore, polygraph does not simply measure lies, it basically measures arousal emotional status. Moreover, even innocents can feel nervous whenever they are investigated.

In 2002, a review by the National Academies of Science found that in populations untrained in countermeasures, polygraph testing can discriminate lying from truth telling at rates above chance, though below perfection. These results apply only to specific events and not to screening where it is assumed that polygraph would work less well, e.g. the utility among sex offenders is poor. In some countries polygraphs are used as an interrogation tool with criminal suspects or candidates for sensitive public or private sector employment. In general, a polygraph cannot differentiate anxiety caused by dishonesty and anxiety caused by something else. Its effectiveness may also be worsened by countermeasures.

Since deception is intrinsically a cognitive event which employs resources from central nervous system (Christ, Van Essen et al. 2009, Shi-Yue and Yue-Jia 2010). More direct

information of central nervous system can be better captured through methods such as EEG and fMRI, which are promising methods in providing features of higher specificity to deception. There are abundance of research results that have been achieved in fMRI community which presents regional hemodynamic changes in response to neural activity changes due to external stimuli with high spatial resolution, and these studies have implicated a diversity of frontal, temporal and parietal areas in involvement of generation for deceptive response. fMRI based lie detection however, is still constrained by its limited accessibility and low affordability in real application. As an alternative, EEG is supposed to provide more cost-effective and accessible measurements in real-life investigation scenarios. Nevertheless, there are still limited theoretical studies that have verified the effectiveness of EEG in distinguishing brain activities associated with lying and truth-telling condition, let alone a consensus yet to be achieved on EEG's correlates to deceptive brain activities. These problems have stimulated research on EEG-based neural correlates for deception. Most EEG studies conducted previously focused on the modulation effect in power spectrum on the scalp level and the neural mechanisms were not associated with any specific areas in the brain. An alternative solution is a frequently used EEG based lie detection paradigm has been used to detect concealed information in the 'guilty knowledge test'(GKT) that depends on the detection of a well-known P300 'oddball' response[It is an increased amplitude relative to baseline occurs 300ms following rarely presented and meaningful stimuli, refer to for a review]. However, the meaningful stimuli should be limited to a few relevant targets among a pool of irrelevant targets throughout the measurement. Different from previous studies, all the experiments conducted for this thesis

focused on two types of signals, (1) ongoing (i.e. oscillatory) components accompanying deception with the hypothesis that there exists rich information about deception in brain's oscillatory activities and (2) an ERP paradigm different from the P300 paradigm was developed which focuses on brain's response to different kinds of feedback to the innocents/liars. These studies were carried out to verify the hypotheses and meanwhile to investigate if there exist robust source level features which may present higher specificity and sensitivity to deception.

1.3 The objective of the thesis

This thesis is concerned about developing new EEG-based deception methodologies that are capable of providing more insightful understanding for deception and granting the future EEG-based deception detection system a more sound theory and detection performance. The specific objectives and contributions can be grouped into four parts:

- (1) To explore deception's underlying neural mechanism by observing the neural anatomies that present significant differences in power spectrum between deception and truth-telling associated brain activities in both instructed and spontaneous lying tasks.
- (2) To provide explanation on the observed difference between truth and falsehood based on EEG signal, from the level of source-to-source connection, and network behavior in order to enrich our understanding of the complex deception phenomenon by turning it into a more easily addressable problem.

- (3) To propose new EEG-based experimental protocols that allows capture of deception features outside deception window, which brings enhanced possibility of successful deception detection.
- (4) To propose novel EEG-based experimental protocols that can effectively simulate realistic deception scenarios to facilitate the differentiation between deception and truth-telling.

This doctoral research contributes to the development of novel EEG-based deception study/application protocols and analysis methods with sound theoretical basis for the results. Moreover, the proposed new methodologies can not only bring up new directions for deception research community but also could potentially empower all the existing deception detection techniques by incorporating the new methods to achieve a more comprehensive and powerful detector. The work might also contribute to inspire the EEG community for inventing and enhancing closely related methods. Also, the explicit concern about the refinement on the deception protocol might draw the researchers' attention to the necessity of fully exploiting human's multiple manifestations of deception that may lies outside of the deceiving process itself. It is still arguable whether deception can be really captured during the deceiving process, however, by recognizing the benefits of exhaustively covering all the phases of deception, i.e. prior to deception, during deception, post deception and post feedback we might be able to produce a comprehensive deception detection tool which captures each step of deception. This thesis specifically focuses on the phase prior to deception and post feedback towards deception/truth-telling, which has never been investigated before. With the help of newly proposed source localization and

network/connectivity analysis methods, to identify neural correlates of deception which is the end goal can be encouraged to step further.

1.4 Thesis outline

Chapter 1 elaborates on the practical value of deception detection researches in real-life, provides an overview of the existing major technologies for deception detection, and made a comparison among these technologies which helps to identify the application gap where needs more research input, and is followed by declaration of the research objectives.

Chapter 2 lays out the background materials that could facilitate reader's familiarity with this research. These background materials include physiology of EEG, history of EEG in clinical application, advantages and limitations of EEG, EEG signal processing methods, inverse solution, and deception studies using various technologies, i.e. polygraph, fMRI and EEG, their pros and cons, and the various categories of deception that have been studied using polygraph/fMRI/EEG. A detailed review is given to the abundant deception protocols and signal modalities, the existing neurophysiology knowledge of deception. From these reviews, limitations of existing researches are analyzed and specific research of this research focus is introduced.

Chapter 3 gives overview of the methodologies/protocols proposed in this research. The experiment designs used in this research are described and corresponding hypotheses are provided for the following experiments. The data collection procedure used in the experiments is described. The recorded data forms the dataset for the subsequent chapters.

Chapter 4 studies the application of the proposed EEG-based source localization method that provides spatial and spectral neural features representing distinguished event-related modulation on the power spectrum by deception or truth-telling condition in the instructed lying and spontaneous lying conditions in the autobiographic memory recalling tasks as well as deception or truth-telling condition in the WE (with prior-experience) and NE (without prior-experience) tasks, respectively. The neurophysiologic interpretation of the spatial and spectral neural features is presented in detail.

Chapter 5 studies the proposed EEG-based network and connectivity analysis method that provides neurophysiologic elaboration on the identified networks functioning with distinguished roles during the time window prior to the action of deceiving. Major differences between two conditions (i.e. instructed lying and instructed truth-telling) from the region-to-region connection and network connection manifestation are discussed.

Chapter 6 studies the proposed novel ERP-based deception protocol that exploits feedbacks to induce differential neural activities from the liars and the innocents. The specific difference observed from the scalp ERP is described, and ICA analysis is exploited to identify the major spatial components that contribute to the observed ERP differences. Finally, source localization is employed to further elucidate the underlying neural sources involved in these major spatial components. The relevant methods and the results are elaborated in detail.

Chapter 7 concludes thesis with overall conclusions, and suggestions for possible future research directions.

CHAPTER 2

LITERATURE REVIEW

2.1 Neurophysiology of EEG (electroencephalography)

In the most basic level, the source in the micro-scale can be formed in a neuron body, and is generated by neurons' polarization and depolarization. When the neighboring neurons excite one neuron through synapse (a junction between a neuron and another cell), the action potential causes calcium channels to open in the plasma membrane of the presynaptic cell. The calcium ions (Ca^{+}) diffuse into the neuron and activate enzymes, which in turn, promote fusion of the neurotransmitter vesicles with the plasma membrane. This process releases neurotransmitter into the synaptic cleft. Neurotransmitter molecules diffuse across the cleft and stimulate the postsynaptic cell, causing Na^{+} channels to open and depolarization of the postsynaptic cell. The depolarization of the postsynaptic cell is referred to as a synaptic potential. The magnitude of a synaptic potential depends on: the amount of neurotransmitter and the electrical state of the postsynaptic cell. If it is already partially depolarized, an action potential can be produced with less stimulation by neurotransmitters. If it is hyperpolarized, it will require more stimulation than normal to produce an action potential. A synaptic potential can be excitatory (they depolarize) or inhibitory (they polarize). Some neurotransmitters depolarize and others polarize. In the

brain and spinal cord, hundreds of excitatory potentials may be needed before a postsynaptic cell responds with an action potential. When the apical dendritic membrane becomes transiently depolarized, consequently the extracellular environment becomes electronegative with respect to the cell soma and the basal dendrites. This potential difference causes a current to flow through the volume conductor from the non-excited membrane of the soma and basal dendrites to the apical dendritic tree sustaining the EPSPs (Gloor 1985).

Excitatory postsynaptic potentials (EPSPs) are generated at the apical dendritic tree of a cortical pyramidal cell and trigger the generation of a current that flows through the volume conductor from the non-excited membrane of the soma and basal dendrites to the apical dendritic tree sustaining the EPSPs. Some of the current takes the shortest route between the source and the sink by travelling within the dendritic trunk, while conservation of electric charges imposes that the current loop be closed with extracellular currents flowing even through the most distant part of the volume conductor.

When the wave of ions reaches the electrodes on the scalp, they can push or pull electrons on the metal on the electrodes. Since metal conducts the push and pull of electrons easily, the difference in push, or voltage, between any two electrodes can be measured by a voltmeter and this recording over time gives us the EEG (Tatum 2008).

However, the electric potentials generated by a single neuron are far too small to be picked by EEG or MEG (Nunez 2006). EEG activity therefore always reflects the summation of the synchronous activity of a cluster of neurons, typically thousands of them, which have

similar spatial orientation as well as good temporal summation. If the cells do not have similar spatial orientation, their currents do not align to create potential that can be detected due to the additive summation requirement. They might just cancel with each other so is difficult to be detected. Pyramidal neurons of the cortex are thought to produce most of the recordable EEG signal as they are well-aligned and have synchronous firing. Large cortical pyramidal nerve cells are organized in macro-assemblies with their dendrites normally oriented to the local cortical surface. This spatial arrangement and the simultaneous activation of a large population of these cells contribute to the spatio-temporal superposition of the elemental activity of every cell, resulting in a current flow that generates detectable EEG and MEG signals. In the most macro-scale, those functional networks made of these cortical cell assemblies and distributed at possibly multiple brain locations are thus the putative main generators of MEG and EEG signals which is related to a specific task or brain condition. The currents associated with the EPSPs generated among their dendrites are believed to be at the source of most of the signals detected in MEG and EEG because they typically last longer than the rapidly firing action potentials traveling along the axons of excited neurons (Nunez 2006).

2.2 Brief history of EEG in practical application

Since the first recordings in humans discovered and performed by the German psychiatrist, Hans Berger in 1929, the electroencephalography (EEG) has become one of the most important diagnostic tools in clinical neurophysiology. EEG used to be a first-line method of diagnosis for tumors, stroke and other focal brain disorders, but this use has decreased

with the advent of high-resolution anatomical imaging techniques such as MRI and CT. Meanwhile, since the 1960s the EEG was also used to measure event-related potentials (ERPs) which refer to averaged EEG responses that are time-locked to more complex processing of stimuli. And the stimuli could be of visual, auditory and somatosensory nature. This technique has been widely used in cognitive science, cognitive psychology, and psycho-physiological research. ERPs could also serve as an instrumental research tool in human disorders research, such as psychiatric and developmental disorders. In addition, resting-state EEG and task-state EEG have been widely explored in various task conditions and pathological states to identify the underlying neuro-physiological and neuro-psychological events and modulation factors.

The ultimate aim of neuroscience research is to seek fully understanding of how human brains function in both normal and pathologic conditions and in turn provide basis for the development of practical tools to serve human's real-life, e.g. to alter pathologic disease state of the brain such as intractable epilepsy, schizophrenia, depression, and Parkinson's and Alzheimer's disease. Electrophysiological measures such as EEG provide one promising way to manifest the underlying processes of brain activities in different states besides hemodynamic, metabolic and neuro-chemical manifestations.

2.3 Advantages and limitations of EEG as a neuro-diagnostic tool

To characterize and understand the underlying neural substrate and its working mechanism responsible for certain neuropsychological events, several imaging tools have been developed. Functional imaging has a twofold objective: localizing the populations of neurons involved in cognitive or behavioral tasks and characterizing the temporal or spectral relationship between those populations. To this end, functional imaging techniques should consequently and ideally offer optimal spatial and temporal resolutions. The spatial and temporal resolutions should reach the order of 1 mm and 1 ms, respectively, to adequately describe the underlying physiological phenomenon of brain activity. Current functional imaging techniques, Positron Emission Tomography (PET), Single Photon Emission Computed Tomography (SPECT) and functional Magnetic Resonance Imaging (fMRI) present rather a good spatial resolution (Barth). However, they all fail to offer a high enough temporal precision. For example, fMRI is capable of producing spatial resolutions as high as 1-3 mm; however, temporal resolution is limited by the slow hemodynamic response to approximately 1 s (Table 1).

Magnetoencephalography (MEG) and EEG (MEG/EEG) are two complementary techniques that noninvasively measure, respectively, the magnetic induction outside the head and the scalp electric potentials produced by electrical activity in neural cell assemblies. They can be used for localizing neural electrical activity by measuring the external electromagnetic signals. Among the available functional imaging techniques, MEG and EEG uniquely have temporal resolutions below 100 ms and offer superior temporal resolution when compared to PET or fMRI, and this high temporal precision allows us to explore the timing of basic neural processes at the level of cell assemblies and

the dynamics of neural networks (Ahlfors, Simpson et al. 1999). MEG/EEG source localization draws on a wide range of signal processing techniques including digital filtering, three-dimensional image analysis, array signal processing, image modeling and reconstruction, and, more recently, blind source separation and phase synchrony estimation.

Table 1 Spatial and temporal resolution of different neuro-diagnostic tools

Neuro-diagnostic tool name	Temporal resolution	Spatial resolution (mm)	Measurement scale
MEG&EEG	Millisecond	10~1000	Map~ Brain
Functional MRI	Second	1~100	Column~ Brain
PET	Minute	10~100	Column~ Brain
Naturally occurring lesions	Hour – Day	10~100	Map~ Brain
TMS	Second- Minute	1~100	Column~ Brain
Multi-unit recording	Millisecond	0.01~1	Dendrite~ Column
Single-cell recording	Millisecond- Day	~0.01	Dendrite ~ Layer Neuron

However, the EEG has a number of limitations. Electrical activity recorded by electrodes placed on the scalp or surface of the brain mostly reflects summation of excitatory and inhibitory postsynaptic potentials in apical dendrites of pyramidal neurons in the more superficial layers of the cortex. Quite large areas of cortex (in the order of a few square centimeters) have to be activated synchronously to generate enough potential for changes

to be registered at electrodes placed on the scalp. Moreover, propagation of electrical activity along physiological pathways or through volume conduction in extracellular spaces may give a misleading impression as to location of the source of the electrical activity. Whether deep sources that play important brain functions can be detected has not reached conclusive stage as well. Spatial sampling in routine scalp EEG is incomplete, as significant amounts of cortex, particularly in basal and mesial areas of the hemispheres, are not covered by standard electrode placement.

2.4 EEG signal processing methods

EEG is the recording of electrical activity along the scalp. As each of the EEG electrodes collects the summation of electrical potential generated by the underlying sources from a specific spatial location, it actually collects a signal with multiple frequency bands information. Typical scalp EEG contains a wide band signal from low frequency wave (~0.5Hz) up to high frequency wave (100 Hz). These frequency components have interesting and valuable properties. However, not all frequency bands are as informative for the interpretation of the underlying brain activities. The basic EEG rhythms are summarized briefly as follows. Delta brainwave (1-4Hz) is the lowest but the strongest brainwave. These waves are usually generated in deepest sleep and dreamless sleep (Roth 2009), not attentive and low arousal level mental status. Theta brainwaves (4-8Hz) also occur in sleep and are also dominant in the deep meditation (Hinterberger, Schmidt et al. 2014), and subjective feeling status such as creative, recalling (Marshall, Kirov et al. 2011). Alpha brainwaves (8-12Hz) is usually a dominant frequency band when subjects close eyes,

it is a band that is closely associated with attentional and task status and has been linked with attention (Klimesch 2012), working load (Kathner, Wriessnegger et al. 2014), etc. Beta brainwaves (usually 12-30Hz) are relatively higher frequency band with large range. It is a brainwave sensitive to moving the arm or leg that leads to ‘sensorimotor rhythm’ (Michael, Krishnaswamy et al. 2005), alertness (Poupard, Sartene et al. 2001), etc. Gamma band ($\geq 30\text{Hz}$) usually indicates a high-level information-rich task processing (Gilbert and Li 2013), thinking/ integrated thought (Lutz, Greischar et al. 2004). These basic EEG rhythms occur with typical distribution on the scalp according to varying subjects’ states, tasks, physiological correlates and the effects of training. However, this brief summary above just serves as a general roadmap and not as fixed and hard rules. Therefore, it maybe ill-conceived to say ‘this is the rhythm for attention’, and we may need to study the patterns that emerge during various specific behavioral, as well as states, and use multi-dimensional representation of some state-space with the help of computer-processing of EEG.

2.4.1 EEG de-noising methods

Although EEG is such broad band signal containing rich cerebral cortex activity information, it can be contaminated with artifact and noise components during measurement. These artifact and noise components are usually electrical signals generated from sites other than the brain or simply collected by the EEG electrode. These artifacts can be divided into physiologic and extra-physiologic artifacts (N Sethi 2006). Physiologic artifacts are generated from the subjects; they arise from sources other than the brain (i.e. body). For example, low frequency component such as EOG (due to eye movement or

blinking) and rhythmic breathing or sweating artifact (Barkoukis, Avidan et al. 2007), or high frequency component such as EMG (through the electrical fields generated by muscle and through a movement effect on the electrode contacts and their leads) can be collected by scalp EEG electrodes (Shackman, McMenamin et al. 2009). Sometimes artifact caused by electrodes themselves can be collected such as electrode pop artifact, electrode contact and lead movement artifact (Solomon 1983). Extra-physiologic artifacts arise from outside the body (i.e. equipment, environment). A typical artifact usually can be seen via a monomorphic frequency of the current, which is 60Hz in North America and 50Hz in much of the rest of the world. This ambient electrical noise is due to the alternating current present in the electrical power supply (Cuong, Ha et al. 2010).

The systematic approach to recognize, separation and elimination of artifacts is an important factor that helps to reduce the chance of misinterpretation of EEG, which is so important for clinical application and human neuroscience research. In fact, the EMG, EOG and the typical 50/60Hz environmental artifact are the most common and significant sources of noise in EEG signal and need to be identified and removed. Although slow roving eye movement shares similar frequency and field pattern compared with perspiration artifact, the eye movement artifact has distinguishing feature with its rhythmicity, phase reversal (because of eye's dipole), and broad, bi-frontal field of eye movement. Moreover, despite the fact that the duration of EMG artifact varies according to the duration of the muscle activity and may ranges from less than a second to an entire EEG record, this artifact occurs most commonly in regions with underlying muscle, specifically the frontalis and masseters and therefore most commonly occurs in channels

including the frontal and temporal electrodes (McMenamin, Shackman et al. 2009). In addition, the EMG artifact has a temporally low autocorrelation property which makes it separable from EEG signal. Out of the three most salient artifacts, 50/60Hz environmental artifact is the most persistent artifact across the time. Although this artifact may be present in all channels or in isolated channels, which means there is no clear-cut spatial distribution associated with this artifact, this rhythmic oscillation is usually easily recognizable from the EEG signal. To remove these artifacts from the EEG signal, various methods have been proposed. The most reliable way is to reject EEG segments that are contaminated by these artifacts. However, this can lead to unacceptable data loss. Based on the spatial/temporal/frequency characteristics of these artifacts, data-driven algorithms are useful in separating out these artifact components.

Typical EOG removal methods have two main branches, 1) Independent Component Analysis (ICA) based method and 2) regression based method. In regression based method, reference electrodes are usually needed which are called EOG electrodes that are pairs of electrodes typically placed either above and below the eye or to the left and right of the eye. Simple time-domain regression (Gratton, Coles et al. 1983), multiple-leg time-domain regression (Kenemans, Molenaar et al. 1991) and frequency domain regression methods (Woestenburg, Verbaten et al. 1983) have been proposed. In all these approaches, calibration trials are first conducted to determine the transfer coefficients between the EOG electrodes and each of the EEG electrodes which estimates the spread of EOG artifacts across the EEG channels. These transfer coefficients are then used for correction by estimating the EOG component in the EEG recording and are removed by subtracting these

components. More recent studies proposed PCA and ICA based methods to separate the EOG signals from the EEG signals through blind source separation (Jung, Makeig et al. 2000). Although PCA method makes use of multichannel EEG information, it cannot completely separate eye artifacts from brain signals especially when they have comparable amplitude (Berg and Scherg 1991). Compared with the regression method and the PCA method, ICA method has been shown more effective in removing EOG components (Jung, Makeig et al. 2000). The EMG artifact has been tentatively distinguished from EEG signal with heavy low-pass filters, such as 10 and 12 Hz low-pass filters. However, it was reported that the frequency spectrum of muscle artifacts has been shown largely overlap with that of brain signals. Moreover, the facial EMG has been shown to present in a broad frequency range from almost DC to 200Hz (Goncharova, McFarland et al. 2003). Although the heavy low-pass filters might be useful to remove the majority portion of EMG artifact, it also constrains the chance to study EEG signal above 12 Hz (i.e. beta) and the estimation of the event related potential with dominant frequency around 10Hz such as visual evoked potential can be seriously affected by applying heavy low-pass filter. More recently, blind source separation technique such as ICA and CCA has been applied to disentangle EMG from EEG. Moreover, most of these ICA-based studies require manual definition of EMG signal based on spatial and frequency characterizations, which predisposes manual error in judgments and the non-existence of an optimal EMG separation method based on the ICA algorithm. On the other hand, CCA algorithm assumes EMG activity has weak autocorrelation over time given the broad spectrum of EMG that resembles white noise signal (De Clercq, Vergult et al. 2006). In contrast, EEG signal tends to be much more

strongly auto-correlated over time. Based on the rationale that EMG and EEG signals are uncorrelated with each other and EEG sources are individually autocorrelated over time, CCA method was proposed and proved to be effective in de-noising EMG from EEG in several studies (De Clercq, Vergult et al. 2006).

To remove the 50Hz/60Hz electrical noise from the background environment, notch filter is normally applied to filter out a narrow frequency band centered around 50Hz/60Hz, and this method has been proven effective evidenced by the significant diminish of power spectrum component at 50Hz/60Hz after notch filtering.

Last but not the least, it is also important to note that some of the dominant noises can be avoided during the EEG measurement, i.e. electrode contact and movement caused artifact, perspiration artifact. Electrode contact and movement caused artifact can be avoided by selecting appropriate size of EEG cap for each subject before EEG recording, since too big the cap can cause loose contact of the electrode with the subject's scalp. And the perspiration artifact can be avoided by making subjects comfortably seated in a room temperature that will not cause any sweating to the subjects.

As a summary, careful selection of an effective artifact removal method plays equally significant role as any method that is attempted for interpretation of the EEG signal itself. Failure to remove artifact especially when the EEG signal is almost as strong as the artifact can lead to mis-interpretation of EEG signals.

2.4.2 Temporal EEG analysis (Event Related Potential - ERP)

Pure EEG signal is a continuous recording of brain activity which is contributed by subjects' ongoing neural activities in a non-task state (resting-state) or task state. Although the ongoing EEG has been proved useful in characterizing the mental status of a subject under a particular situation (normal/disease state, trained/un-trained state, alert/drowsy state), it becomes difficult for assessment of highly specific neural process that are the focus of cognitive neuroscience due to the fact that it is difficult to isolate individual neuro-cognitive processes based on the pure EEG data. On the other hand, ERP has offered a more sophisticated method of extracting more specific brain response induced by a specific sensory, cognitive or motor event by simple averaging technique (Woodman 2010). This ERP normally represents subjects' stereotypical electrophysiological responses to a stimulus. The pure EEG signal reflects thousands of simultaneously ongoing brain processes. In a single trial to a specific event, brain response to that particular event is normally invisible due to the strong non-task related background EEG signal that obscure the signal of interest. To see brain's response to a stimulus, many trials have to be conducted / repeated and averaged, causing brain activity irrelevant to the task/stimulus (i.e. EOG, EMG, random background brain activity) to be averaged out and the task-relevant waveform to remain. This averaging procedure significantly increases the signal-to-noise ratio (SNR) of the recorded ERPs, and therefore rendering the ERP more discernible and allowing for interpretation. The assumptions behind this technique is that

- 1) signal of interest that is caused by an event has negligible variance of latency and shape,
- 2) the noise can be approximated by a zero-mean Gaussian random process which is uncorrelated between trials and not time-locked to the event (Limpiti, Van Veen et al.

2009). Although random brain activities can easily fulfill point (2) as a noise component, EOG/EMG artifact that are often several orders of magnitude larger than the underlying ERPs should be removed from affected trials by performing manual or automated artifact removal procedures.

As a standard EEG analysis technique, ERP method has its advantages and disadvantages. The major advantages of ERP is that it can provide a measure of processing of stimuli in a more specific way even without behavioral or peripheral nerves system's activity change. Moreover, ERP provides excellent temporal resolution of 1ms or better. However, given the small amplitude of an ERP, it usually requires repeating a large sample size to ensure accurate measurement of ERP. In addition, spatial resolution of an ERP is currently undefined making it difficult to localize the neural generators of ERP. This renders ERP less competitive compared with fMRI and PET in identifying source generators to a stimulus. Sophisticated methods such as PCA/ICA are usually required to decompose the ERP components into several single ERP components, before source localization method can be applied to isolated ERP components (Makeig, Westerfield et al. 1999).

Experimental psychologists and neuroscientists have used ERP extensively in neuroscience, cognitive psychology, cognitive science and psycho-physiological researches. Various ERP signals in response to visual, auditory, motor and cognitive events have been identified, providing a measure of the timing (latency) and the degree (amplitude) of brain's communication/information processing to the stimulus/event. For example, Visual N100 has been associated with visual stimulus processing and is an ERP

with a negative peak around 150-200 ms post-stimulus. The N1 can be found over the entire scalp and studies have suggested that its magnitude/latency can be modulated by spatial selective attention (Rugg, Milner et al. 1987). Visual C1 and P100 are other early event-related components that are associated with visual event-related potential, with the onset of C1 at around 40-60 ms post-stimulus and peak around 65-90 ms post-stimulus (Stolarova, Keil et al. 2006) followed by P100, a positive potential peaks around 100-130 ms (Di Russo, Martinez et al. 2003). It has been shown by studies that both C1 and P100 are sensitive to stimulus parameters, and P100 can also be tuned by attention (Luck, Heinze et al. 1990). Another type of visual evoked potential is termed N170, which is usually associated with the neural processing of faces. It was reported that face stimuli can elicit a more negative potential than other visual stimuli over occipio-temporal sites, which peaks at about 170 ms post-stimulus (Bentin, Allison et al. 1996). Late component such as P300 whose latency ranges from 300 to 600 ms after the presence of the targets is thought to reflect processes involved in stimulus evaluation and categorization and not correlated with post-categorization processes such as response selection and execution (Magliero, Bashore et al. 1984). It is a famous peak elicited using the oddball paradigm (Polich and Margala 1997), in which low-probability task-relevant stimuli (target items) are mixed with a large number of high-probability standard stimuli (non-target items). N400 is another type of late component as part of normal brain response to words and other meaningful stimuli, including visual and auditory words, sign language, picture, faces, sounds and smells (Kutas and Federmeier 2000) and has been shown modulated by expectancy (Curran, Tucker et al. 1993).

In summary, ERP is a standardized and important EEG technique that allows extraction of subjects' stereotypical event-related waveforms to a certain stimulus. This waveform not only offers timing and coarse spatial information in stimuli processing, it may also be modulated by contrastive conditions and present with differences in the amplitude as a measurable index to quantify the difference.

2.4.3 Spectral EEG analysis (Event Related Synchronization/De-synchronization- ERS/ERD)

Neural oscillations represent common neural activities at all levels, e.g. spike trains, local field potentials and large-scale oscillations that can be measured by EEG. These oscillation signals can be generally characterized by their frequency, amplitude and phase and analyzed via time-frequency analysis. In some conditions, external stimuli/event can induce brain activity, which generally reflects the activity of numerous neurons by amplitude changes in oscillatory activity that are thought to arise from the change in the synchronization of neural activity, for instance by synchronization of spike timing or membrane potential fluctuations of individual neurons (Varela, Lachaux et al. 2001). This change of oscillation amplitude can be used to quantify the induced change in signal band power as difference between a baseline prior to the event and the post-event period. As a result, the spectrum modulation induced by stimuli/event or movement preparation has two forms, i.e. event-related synchronization and event-related de-synchronization, which correspond to a positive value (increased signal power) and a negative value (decreased signal power) respectively to the baseline period, and the direction of change depends on

the frequency band in question. For instance, presentation of a visual stimulus, typically results in a decrease in the alpha amplitude (alpha de-synchronization) and increase in the theta amplitude (theta synchronization) (Pfurtscheller and Lopes da Silva 1999). This concept has received wide adoption in human sensory, cognition and memory studies as well as practical application such as motor imagery neural modulation and recently in deception.

In summary, parallel to the event related potential analysis that characterizes time-locked and phase-locked neural modulation evoked by the external stimuli, event-related de-synchronization /synchronization characterizes time-locked modulation effect induced in the synchronization of neural activity. These two index provide complementary information that enable neuroscientists to explore neural mechanisms underlying brain's response to external stimulus, which is of great significance for studying both subjects with normal and diseased status and investigating distinguished features that lie in different conditions.

2.5 Inverse problem and source localization

2.5.1 Lead field theory

The lead field theory introduced by McFee and Johnston (1953) is an extension of the lead vector theory introduced by Burger and Van Mialann (1946). The lead field theory generalizes the physical relationship between the electrical current source in a 3D space and the voltage potential measured on any scalp lead through an integration of a lead-field

matrix multiplied by current source density extending over a finite volume where the sources are believed to lie. The mathematical formula is shown in Eq. 1.

$$V_i(t) = \int_V K_i(r) j^p(r, t) d^3r \quad (1)$$

Eq.1 basically implies a forward model from underlying source to the measured scalp potential. Fig.1 illustrates this relationship between the forward and inverse problem through source and volume conductor model. Basically, forward problem is for estimation of the output EEG data given the known source information and the volume conductor model; and inverse problem is for estimation of the underlying source information (i.e. location and moment) given the EEG data and the volume conductor model.

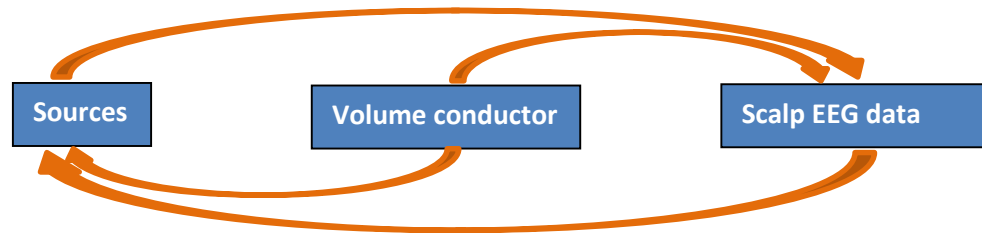


Figure 1 The relationship between forward problem and inverse problem, the connection between them is source model and volume conductor model.

2.5.2 Inverse problem

It has been a keen pursuit of neuroscientists to decipher brain activity by looking into the neural substrate that contribute to the measured scalp EEG signal, which can be defined as solving an ‘inverse problem’. It is important to be aware that scalp EEG electrodes are most sensitive to a particular set of post-synaptic potentials that are generated in superficial layers of the cortex, on the crests of gyri directly abutting and radial to the skull. The

dendrites that are located deeper in the cortex inside sulci, in midline or deeper structures, or producing currents that are tangential to the skull, have far less contribution to the EEG signal. Moreover, EEG recordings do not directly pick up axonal action potentials due to the reason that an action potential is more like a quadrupole that produces field decreasing much more rapidly than the one produced by the current dipole (Hämäläinen, Hari et al. 1993). In addition, EEG captures summation of activity by thousands of synchronized neurons, which means that there is weak possibility for the fast action potential to sum up and recorded in EEG. Therefore, to inversely decipher source information from scalp EEG may only allow extraction of information that can be captured by EEG.

However, this is an ill-posed linear equation, with far more unknowns (sources' current density) than known parameters (scalp EEG voltage). From mathematical point of view, there is no unique solution behind this equation. As such, seeking the contributing source underlying a given measured EEG signal is deemed as an ill-posed inverse problem. Fortunately, despite this notorious ill-posedness by nature, there are some developed techniques which provide good estimation of the current source information given adequate and proper assumption of the characteristics of the underlying sources.

2.5.3 Inverse model (source localization)

There are many methodologies developed in the spirit of looking for the underlying sources of EEG signal. The reason why there are so many different inverse solutions to the problem is due to the fact that the solution itself is none-unique, and therefore neurophysiologic plausible and computational achievable constraints should be applied to get the unique

solution for the problem. Among these techniques, there is no single constraint that performs best in all conditions in localizing the sources. In fact, each constraint has its underlying assumption, and is called regularization operator for the solution space which reduces the whole large source space to a much smaller source-activated space that produce best matched voltage value compared with the given EEG signal.

There is abundance of many other sophisticated approaches proposed to tackle the ill-posedness of EEG inverse problem and to strike a balance between accurately localizing the source location and providing solutions with excellent spatial resolution for the purpose of results interpretation. However, it is interesting to note that the majority of the neuroscientists actually have applied LORETA/SLORETA as a standardized method for source reconstruction for their neuroscience research. sLORETA is a well-recognized inverse solution technique that estimates the distribution of the standardized electrical current density by normalizing the voxel's estimated electric current density over its expected standard deviation in the three-dimensional space and is reported to have zero-localization error in non-noise and even with-noise conditions (Pascual-Marqui 2002). According to the nature of this algorithm, sLORETA is most suitable for calculation of distributed cortical sources or limited amount of focal cortical sources with distinct field, given the low spatial resolution of this technique (Wagner, Fuchs et al. 2004). In this thesis, sLORETA is widely adopted for source localization to infer the neuro-anatomy underlying the differences between two different conditions under investigation.

2.6 Deception protocol/signal modalities and neural correlates of deception

Deception can cause serious social and economic harm to the society by incurring huge social economic loss and safety threat to the society. It is an impactful social event and has been the focus of an abundance of researches over recent decades. Despite decades of researches in finding the neuronal mechanism of deception, this complex neuropsychology phenomenon remains obscure. Therefore, it is of significant importance to improve on the existing methods or proposing new methods to promote the fundamental research or algorithm development for deception studies and applications. Since deception detection is largely based on the knowledge of neural correlates / features underlying deception, it is of paramount importance to be aware that the so-called neural correlates of deception is derived and largely dependent on the protocols that employed to induce deception trace in brain activities that can be recorded in certain signal modalities. Therefore, the importance of the development of effectively valid deception protocols cannot be underrated and overwhelmed by sophisticated mathematical algorithms that come in for feature extractions or pattern recognition only after the relevant brain activity has been recorded, with the brain activity determined by the protocols in the first place.

2.6.1 Developed deception study protocols and signal modalities in literature

Practically, lie detection has been used in the criminal investigation, employee honesty pre-screening and forensic settings. Unfortunately, the existing lie detectors are lack of sensitivity and specificity to deception and hence new methodologies need to be researched and proposed. There are several methods that have been attempted to detect lies, i.e. polygraph (Matte 2007, Grubin 2010), fMRI (Davatzikos, Ruparel et al. 2005, Christ, Van Essen et al. 2009), personality screening (Zickar and Drasgow 1996), EEG/MEG (Seth, Iversen et al. 2006, Kim, Jung et al. 2012), and fNIR (Ding, Gao et al. 2013).

There is an abundance of research on deception in fMRI community (Langleben, Schroeder et al. 2002, Ganis, Kosslyn et al. 2003, Abe, Suzuki et al. 2006, Langleben 2008, Simpson 2008, Christ, Van Essen et al. 2009, Greene and Paxton 2009), these studies have shown that a diversity of frontal, temporal and parietal areas involve in deceptive responses. The previous fMRI studies have highlighted important roles of prefrontal and anterior cingulate cortex (ACC) in deception (Langleben, Schroeder et al. 2002, Ganis, Kosslyn et al. 2003, Abe, Suzuki et al. 2006, Greene and Paxton 2009), highlighting ‘executive control’ as a core component of deception. In a wider sense, a review study using the Activation Likelihood Estimation (ALE) method has identified working memory, inhibition control and task switching as the most basic components underlying various kinds of deception through meta-analysis over published fMRI studies on deception irrespective of the specific property of the task (Christ, Van Essen et al. 2009). Despite the exciting discoveries with fMRI studies on deception, fMRI-based lie detection is still constrained by its limited accessibility in real-life application.

As an alternative, EEG is supposed to provide more cost-effective and accessible measurements in real-life investigation scenario. Nevertheless, there are still limited theoretical studies that have verified the effectiveness of EEG in distinguishing brain activities associated with the lying and the truth-telling conditions, let alone a systematic theory and a consensus yet to be achieved on the feasibility of EEG for lie detection. Most EEG studies conducted previously focused on the modulation effect on EEG power spectrum observed from the scalp level and specific EEG frequency band (i.e. alpha) has been associated with deception, demonstrating that risk monitoring/expectation and increased cognitive load play important roles in deception (Jung and Lee 2012, Kim, Jung et al. 2012). However, the underlying neural mechanisms were not associated with any specific areas in the brain by any of these studies (Seth, Iversen et al. 2006, Abootalebi, Moradi et al. 2009, Shi-Yue and Yue-Jia 2010, Kim, Jung et al. 2012). Moreover, a frequently used EEG based lie detection paradigm (Abootalebi, Moradi et al. 2009) has been used to detect concealed information in the ‘guilty knowledge test’(GKT) (Carmel, Dayan et al. 2003) that depends on the detection of a well-known P300 ‘oddball’ response (Lawrence A. Farwell 2013). However, P300 is considered not merely specific to deceptive brain activities and stimuli used in the test are limited to visual items.

In terms of EEG-based neural correlates for deception, although several EEG studies have reported alpha event related de-synchronization (ERD) as a global/regional feature characterizing enhanced cognitive load caused by deception (Jung and Lee 2012, Kim, Jung et al. 2012), the degree of ERD actually depends on deception type as well as observation window. Compared with spontaneous lying which involves higher cognitive

load contributed by decision making, selective attention, memory retrieval and response planning, instructed lying however focuses on inhibition of the truth while generating the lie and is more likely to be associated with an increase of alpha power event related synchronization (ERS) evidenced by the observations that alpha ERS is associated with inhibition of task irrelevant and potentially interfering processes. From the perspective of neuro-psychological process, it is likely that the major difference between the spontaneous lying and the instructed lying is an additional decision making process involved in the former scenario. Meanwhile, it is possible that inhibition and controlled access to memory are the other two unavoidable processes involved in both types of lying task w.r.t their truth-telling counterpart.

Based on the above review of the existing methods, it can be concluded that the existing methods for lie detection still suffer from various reasons for lack of feasibility to be utilized in real-life scenarios, and therefore, new methods should be open-mindedly proposed and evaluated in exploration of more feasible methods.

2.7 Specifying the research topics that merge the research gap

This thesis takes an initiative in several aspects in deception research, and can be summarized as below points:

- (1). Most previous deception studies focused on the effect of deception types on brain activities such as instructed/spontaneous lying, lying about self- and other-referential information, and memorized/created lying. Few cast attention on lying about

experienced/un-experienced events. This thesis thus will discuss the theoretical study on lying about experienced/un-experienced events.

(2). The underlying neural mechanisms were not associated with any specific neuro-anatomy in the brain by the previous EEG studies, making it challenging to interpret the neuropsychological implication behind the condition differences. Source localization technique has been employed in this thesis at several chapters which seek to elucidate the underlying neural substrates that contribute to the distinguished neural activity between lying and truth-telling measured by EEG.

(3). Previous studies, regardless of signal modalities (EEG/fMRI/fNIR), have never taken any initiative to investigate into the underlying functional networks associated with the deception process, given the daunting fact that deception is such a complicated and largely unknown phenomena. This thesis has made some preliminary contribution to unveil the functional networks associated with the deception process, by selecting a cleaner data segment bearing more or less predictable neuro-psychological processes with the adoption of a network analysis method. This is also a piece of work for the first time investigated into the window prior to the deception process, (i.e. the stimulus delivery period- SDP), thus providing additional coverage of the complete deception processes.

(4). The majority of previous studies have investigated deception from the perspective of a liar. Little attempt has been taken to look into the distinguished neural features from the perspective of an innocent due to the conventional way of understanding that telling-truth is a default mode of the brain which makes deception a more salient and distinguished state. However, just by making use of the innocents' default mode neural responses towards

‘trustful’ and ‘doubtful’ feedbacks, interesting innocent neural correlates were found which can be potentially used to indirectly identify the liars.

In summary, the identification of the research gap is the major driver of all the research work underlying this thesis. To recognize these gaps drives the thinking and finding of more ways of looking at deception which helps complementing our understanding of neural mechanisms underlying this multi-faceted complicated phenomenon.

CHAPTER 3

EXPERIMENTAL PROTOCOLS

ESTABLISHED IN THIS THESIS

This research has carried out 3 different experiments in order to verify the effectiveness of the proposed methods applied in the corresponding protocols. This chapter gives an overview of the methodologies/protocols proposed in this research. The experiment designs used in this research and the data collection procedures used in the experiments are described. This chapter has described three different types of protocols, and each protocol has its respective novelty. The experimental design is mainly driven by the hypotheses and developed based on some existing well-established protocols to customize the verification purpose of the new hypotheses.

The first and second protocols investigated two types of deception scenarios, i.e. lying with prior experience (WE) and without prior experience (NE). Both of the first and second protocols investigated the period prior to the execution window of deception in two types of deception scenarios in each task, i.e. with prior experience vs. without prior experience in the first task and instructed lying vs. spontaneous lying in the second task. These two

experiments share similar experimental design except that the questions (stimulus) used in each of the experiments are different. The purpose of designing these two different experiments is to investigate in depth whether different types of lying tasks would present different neural correlates. Deception in real life can be complicated by the diverse scenarios of deception. To identify the potential categories of deception can facilitate relevant neural scientific research, from which promising neural correlates/mechanisms can be well investigated which in turn serves future practical application when applicable features have been identified. The third protocol investigated subjects' neural responses to doubtful/trustful feedbacks as a liar or innocent. Different from previous studies, the protocols proposed in this thesis explored the windows outside the deception execution window.

3.1 Deception tasks for experiment I and II

3.1.1 Experiment design and protocol

This section concerns about the explanation on the experimental design for experiment I and II. The experiment I contained four blocks, among which two belong to the WE task (instructed lying: IL, instructed truth-telling: IT), which are related to autobiographic declarative/episode questions. The other two blocks belong to the NE task, which require subjects to fabricate lies for non-experienced events. The experiment II also contained four blocks, with the first two blocks contributing to the instructed lying and instructed truth-telling tasks (I) and the other two contributing to spontaneous lying and spontaneous truth-

telling tasks (S) on autobiographic memories. In each experiment, the four blocks were separated by 10-min breaks. The sequences of the four blocks were randomized across all of the subjects, and the sequences of the questions were randomized within the block. The question pool with 50 questions/condition in each experiment were pre-screened by 15 volunteers (non-subject undergraduate students with similar population characteristic as the subjects) to score the understandability of each question into 4 levels (i.e. very easy-1, easy-3, moderate-difficult-5, very difficult-7). Understandability is a subjective score that measures how difficult it is for the volunteers to understand a particular question by asking the question once with the same speech rate. Examples were provided in advance as customized calibration for each subject to know which level a particular question should fall into. After ranking the questions according to the understandability score, 25 questions with the lowest mean score were selected for each condition. In fact, the selected questions have been tested non-significantly different between the lying and the truth-telling conditions in understandability in experiment I: (paired t-test: $p=0.75$ for WE, and $p=0.82$ for NE); in experiment II (paired t-test: $p=0.74$ for I, and $p=0.73$ for S) and question length in experiment I: (paired t-test: $p=0.78$ for WE, and $p=0.76$ for NE); in experiment II (paired t-test: $p=0.85$ for I, and $p=0.66$ for S). The short-listed questions also share a similar time-window between 2.2s-2.7s. In addition, prior to the experiment, subjects were instructed to give up the trial during the experiment by pressing a specific button if they cannot understand the question correctly. Truthful answers for all of the questions in the WE/I task were acquired in a pre-experiment investigation one week prior to the experiment for monitoring purposes during the experiment. The NE task mimics an interview scenario in

which the questions are related to working experience in a target field (i.e., oil exploration) where none of the participants had prior experience. A pre-experiment survey was conducted on the spot to ensure that all subjects knew the terms that would be covered during the ‘mock interview’, and the subjects were instructed to pretend to be an experienced job candidate by lying when answering the questions for which they had no experiential knowledge.

The procedure in each block in both experiments followed the same sequence (see Fig. 2). Each trial was initiated with a fixation period (3 s), after which an auditory stimulus was delivered to the subjects for 2.2-2.7s. After the subjects provided an answer to the questions, a ‘mentalization’ phase lasting for 5 s was added. This was triggered manually in the experiment by attending to the subjects’ verbalizations indicating the completion of an answer. The brain activities during this phase are not within the scope of this study. After this phase, an auditory judgmental sentence with a varying degree of trust (i.e., believe/don’t believe/suspicious) was delivered to the subject and was simultaneously accompanied by a visual image of an interrogator in order to enhance the subject’s sense of reality in the experimental environment. The judgment was converted to an accumulated score with a deduction of 10 points for a judgment of lying, a deduction of 5 points for a judgment of a suspicious answer, and an addition of 10 points for the judgment of a lie as the truth. All updates were presented at the end of each trial, but the accumulated score was not reported to the subjects until the end of the experiment to avoid direct emotional interference imposed by the current score during the experiment. The ISI (inter-stimulus

interval) varied from 3000 ms to 3500 ms; this length was used to avoid emotional effects caused by the procedure of the previous trial (Asma 2008).

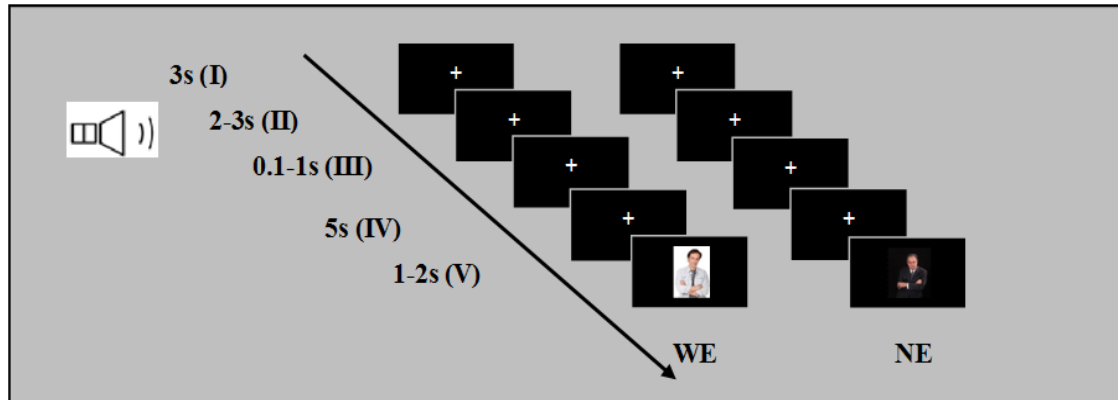


Figure 2 The IL and IT conditions for both the WE and the NE tasks share the same schematic procedures: (I) fixation phase; (II) attending to auditory question; (III) answering phase; (IV) mentalization phase; (V) feedback phase, except that the visual images accompanying the auditory feedbacks were different in the two tasks to match the specific contexts.

3.1.2 Instruction protocol

In both two experiments, the subjects were informed prior to the experiment that they would be given a maximum of \$50 once they successfully finished all of the blocks and that the actual reward would be adjusted based on the score achieved. However, if the frequency of the detected lies reached a pre-determined value in the lying block, they would receive only \$25. This financial punishment helps to prevent low attention levels and effortless lying by the subjects. The subjects were required to answer as quickly and concisely as possible, but not to compromise the quality of the answer. To further engage the subjects' attention, they were informed that each answer was judged by an experienced interrogator who did not know if they would tell lie or truth beforehand and monitored the

answers in another room by receiving video and audio information from the experiment room. However, the actual judgment was manipulated based on a decision made by the experiment operator in the experiment room who knew the truthful answers and was monitoring the experiment via video and the verbal responses from the subjects. Additionally, the decision strategy for the judgment was integrated with a random effect to produce a 40% to 50% (true positive) chance of detection when the subjects were lying, and the misjudgment of truthful answers as lies was maintained below 20% (false positive). Feedback being used in this experiment is mainly because that the type of lying tasks under investigation intrinsically involves incentives and potential risk. Without such feedbacks, subjects' perception of their ongoing behavior (i.e. lying/telling-truth) could be different and the relevant awareness of being a liar/innocent would be weakened since their action is not associated with any consequence. The numbers picked up for chance of detection and false positive rate mainly serve the purpose to make the interrogator 'appears' with reasonably overall accuracy, and therefore helps maintain subject's realistic feeling with the role of the interrogator and maintain their attention focus on the ongoing task. Furthermore, this detection rule was not informed to the subject. Instead, subjects were informed that each feedback was given based on the information captured (e.g. video and verbal response) during the particular trial. To familiarize the subjects with the experiment procedure, they were provided with a training session with 10 sample questions for each condition, and they were required to repeat the rules to the operator to ensure that they fully understood all of the instructions.

3.2 Deception task for experiment III

3.2.1 Stimuli

In this study, the protocol based on custom inspection setting was modified from an original paradigm (Seth, Iversen et al. 2006) and was contextualized locally by mirroring the inspection targeted items classified in Singapore's custom procedures (Customs 2013). The number of the targeted items have been expanded from four in the original study (Seth, Iversen et al. 2006) to twenty different items in three categories, in order to reduce the habituation effect caused by repeatedly showing the same items as well as to enhance subjects' awareness of being a liar/innocent throughout the whole experiment. These items essentially represent what the subjects would be 'carrying' as they attempt to pass through the customs (see Fig.7 for the item list) and these items were presented to them at the beginning of each block. Each category and its associated condition were introduced to them prior to the commencement of the experiment.

As shown in Table 3, the three categories of items are namely the 'Dutiable item', 'Prohibited item', and 'Allowed item'. Each item was assigned a punishment (\$P) and/or duty (\$D) value. These values were not specifically selected but served the purpose to have impact on the total amount of remuneration that subjects can gain from participation. All the items and their corresponding \$P/\$D were shown to the subjects prior to the experiment, and they were examined in a separate test to make sure enough familiarity to recognize the items during the experiment.

3.2.2 Instruction protocol

Subjects were briefed clearly prior to the experiment regarding the background story behind all the scenarios and conditions. The subjects were instructed not to declare but to smuggle the ‘Prohibited items’ all the time (i.e. instructed lying (IL) condition) while they were instructed to declare all the ‘Allow items’ (i.e. instructed truth-telling (IT) condition). To make these two item categories more distinguishable, prohibited items such as firearms were employed for the IL condition while neutral items were used for the IT condition (see Fig.7). Heavy punishment would be incurred if the subjects would be detected carrying one of the ‘Prohibited items’, while there is a nominal small amount of charge for declaring ‘Allow item’. On the other hand, the dutiable items were employed for the spontaneous lying/truth-telling (SL/ST) conditions. In this condition, subjects were assigned a quantity of two units for each item and had the freedom to choose to smuggle 1 unit (i.e. SL) or declare the full quantity (i.e., ST). On average, subjects were required to tell lie and the truth for half of the total stimulus for the spontaneous lying condition (Seth, Iversen et al. 2006). Each subject was given an initial amount of money \$150.00 which could decrease if they are caught smuggling or when they choose to pay duty for honest declaration. They were instructed that their aim in the task is to keep as much money as possible at the completion of the task.

3.2.3 Experimental design

All the participants were requested to sit at a fixed distance away from a computer screen, and they were comfortably seating in a quiet room with controlled temperature at 25°C. The stimuli item was approximately 12cm (width) ×10cm (height) in size. A program developed based on the Presentation® (Neurobehavioral Systems, Inc., Albany, CA) software was used for stimulus delivery. The subject had to undergo a total of 6 blocks, and each block had both the SL/ST and the IL/IT conditions with mixed pseudorandom sequence of Dutiable, Prohibited item and Allowable items. There were total 320 trials that each subject would undergo for the whole experiment. The specific number of trials used in each condition is included in Table 2. As shown in Fig.5, each trial begins with a visual fixation (3.0s), followed by a visual presentation of the stimuli (1.0s) together with a probe question ‘Are you going to declare this item?’ indicating that subjects can start to respond. Subjects were instructed to make their responses as quickly as possible but without hurrying and they must verbally speak out their responses while simultaneously pressing a button associated with an answer. A visual presentation of the feedback with a ‘STOP, CHECK!’ or ‘GO!’ sign (see Fig.6) indicating doubt or trust (2.0s) was delivered to the subject after their response. As shown in Fig.6, each doubtful or trustful feedback consists of three components in a single graph, with the top half of the picture showing a custom scenario, as well as the bottom half of the picture showing a ‘stop check’ or ‘go’ sign and at the middle line showing either a ‘doubtful feedback’ sentence mimicking the real-life situation where custom officers are announcing their suspiciousness to the passenger or a ‘trustful feedback’ sentence mimicking the real-life situation when the custom officers tend to trust the passenger. Similar to the instructed lying task, feedback used in the spontaneous

lying task also consists of three components except that the top half of the picture shows a permission sign and the bottom half of the picture shows a 'duty charge' sign, with the middle line showing 'Please pay your duty before entry'. The 'trustful' feedback essentially was no checks and implied a freedom of pass for that item. For trials that involved 'doubtful' feedback, the subjects had to symbolically go through a checking phase lasting for 5s, during which a word 'CHECK' was presented on the screen. Two types of checking statements were employed in this study, one was for the SL/ST condition and the other was for the IL/IT condition (see in Table 4). Within each set, the statements had two levels of 'suspicion', each with four variations of statement (Table 4); this was designed to avoid repeating the same level of suspicion that could lead to the subjects' habituation towards the same feedback. For trials that involve checking, the eventual checking result for that trial was announced together with the updated current points. This 'announcement' segment was of primary importance as the showing of the subjects' updated points would ensure their continued engagement in their task. Lastly, the ISI (inter-stimulus interval) varied from 3000 ms to 3500 ms. This length was used to avoid emotional effect caused by the procedure of the previous trial (Asma 2008). A trial run was conducted prior to the experiment for the subjects to familiarize themselves with the task. They were allowed a resting period for 10 minutes in between each block.

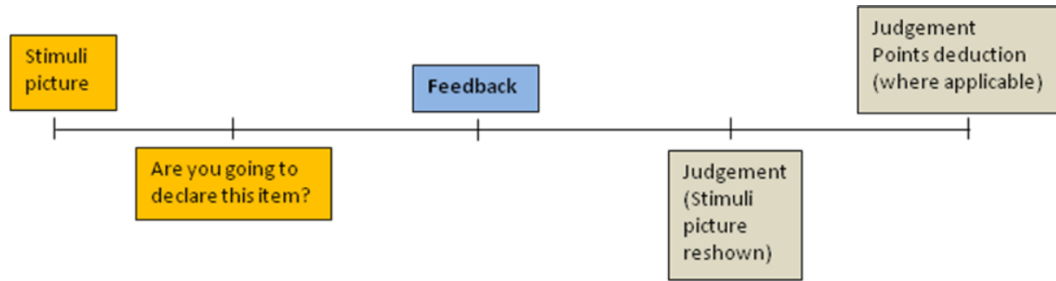


Figure 3 Timeline showing the different component and their sequence in a trial.

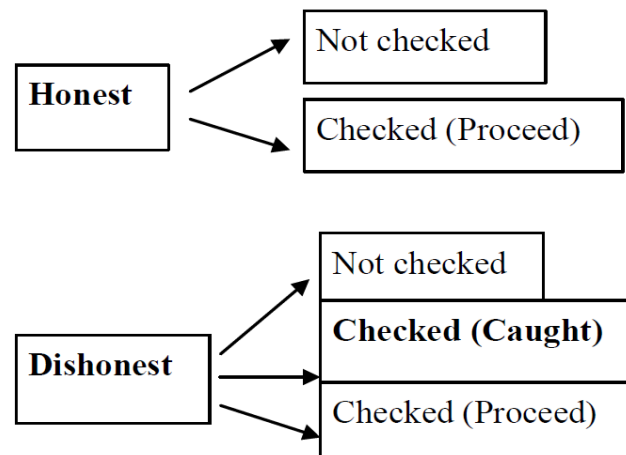


Figure 4 The structure of all the conditions involved in experiment III.

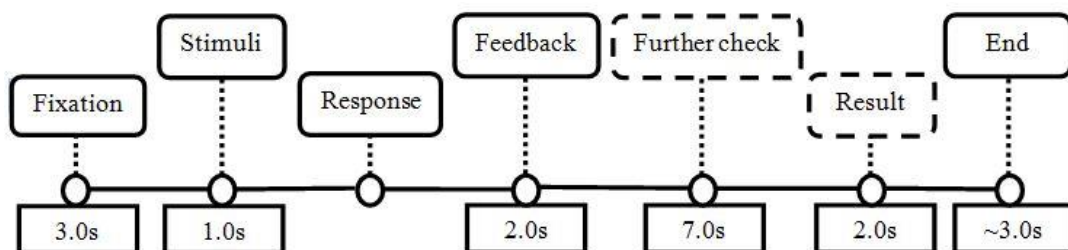


Figure 5 Schematic demonstration of the timeline for a single trial in the experiment. The steps with dashed rectangular only appeared for trials that involve doubtful feedback which triggers further check on subject's response, after which a result announcement was delivered. The steps without dashed rectangular appeared for trials that involve only trustful feedback. The time spent on each step was listed below its corresponding step.



Figure 6 The feedback stimuli used in the experiment. An example of (a).doubtful feedback and (b).trustful feedback in the instructed lying/truth-telling task (c). trustful feedback in the spontaneous lying/truth-telling task (d). the negative result feedback that indicates a punishment for detected lying in both the instructed and the spontaneous lying tasks.



Figure 7 The item categories that the subjects would encounter in each block. The label '2' indicates that the subjects are carrying 2 units of one of the items at one time, and they can cheat by declaring '0' or '1', or tell the truth by declaring '2'; the label '×' instructs that the subjects are carrying 1 unit of one of the illegal items at one time, and the subjects have

to cheat by declaring none; the label ‘√’ instructs that the subjects are carrying 1 unit of one of the permitted items at one time, and the subjects have to tell the truth.

Table 2 Number of trials per condition (spontaneous lying/truth-telling condition has a reported average number of trials since the real number of trial is dependent on the frequency of lying/truth-telling by the subject in the experiment, and they are constrained to be roughly the same)

Conditions	Feedback	Judgment	Probability	Trials
Duitable Items	Trusted	Positive	50%	40 in average
(SL condition)	Checked	Negative	25%	20 in average
	Checked	Positive	25%	20 in average
Duitable Items	Trusted	Positive	50%	40 in average
(ST condition)	Checked	Positive	50%	40 in average
Prohibited Items	Trusted	Positive	50%	40
(IL condition)	Checked	Negative	25%	20
	Checked	Positive	25%	20
Allowed Items	Trusted	Positive	50%	40
(IT condition)	Checked	Positive	50%	40

Table 3 Punishment and Duty values for the different items.

Duitable Items	\$P	\$D	Comment
Alcohol Cigarettes Phones & Tablets Laptop	-28 ¢	-14 ¢	Punishment is higher than duty
Allowed Items Currency Jewellery Watches	-0 ¢	-1 ¢	Nominal fee for declaring these items

Table 4 The sentences used in the doubtful feedbacks for instructed lying/truth-telling and spontaneous lying/truth-telling conditions respectively.

Instructed Lying/Truth-telling	Spontaneous Lying/Truth-telling
We think you must be a liar	We think you are hiding extra units
We think you're carrying illegal items	We think your item declaration is fake
We think you're smuggling illegal items	We think you reported a fake number
We think you must be cheating	We think you cheated in declaration

3.3 Participants

Sixteen right-handed university students (8males, 8 females) with mean age of 22.5 years (SD=4.5) have been recruited at the National University of Singapore and participated in the first and the second experiments. The third experiment has recruited nineteen right-handed university students sharing similar population property. All the subjects underwent a detailed health questionnaire before admission for participation. Their hearing ability and English proficiency were evaluated for participation. Only those with no current or previous history of neurological or psychiatric disorder or alcohol and drug abuse were selected to participate in the English proficiency screening, and only those whose English proficiency are satisfactory were finally selected to participate in this study. Each subject was given a detailed explanation of the experimental procedure and each signed a consent form prior to the experiment. The study was approved by the National University of Singapore Institutional Review Board (also referred to as the Research Ethics Committee in some countries), which requires all experiments to comply with all relevant laws and regulations in Singapore.

3.4 Data acquisition and Pre-processing

EEG signals were collected with an EEProbe recording system (Advanced Neuro Technology (ANT) Enschede, The Netherlands). The EEG cap with 64 Ag/AgCl electrodes was placed on each participant's scalp according to the 10/10 system of electrode placement. Impedances for over 98% of the electrodes were maintained below 20 kOhm

as shown in Fig.9 (Brodbeck, Spinelli et al. 2011). The sampling frequency was 250 Hz, and the common average served as the recording reference (Ludwig, Miriani et al. 2009). Presentation® software (Neurobehavioral Systems, Inc., Albany, CA) was used to control the timing of the events in each trial. The auditory stimuli were prepared prior to the experiment using Ivona Reader software (IVONA® Software, Poland), which transforms text information to standard auditory stimuli, which were delivered to the participants through an earphone. To minimize the variation between the stimuli, the speed and intensity of the auditory stimuli were constant for all of the questions. During the experiment, the participants were comfortably seated in a quiet room with a controlled temperature of 25°C. A computer screen was displayed in front of the subjects with a fixed viewing distance of 80 cm (Fig.8). A webcam was mounted on the top of the computer screen for online video recording, which enabled the experiment operator to provide a trial-based decision to the trial. This operation could not be detected by the participants. An electromyography (EMG) signal was simultaneously recorded with an electrode that was attached to the subject's face, and the location was found to not interfere with speaking. This signal was used to determine the onset time of the verbal response. An electrooculography (EOG) signal was simultaneously recorded using two Ag/AgCl electrodes placed on the vertical midline of the right eye above the eyebrow and approximately 1 cm below the lower lid. In the off-line analysis, the signals were band-pass filtered at 1-30 Hz. The EOG and EMG artifacts of the collected EEG data were removed using open-source artifact removal software (Gómez-Herrero 2008), with the application of independent component analysis (ICA) algorithms, i.e. canonical correlation

analysis (CCA) as a blind source separation technique for EMG removal (De Clercq, Vergult et al. 2005) and sobi for EOG removal (Gomez-Herrero 2006) for each individual trial. Since band pass filtering, EOG and EMG removal were applied simultaneously to de-noise the data, only a few trials still produce noisy data after de-noising (might be caused by subject's body motion at some trials) and have to be discarded. Thus, a minimum of 22 and a maximum of 25 valid trials were collected for each condition (condition WE-IL: mean: 24.43, variance: 1.06; condition WE-IT : mean: 24.50, variance: 0.80; condition NE-IL: mean:24.44, variance: 0.80; condition NE-IT: mean: 24.50, variance: 0.53; condition SL: mean 24.32, variance: 0.58; condition ST: mean: 24.32, variance: 0.64), which approximates the starting trial number (i.e. 25) for time-frequency analysis as suggested by (2009). Moreover, this study adopted frequency domain connectivity analysis, with 2s per trial altogether providing 44-50s data length per subject, which should render reasonably accurate estimation with the employed estimator given the fair signal-to-noise ratio (SNR) after the de-noising procedures (Astolfi, Cincotti et al. 2007).



Figure 8 Scenario showing experimental setting during the EEG recording.

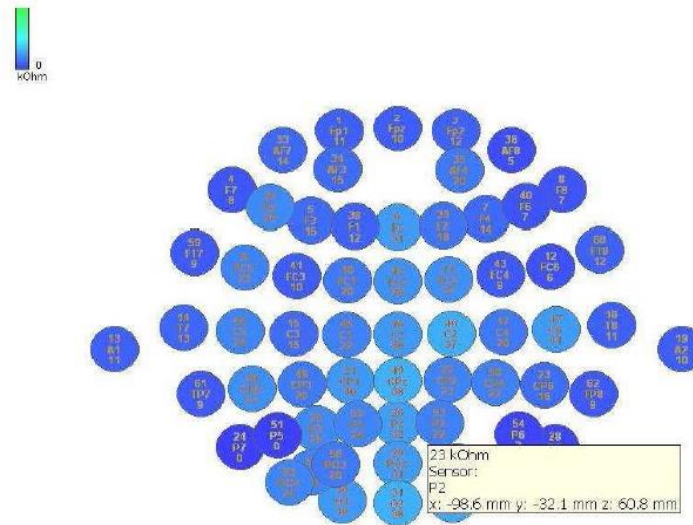


Figure 9 Topography showing the distribution of electric impedance across the whole head. The darker the blue color, the lower the impedance. Each electrode was guaranteed to have impedance below 20k Ohm.

3.5 Concluding Remarks

This chapter has described three different types of protocols, and each protocol has its respective novelty. The experimental design is mainly driven by the hypotheses and developed based on some existing well-established protocols to customize the verification purpose of the new hypotheses. The first protocol investigated two types of deception scenarios, i.e. lying with prior experience and without prior experience. The second protocol investigated the period prior to the deception action in two types of deception scenarios, i.e. instructed lying and spontaneous lying. The third protocol investigated subjects' neural responses to doubtful/trustful feedbacks as a liar or innocent. Different from previous studies, the protocols proposed in this thesis explored the windows outside

the deception execution window. However, the new experimental protocols and data analysis methods proposed in this thesis are not claimed to be better than existing technologies. Or rather, the features identified by the proposed methods can complement all the existing lie detection technology as an independent feature or one of the integrated features.

CHAPTER 4

HUMAN ELECTROENCEPHALOGRAPHY - BASED SOURCE LOCALIZATION METHOD TO STUDY VARIOUS DECEPTION TASKS

In this chapter, two experiments were carried out to study whether electroencephalography (EEG) could distinguish between (1) instructed lying processes and their corresponding truth-telling processes; (2) instructed lying (truth-telling) and spontaneous lying (truth-telling) conditions. In the first experiment, two types of instructed lying (IL) tasks differentiated by subjects' own authentic experience and fictional experience were investigated on sixteen subjects. One task required the subjects to deceive on autobiographic information for which they have prior experience (WE: with prior experience) and the other required the same subjects to deceive on working experience in a target field where they in fact have no prior experience (NE: no prior experience) in a mock interview scenario. In both deceptive tasks, subjects were instructed to lie to all the questions in the lying block and tell the truth in the truth-telling block. In the second experiment, under the same category of deception on autobiographic memories (with prior

experience), two types of deception were studied. One task required the subjects to deceive and tell the truth in an instructed way. The other task required them to provide spontaneous answer to the probe question, i.e. by either lying or telling the truth based on their own decision. To elicit ecologically valid situation, the lying tasks involved greater monetary reward and higher risk of punishment compared with truth-telling tasks. The EEG data were analyzed based on frequency-domain source localization which provides higher resolution information on the underlying mechanism of deception. A more comprehensive and detailed understanding of neural mechanism and correlates for various types of deception is of great significance in real-life application of lie detection.

4.1 Introduction

It is noteworthy that most previous deception studies focused on the effects of deception types on brain activities such as instructed/spontaneous lying, self-referential/other-referential lying, memorized/created lying (Ganis, Kosslyn et al. 2003) and there is little attention cast on lying about experienced/non-experienced events except Ganis et al.(2009) and Abe et al.(2006). The former study investigated neural correlates for self-relevant and other-relevant deception which identified several brain registration areas responsible for such agent effects (Ganis, Morris et al. 2009). In the other fMRI study (Abe, Suzuki et al. 2006), subjects were asked to experience 20 real-world events using one implement per event in the experience phase. By presenting pictures of the stimuli from a stimuli pool mixed by 20 new (subjects have not experienced) and 20 old stimuli (subjects have experienced) on the screen, subjects were instructed to tell lies/truths on events they have

either experienced or not by answering ‘I know’ or ‘I don’t know’. This fMRI study considered both experienced and non-experienced events in the deception task; however it recruited neural circuits from no more than recognition memory and inhibition control since no new information need to be generated. In the current study, as an extension to the design in which instructed lies were elicited from participants based on their autobiographic information (Lee, Liu et al. 2002, Abe, Suzuki et al. 2007, Sartori, Agosta et al. 2008), the novel NE (no prior experience) paradigm was also investigated on the same group of participants by instructing them to cheat on non-experienced events. It was hypothesized that the main difference between these two instructed lying tasks in the aspect of cognitive process is, the WE (with prior experience) task should be dominant by inhibition related execution control process while the NE task involves mental imaginary activities and a decreased level of self-referential processing. In this study, commonalities and differences between these two instructed lying tasks were explored. In the second study, instructed lying/truth-telling task was compared against spontaneous lying/truth-telling task, and distinguished neural substrates were found for lying against truth-telling conditions in both tasks. To study on the neuro-anatomies allows inference of the neuro-psychological processes involved in these various types of lying tasks which may potentially complement our understanding of neural mechanisms underlying deception.

EEG and simultaneous EEG/fMRI studies have corroborated the role of alpha-band oscillation (upper alpha) in working memory tasks especially localized in occipital areas which reflects working memory maintenance or active inhibition of task-irrelevant areas (Michels, Moazami-Goudarzi et al. 2008, Michels, Bucher et al. 2010). According to

(Klimesch 2012), the role of event-related synchronization (ERS) can be generalized to serve an inhibitory as well as information processing function which are closely linked to two fundamental functions of attention, i.e. suppression and selection. The classical view holds that suppression of alpha-band event-related de-synchronization (ERD) activity is the ‘typical’ event-related response indicating activation of cortical areas while alpha-band ERS activity marks cortical areas at rest or in an idling state with task-irrelevant processing (Pfurtscheller 1992). Nevertheless, increasing recent evidences suggest that alpha-band oscillations have an inhibitory function and ERS rather than ERD would have to be considered the ‘active’ task-engaging alpha-band response (Klimesch 2012). For example, alpha enhancement was observed over visual area during a motor task (Jeon, Nam et al. 2011, Müller and Anokhin 2012), or during a visual task over a sensori-motor region (Pfurtscheller 1992), and memory task (Krause, Sillanmaki et al. 2000).

In summary, EEG is a promising tool to study deception which provides information generated by the central nervous system. Previous studies suffer from various shortcomings for real-life application, i.e. either due to low accessibility or lack of specificity. Even EEG-based studies did not provide neuro-physiological basis for the genesis of EEG signals for deception. In addition, previous studies for instructed lying might have only considered limited possibilities, i.e. creating lies for events experienced by/known to the subjects, and therefore is not comprehensive enough to cover real-life possible instructed lying scenarios. To address these issues, 1) method with higher resolution was employed in the source space with the help of frequency domain EEG source localization, with which neuro-physiological basis of deception can be studied; 2) a new protocol was developed which

considers lying about events non-experienced by the subjects and induces subjects to fabricate lies about the event.

4.2 Data analysis

The neural modulation effects by the various conditions were analyzed through frequency domain source localization analysis which provides resourceful information on regional brain activities underlying deception. Standardized low-resolution brain electromagnetic tomography (sLORETA) (Pascual-Marqui 2002) was used to compute the estimated intracerebral electrical sources current density (A/m^2) that contribute to the scalp EEG. The source solution space consists of 6,239 voxels (each voxel with dimension $5 \times 5 \times 5$ mm), and is restricted to the cortical gray matter and hippocampi. The whole space was defined according to MNI atlas (Mazziotta, Toga et al. 2001).

sLORETA is a well-recognized inverse solution technique that estimates the distribution of the standardized electrical current density by normalizing the voxel's estimated electric current density over its expected standard deviation in the three-dimensional space and is reported to have zero-localization error in non-noise and even with-noise conditions (Pascual-Marqui 2002). sLORETA is most suitable for calculation of distributed cortical sources or limited amount of focal cortical sources with distinct field, given the low spatial resolution of this technique (Wagner, Fuchs et al. 2004). Therefore, sLORETA is most likely a suitable source localization method for estimating sources in the frequency domain based on spontaneous EEG that involves widespread contributing sources. Several

previous studies with different research topics have employed this LORETA/sLORETA for source analysis (Mulert, Jager et al. 2004, Zaehle, Frund et al. 2009, Shao, Shen et al. 2012). Technically, sLORETA computes three-dimensional linear solutions for the EEG inverse problem within a head model co-registered to the Talairach probability brain atlas and viewed within MNI at 5mm resolution (Mazziotta, Toga et al. 2001). According to (Pascual-Marqui 2002), the inverse problem can be formulated as follows,

$\boldsymbol{\phi} = \mathbf{K}\mathbf{J}$, $\boldsymbol{\phi}$ represents the electrical potential measured on the scalp, \mathbf{J} represents the electrical current density generated from the voxels, while \mathbf{K} represents the lead field matrix that establishes the physical volume conduction relation between the primary current source and the electrical potential measured from the electrodes. The target function to be addressed can be formulated as $\mathbf{F} = \|\boldsymbol{\phi} - \mathbf{K}\mathbf{J}\|^2 + \alpha\|\mathbf{J}\|^2$, the real solution is the one that minimizes the target function which physically means the best solution is the one that can minimize the energy of the system (the smoothest solution that best approximates the measured electrical potential). The solution therefore can be formulated as $\hat{\mathbf{J}} = \mathbf{T}\boldsymbol{\phi}$, with $\mathbf{T} = \mathbf{K}^T[\mathbf{K}\mathbf{K}^T + \alpha\mathbf{H}]^+$, and $\mathbf{H} = \mathbf{I} - \mathbf{1}\mathbf{1}^T/\mathbf{1}^T\mathbf{1}$. Here \mathbf{H} is an average reference operator. The variance of the electrical current density S_j can be represented as $\mathbf{T}\mathbf{S}_\phi\mathbf{T}^T = \mathbf{K}^T[\mathbf{K}\mathbf{K}^T + \alpha\mathbf{H}]^+\mathbf{K}$. Therefore, the variance of the electrical current density consists of two components: variance of the actual source, and variance due to noisy measurement. Finally, the solution of sLORETA corresponds to $\hat{\mathbf{J}}_l^T\{[\mathbf{S}_j]_{ll}\}^{-1}\hat{\mathbf{J}}_l$. This solution also mimics the pseudo-statistic which has the form of an ‘F’ statistic. Compared with other minimum norm inverse solutions, this solution provides more robust estimation which also captures deep

source activity with least bias. As such, the power of each voxel at frequency f is $\left[\frac{\hat{J}_l}{[S_j]_{ll}}\right]_f$, called standardized power spectral density for voxel l .

The integrated power spectral density of each voxel was calculated in six standard frequency bands ('delta': 1-4Hz; 'theta': 4-8Hz; 'alpha1/lower alpha': 8-10Hz; 'alpha2/upper alpha':10-12Hz; 'beta1':12-18Hz; 'beta2': 18-30Hz) in the source space (Canuet, Ishii et al. 2011). In this study, frequency domain source localization was followed by event related synchronization (ERS) computation based on power spectral density calculated for the stimulus period and the baseline period, i.e. the ERS was computed for the first 2s of the stimulus existent period (auditory question) relative to the last 2s of the fixation period as baseline. A fixed frequency resolution of 0.4883Hz was utilized for the analysis. The results from sLORETA computation for the paired-conditions in each task were further analyzed by multiple voxel-by-voxel comparisons using a non-parametric permutation test(with 5000 randomizations) with the maximum-statistic (Nichols and Holmes 2002) adopted to adjust for multiple comparisons. The application of source localization method in this study is justifiable. Despite the fact that the complete network of sources underlying deception/ truth-telling are widespread and extremely complicated to be fully investigated, the application of source localization in this study is not used for addressing this problem. Similar to the most of the fMRI studies for deception, only neural substrates with significantly different neural activity levels between the IL/SL and the IT/ST conditions could be identified. Such comparison makes the sources to be identified limited to several key sources which demonstrate highest distinguishability and this is then

addressable by source localization technique together with the paired t-test. On the other hand, the complete neural mechanisms underlying deception is not fully known yet and there is no existing EEG-based database or deception neural anatomy models to be referred to or used for comparison. Most of the source localization study for deception is based on protocol designs that are supposed to elicit deceptive/truthful responses from the subjects and the source results are dependent on the particular experimental protocol employed. Cross validation by other similar EEG studies therefore play an important role in EEG-based source localization study for deception. This study has not addressed the database issue for deception which requires big data resources for further data mining.

For the behavioral data, response times for each condition were extracted based on the filtered EMG signal (band-pass: 1-15Hz) recorded from a separate EMG channel.

4.3 Results

4.3.1 Behavioral data for experiment I and II

All the subjects successfully completed the experiment with acceptable performance by following the instructional rules to tell truth or construct lies in the corresponding block and their responses were concise. Average response time was obtained from EMG signals for each subject in each condition. Significantly longer response time was found in the IL condition relative to the IT condition in the WE task as shown in Fig.10(a); and significantly longer response time was found in the IL condition relative to the IT condition in the NE task as shown in Fig.10(b). To summarize, both of the two deceptive tasks are

associated with longer response time. This result is consistent with previous findings and can be explained by the longer time spent on generating deceptive answers by adding extra component to the known truthful answers (Vendemia, Buzan et al. 2005). On the other hand, there is no significant difference in response time between the SL and the ST conditions as shown in Fig.11(b). It can be understood that in both the SL and the ST conditions, subjects will spend the majority of time on decision making, with the remaining time spent on preparing for answers. The component of decision making that takes the bulk of time leads to the insignificant response time between the two conditions.

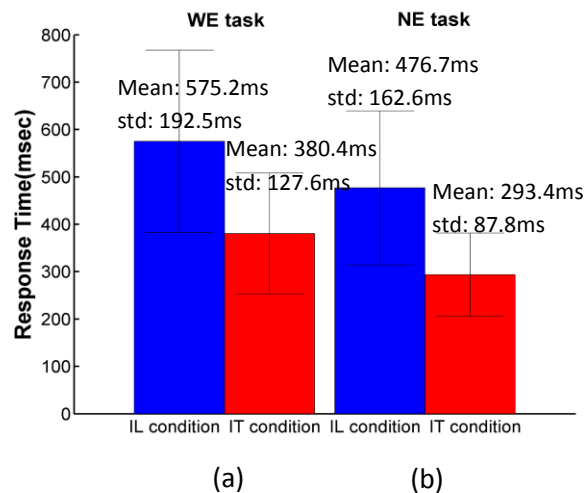


Figure 10 Response time statistics for the IL and IT conditions in WE task and NE task (unit: ms). Paired t-test shows significantly longer response time ($p < 0.05$) for the IL condition compared to the IT condition in the WE task; significantly longer response time ($p < 0.05$) was also found for the IL condition compared to the IT condition in the NE task.

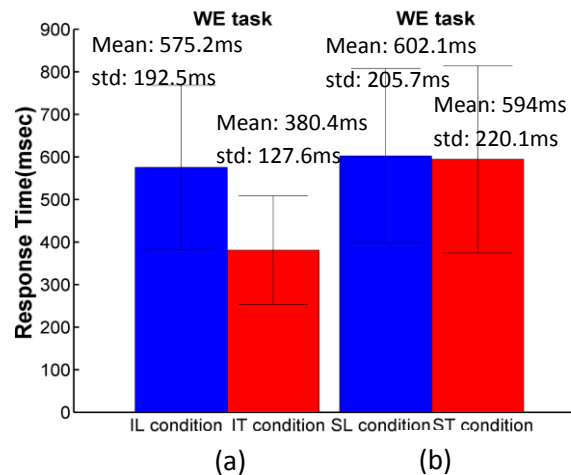


Figure 11 Response time statistics in IL task and SL task (unit: ms). Paired t-test shows significantly longer response time ($p < 0.05$) for the IL condition compared to the IT condition; there is no significant difference in response time found for the SL condition compared to the ST condition.

4.3.2 Source localization for experiment I and II

Source localization in the frequency domain was carried out in each condition, the voxels that survive the significant test between the lying and the truth-telling conditions with multiple comparison permutation test (corrected $p < 0.05$) are highlighted and these results are depicted in Fig.12 for the WE task, and in Fig.13 for the NE task, and in Fig. 15-16 for the spontaneous lying task. The detailed source information is demonstrated in Table 5-7 for these tasks respectively. Moreover, instructed lying with spontaneous lying, instructed truth-telling with spontaneous truth-telling are cross-compared with the same source localization method in order to study the differences that might lie in different types of lying and truth-telling conditions.

In the WE task, significantly increased ERS was observed in the lower alpha band in left inferior frontal gyrus and was also observed in the upper alpha band in cuneus while comparing the IL and the IT conditions (Fig.12). As compared with the instructed lying condition in the WE task, the same condition in the NE task seems to involve more regions. It can be seen from the source localization results as depicted in Fig.13 (a-c), increased delta band ERS in the lying condition was observed in several brain areas that are hemispheric-symmetrically distributed and largely overlapped with the regions associated with self-perception and self-consciousness processing networks. Moreover, Fig.13 (d-f) show that there are multiple occipital and temporal regions present significantly increased ERS in upper alpha band in the NE-IL w.r.t the NE-IT condition. In order to quantitatively present these ERS results, mean and standard deviation (std) was calculated for voxels that mark significant differences between the two conditions, and the corresponding results are presented in Fig.14 (a-d).

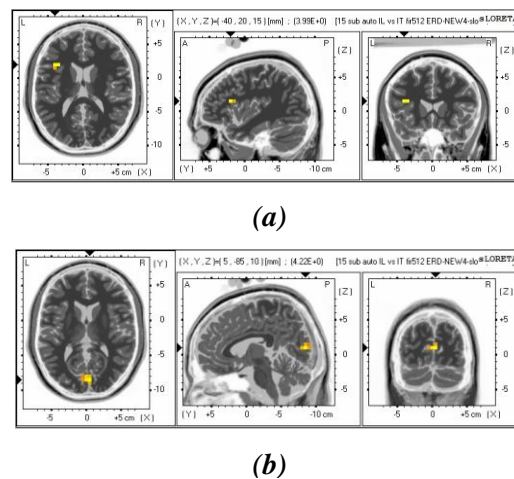


Figure 12 Frequency domain EEG source localization results indicate a significantly increased ERS (a) in the lower alpha band in left inferior frontal gyrus and insula as well as (b) in the upper alpha band in cuneus in the IL w.r.t the IT condition in the first 2s of the

stimulus presence, significant voxels (corrected $p < 0.05$) are highlighted with yellow and are color-intensity coded with t-statistics.

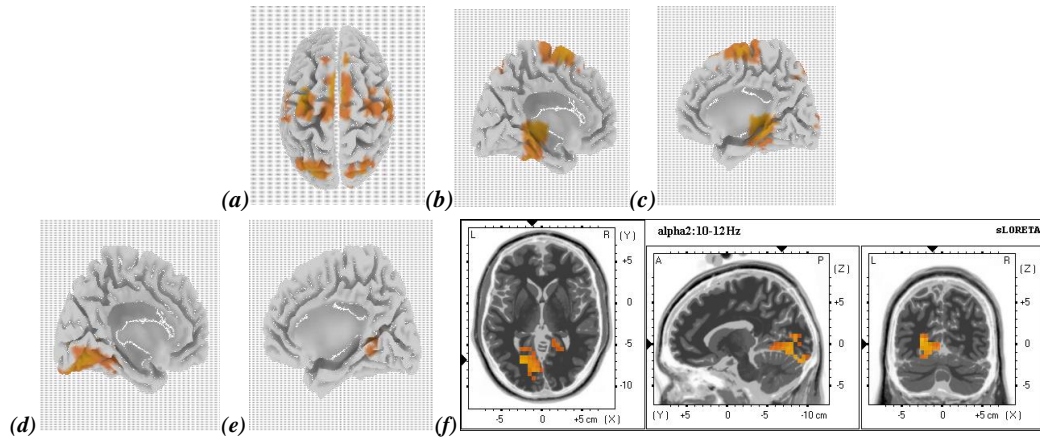
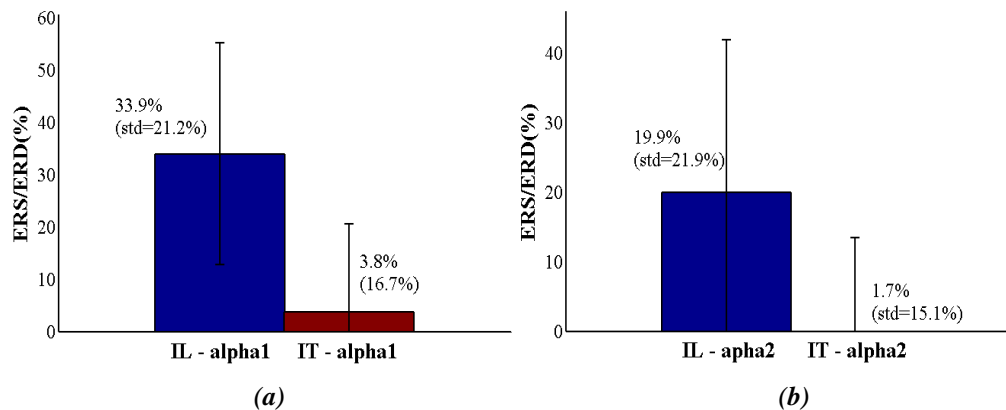


Figure 13 EEG source localization in the frequency domain indicates increased ERS in delta band in multiple regions of the brain in the NE-IL w.r.t the NE-IT condition in the first 2s of the stimulus presence. (a). transverse view; (b). left sagittal view; (c). right sagittal view. Results also indicate increased ERS in the upper alpha band in multiple regions of the brain (d-f), significant voxels (corrected $p < 0.05$) highlighted with orange are color-intensity coded with t-statistics (d). left sagittal view; (e). right sagittal view; (f). transverse, sagittal and coronal cross-sectional views are presented in sequence.



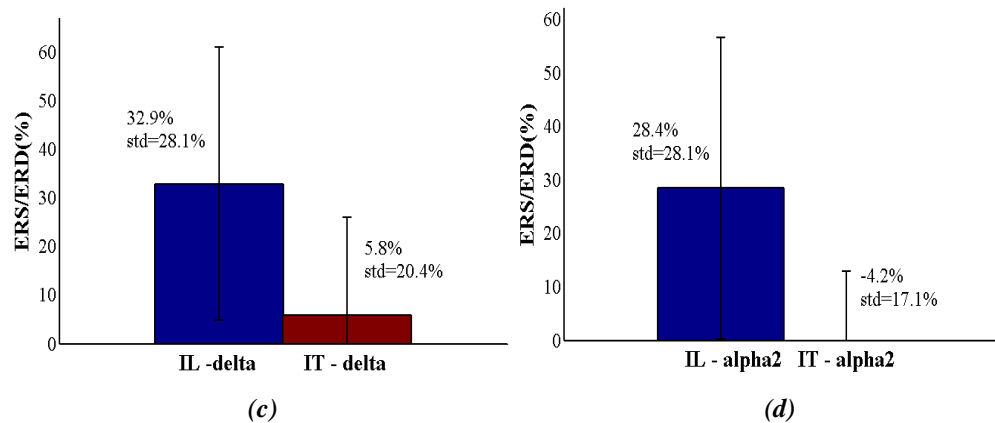
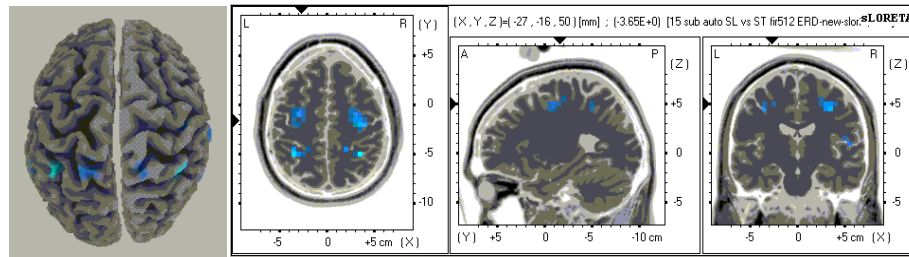
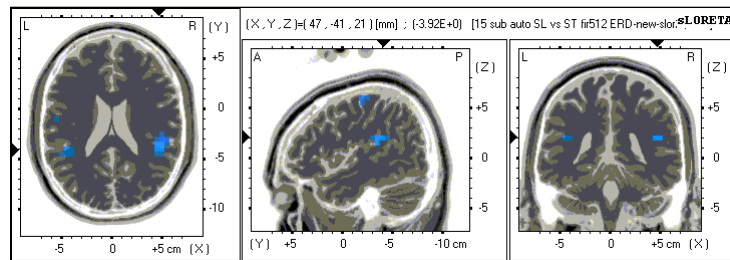


Figure 14 (a)-(d) show quantified ERS/ERD results in the IL and IT conditions in the WE task (a-b) and in the NE task (c-d) respectively. Mean and standard deviation for the ERS value calculated for voxels that present significantly increased ERS in (a). lower alpha band, (b). upper alpha band, (c). delta band, (d). upper alpha band.

In the SL-ST task, significantly decreased ERS in the lower alpha band was observed in the bilateral inferior parietal lobe, superior parietal lobe, precentral gyrus, precuneus, middle frontal gyrus, superior temporal gyrus, right postcentral gyrus and left inferior frontal gyrus while comparing the SL and the ST conditions during the first 2s presence of the stimulus (Fig.15 (a-b)). It is also found for the last 2s presence of stimulus that lower alpha band ERS is significantly higher in cuneus and precuneus in the SL w.r.t the ST condition (Fig.16). Interestingly, these two phases have shown different trend and responsible neural substrates, and this could be related to the underlying neuropsychological processes. The quantitative results presented by mean and standard deviation (std) was calculated for voxels that mark significant differences between the two conditions, and the results are shown in Fig.17 (a-b).



(a)



(b)

Figure 15 Frequency domain EEG source localization results indicate a significantly decreased ERS during the first 2s presence of the stimulus (a) in the lower alpha band in bilateral inferior parietal lobe, precentral gyrus, postcentral gyrus, precuneus, middle frontal gyrus and left insula as well as (b) in bilateral superior temporal gyrus in the SL w.r.t the ST condition, significant voxels (corrected $p < 0.05$) are highlighted with blue and are color-intensity coded with t-statistics.

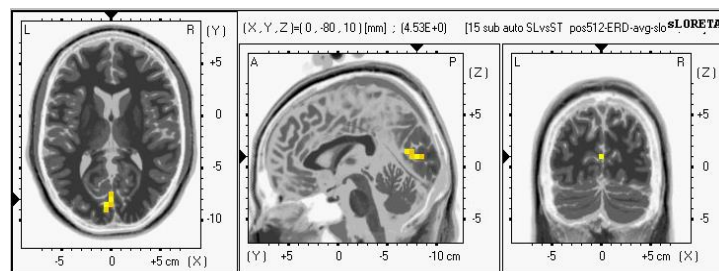


Figure 16 Frequency domain EEG source localization results indicate a significantly increased ERS during the last 2s presence of the stimulus in the lower alpha band in cuneus in the SL w.r.t the ST condition, significant voxels (corrected $p < 0.05$) are highlighted with yellow and are color-intensity coded with t-statistics.

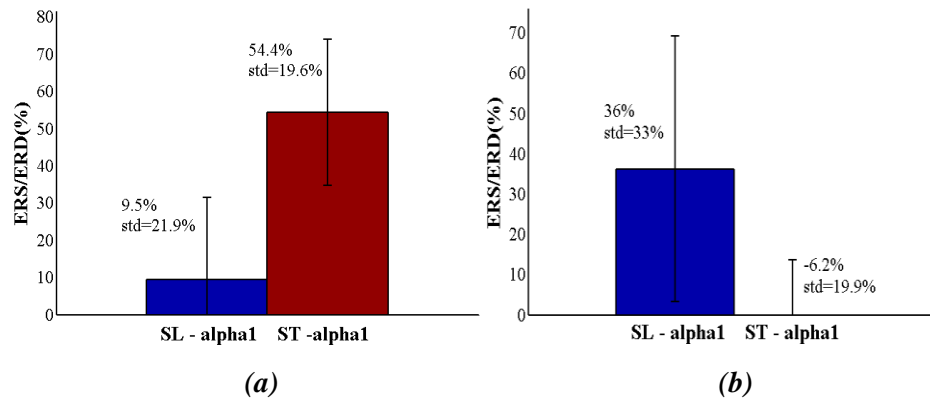


Figure 17 (a)-(b) show quantified ERS/ERD results in the SL and ST conditions for the (a). first 2s and (b). last 2s of the stimulus presence, respectively. Mean and standard deviation for the ERS value calculated for voxels that present significantly (a).decreased ERS in lower alpha band, (b).increased ERS in upper alpha band.

In the comparison of the ST and the IT condition, significantly increased ERS in the upper alpha band was observed in cuneus in the ST w.r.t the IT conditions during the first 2s presence of the stimulus (Fig.18 (a)). The quantitative result presented by mean and standard deviation (std) was calculated for voxels that mark significant differences between the two conditions, and the results are shown in Fig.18 (b).

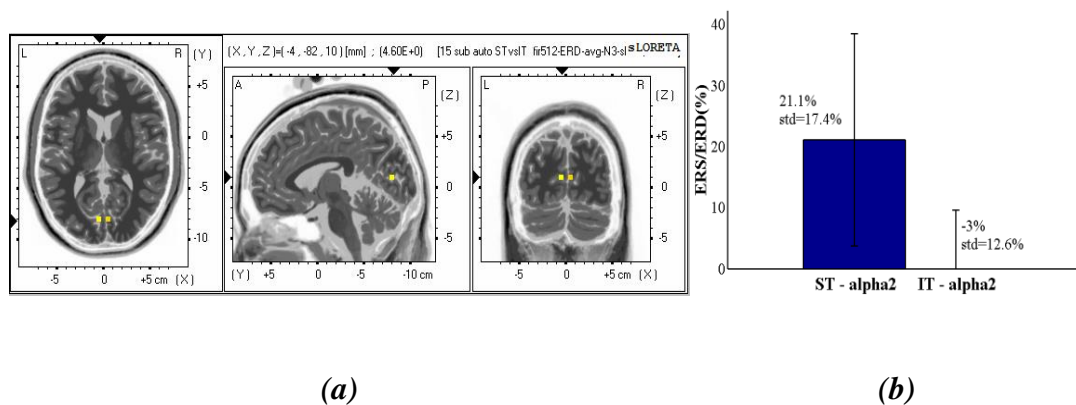


Figure 18 Frequency domain EEG source localization results indicate a significantly increased ERS (a) in the upper alpha band in cuneus in the ST w.r.t the IT condition in the first 2s of the stimulus presence, significant voxels (corrected $p < 0.05$) are highlighted with yellow and are color-intensity coded with t-statistics. (b). shows quantified mean and

standard deviation for the ERS/ERD results in the ST and the IT conditions for the first 2s of the stimulus presence calculated based on voxels that present significantly increased ERS in the upper alpha band.

In the comparison of the SL and the IL conditions, in the first 2s of the stimulus presence, significantly decreased ERS in the theta band was observed in left and right frontal gyrus, left insula and precentral gyrus and right middle frontal gyrus (Fig.19 (a)) and also in the lower alpha band in left inferior frontal gyrus and left insula (Fig.19 (b-c)) in the ST w.r.t the IT conditions. The quantitative result presented by mean and standard deviation (std) was calculated for voxels that present significant differences between the two conditions, and the results are shown in Fig.20 (a-b).

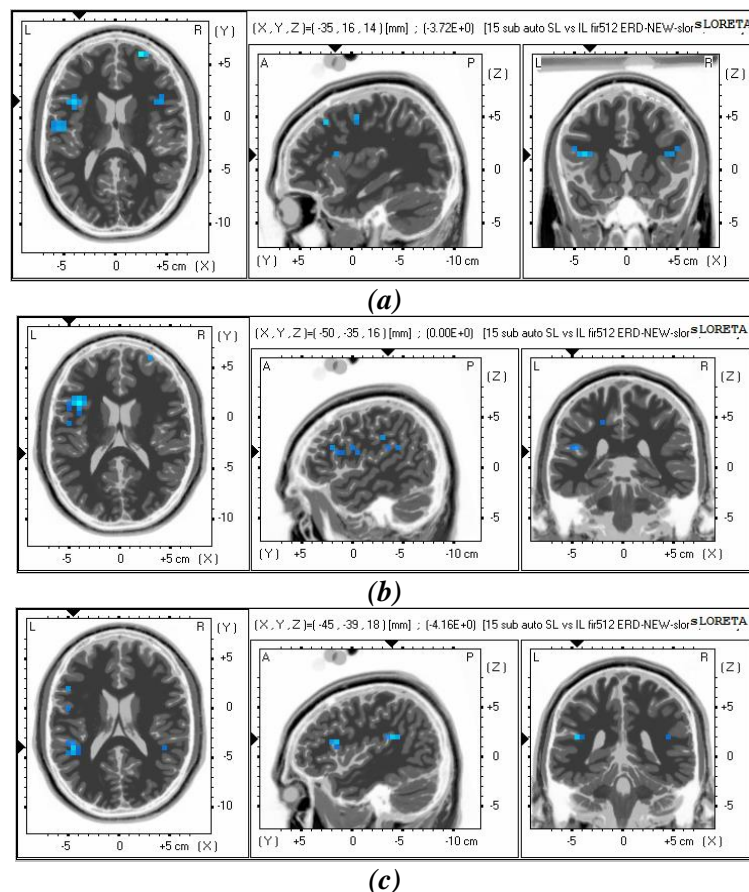


Figure 19 Frequency domain EEG source localization results indicate a significantly decreased ERS (a) in the theta band in left and right frontal gyrus, left insula and precentral

gyrus and right middle frontal gyrus as well as in the lower alpha band in (b). left inferior frontal gyrus and (c). left insula in the first 2s of the stimulus presence, significant voxels (corrected $p < 0.05$) are highlighted with blue and are color-intensity coded with t-statistics.

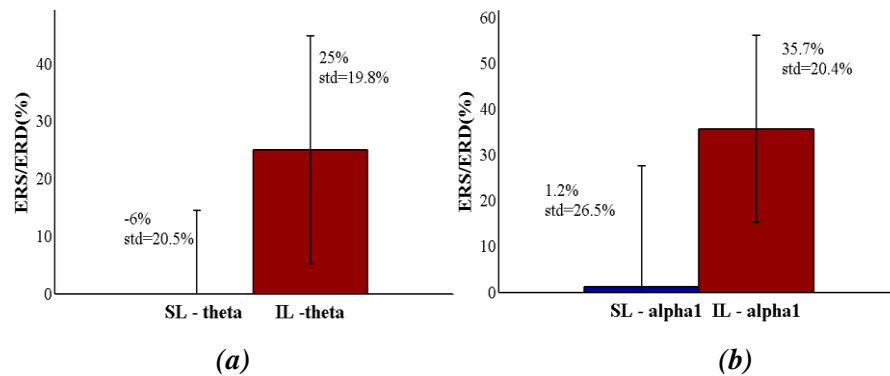


Figure 20 (a) and (b) show quantified ERS/ERD results in the SL and the IL conditions for the first 2s of the stimulus presence in the theta band and the lower alpha band, respectively. The mean and standard deviation for the ERS values were calculated for voxels that present significantly decreased ERS (a). in the theta band; (b) and in the lower alpha band.

Table 5 Detailed information on identified sources through frequency domain EEG source localization between the NE-IL and the NE-IT conditions.

Structural Names	Brodmann Area	Averaged statistic		t-	Volume Size (voxel number)		Frequency band (ERS)
		L	R		L	R	
Insula	13	4.740	4.787		3	9	Delta
Parahippocampal gyrus	19,27,28,30,35,36,37	5.172	5.104		73	61	Delta
Fusiform gyrus	20,36,37	4.984	4.824		45	31	Delta
Superior frontal gyrus	6,8	4.654	4.730		11	10	Delta
Superior parietal lobule	7	4.581	4.636		19	13	Delta
Precentral gyrus	4,6	4.730	4.620		20	19	Delta
Precuneus	7	4.650	4.652		7	6	Delta
Middle frontal gyrus	6	4.794	4.619		12	8	Delta
Middle temporal gyrus	19,21,39	4.570	4.680		5	4	Delta
Posterior cingulated	23,29,30	4.867	4.852		3	5	Delta
Medial frontal gyrus	6,8	4.530	4.597		2	3	Delta

Inferior temporal gyrus	20,21,37	4.593	0	10	0	Delta
Lingual gyrus	19,18	4.665	4.850	4	4	Delta
Poscentral gyrus	1,3	0	4.528	0	5	Delta
Lingual gyrus	17,18,19	5.629	4.995	90	55	Upper Alpha
Posterior cingulated	29,30,31	5.233	5.021	20	11	Upper Alpha
Fusiform gyrus	18,19,20,36,37	5.199	4.933	53	36	Upper Alpha
Cuneus	17,18,23,30	5.176	5.044	40	9	Upper Alpha
Parahippocampal gyrus	19,36,37,30,27,35,28	5.368	5.276	63	56	Upper Alpha
Inferior occipital gyrus	17,18	4.955	0	4	0	Upper Alpha
Middle occipital gyrus	18,19,37	4.900	4.710	6	2	Upper Alpha
Superior temporal gyrus	13,39,41	5.645	4.500	2	1	Upper Alpha

Table 6 Detailed information on identified sources through frequency domain EEG source localization between the WE-IL and the WE-IT conditions.

Structural Names	Brodmann Area	Averaged statistic		Volume Size (voxel number)		Frequency band (ERS)
		L	R	L	R	
Cuneus	17,18	4.05	4.20	4	5	Upper Alpha
Inferior frontal gyrus	45	3.82	0	1	0	Lower Alpha
Insula	13	3.99	0	2	0	Lower Alpha

Table 7 Detailed information on identified sources through frequency domain EEG source localization between the SL and the ST conditions.

Structural Names	Brodmann Area	Averaged statistic		Volume Size (voxel number)		Frequency band (ERS)
		L	R	L	R	
Insula	13	-3.68	-3.71	3	5	Lower Alpha
Inferior parietal lobe	40	-4.21	-3.95	4	3	Lower Alpha
Superior parietal lobe	7	-3.78	-3.63	1	1	Lower Alpha
Precentral gyrus	4,6	-3.68	-3.71	5	5	Lower Alpha
Postcentral gyrus	3	0	-3.72	0	3	Lower Alpha
Precuneus	7	-3.71	-3.74	5	3	Lower Alpha
Middle frontal gyrus	6	-3.82	-3.75	6	4	Lower Alpha

Superior temporal gyrus	13,41,42	-3.69	-3.76	2	6	Lower Alpha
Cuneus	17,18	4.43	0	5	0	Lower Alpha

Table 8 Detailed information on identified sources through frequency domain EEG source localization between the ST and the IT conditions.

Structural Names	Brodmann Area	Averaged t-statistic		Volume Size (voxel number)		Frequency band (ERS)
		L	R	L	R	
Cuneus	17	4.60	4.41	1	1	Upper Alpha

Table 9 Detailed information on identified sources through frequency domain EEG source localization between the SL and the IL conditions.

Structural Names	Brodmann Area	Averaged t-statistic		Volume Size (voxel number)		Frequency band (ERS)
		L	R	L	R	
Inferior frontal gyrus	44,45	-3.75	-3.68	4	2	Theta
Insula	13	-3.79	-3.69	3	1	Theta
Precentral gyrus	4,6,43	-3.72	-3.66	7	1	Theta
Middle frontal gyrus	10	0	-3.95	0	2	Theta
Inferior frontal gyrus	44,45	-3.83	0	6	0	Upper Alpha
Insula	13	-3.75	0	10	0	Upper Alpha

4.4 Discussion

4.4.1 Experiment Stimuli Control

Different from those ERP studies that trigger deceptive brain responses to transient stimuli, this study employed auditory questions that sustained for a few seconds, and accordingly, we focused on ongoing (i.e. oscillatory) components. In addition, real-life lie detection in many situations involves investigation through a series of questions which require semantic

processing while deception is concurrent. Several critical factors were identified for experimental control, i.e. i) the auditory volume, ii) window length of the stimuli and iii) the content of the probe questions. Attempts have been made to control these variation factors of the stimuli by i) converting questions from texts to audio sounds with standard auditory volume and pitch throughout the measurement. ii) randomizing the question sequence in each condition for each subject and guaranteeing the questions' length in the lying and its corresponding truth-telling conditions non-significantly different. iii) conducting a prior-experiment test to screen for the subjects' eligibility in English proficiency; on the other hand, the probe questions used in the experiment were examined by a group of non-participants who have similar English proficiency level with those participants, questions that are ambiguous or difficult to understand were excluded. The probe questions were screened in advance to make sure the difficulty level of the questions is similar to each other. In addition, since the particular brain activity for each specific question is not to be studied, trials that belong to each condition were grouped and averaged. As a result, the results were evaluated based on the mean effect which is justifiable since there exists non-obvious difference in the difficulty level among the questions.

4.4.2 Source localization in experiment I and experiment II

In the WE task, significantly increased ERS in cuneus in the upper alpha band was observed in the WE-IL condition compared with the WE-IT condition. The ERS in cuneus in the upper alpha band has been reported associated with inhibition of task-irrelevant information in working memory task (Michels, Moazami-Goudarzi et al. 2008, Michels,

Bucher et al. 2010). Since in the lying task, truthful answers are task-irrelevant information which needs to be inhibited, the increased ERS observed might represent inhibition of the truthful answers. Moreover, the ERS observed in cuneus could not be simply related to the suppression of the visual function in the IL condition since visual stimuli processing was not involved in the deception task. Therefore, the observed increased ERS in cuneus in the upper alpha band is most likely associated with task-related inhibition control instead of a generic inhibition of visual processing. In addition, complementary to this result, significantly increased ERS in the left inferior frontal gyrus and insula was observed in the same comparison. Left inferior frontal gyrus has been suggested as a critical region involved in response inhibition and in general habitual behavior inhibition (Matsubara, Yamaguchi et al. 2004, Swick, Ashley et al. 2008). Moreover, left insula has also been indicated as a region correlated with response inhibition (Prisciandaro, Joseph et al. 2014). As such, all the above ERS findings seem to strongly suggest a response inhibition sign that is involved in the IL w.r.t the IT condition. Correspondingly, longer response time in the WE-IL condition is most likely associated with increased amount of time spent on inhibitive processing before response.

On the other hand, in the NE task which is a mock interview scenario, increased ERS in delta band was observed in multiple regions across the brain in the NE-IL condition compared with the NE-IT condition. Delta band has been found negatively correlated with the default mode network's activity (Knyazev 2013), with which self-consciousness and self-processing are consistently associated (Hlinka, Alexakis et al. 2010). This network is most frequently associated with deactivation when task load increases (Buckner, Andrews-

Hanna et al. 2008). However there is a noticeable exception to this general pattern of deactivation during goal-directed activity which occurs in tasks requiring self-referential thought and social cognition (Mitchell 2006, Gobbini, Koralek et al. 2007). It is therefore suggested that DMN likely mediates active cognitive processes rather than being strictly a 'default' network. In this study, increased ERS has been found for the NE-IL condition compared with the NE-IT condition in several regions. Among these regions, insula, fusiform gyrus, middle frontal gyrus, superior parietal lobe, precuneus, middle temporal gyrus, posterior cingulate, and medial frontal gyrus are sources from the DMN (Buckner, Andrews-Hanna et al. 2008, Fransson and Marrelec 2008, Sridharan, Levitin et al. 2008). Increased delta ERS in these regions that largely overlap with the DMN might indicate a decreased level of self-referential in the NE-IL task. In contrast to the truth-telling condition, which involves more self-referential processing to retrieve exact personal information about subjects' prior experience, the lying condition involves more visual imagery processing of the non-experienced events which reduces the requirement for self-referential processing.

Apart from the finding in the delta band for the NE task, the upper alpha band ERS was found increased in several occipital and temporal regions. Activation of the occipital and temporal regions in memory tasks is associated with memory processing (Yonelinas, Hopfinger et al. 2001). The involvement role of the occipital regions in the memory task without visual perception of any stimulus is likely to be linked with mental imagery (Kosslyn and Ochsner 1994, Aleman, van Lee et al. 2001, Ganis, Thompson et al. 2004), which is an experience that significantly resembles the experience of perceiving some

object, event or scene without the presence of the relevant targets. Visual imagery is not only considered a bottom-up visual perception process used to build mental pictures, it is also a form of memory retrieval (nonverbal recall) and is involved in memory processes (De Volder, Toyama et al. 2001). Primary visual cortex, visual associative cortex, temporal cortex and parietal cortex have been reported in visual mental imagery tasks (Mellet, Tzourio et al. 1996). For example, fusiform gyrus was found with increased activity while generating images in response to concrete words and its activation is more associated with engagement in visual knowledge retrieval compared with non-visual knowledge retrieval. It has also been reported that both ventral and dorsal neuro-anatomical pathways are involved in visual imaging tasks in sighted or blind subjects (Lambert, Sampaio et al. 2004). Along the ventral pathway, lingual gyrus and fusiform gyrus specifically deal with the figurative features of the imaged stimuli. On the other hand, the dorsal pathway deals with the dimensional and spatial features of the stimuli which involve the parietal and temporal regions in participation (Baizer, Ungerleider et al. 1991). Along the dorsal pathway, the parahippocampal gyrus is associated with contextualizing of visual scenes, and parahippocampal place area is part of this gyrus responsible for encoding and recognition of scenes (Mullally and Maguire 2011). The anterior part of the parahippocampal gyrus includes the perirhinal and entorhinal cortices. The perirhinal cortex (BA 35, 36) is involved in both visual perception and memory processing (Murray, Bussey et al. 2007); it facilitates the recognition and identification of environmental stimuli. The entorhinal plays an important role in the autobiographical/declarative/episodic memories and in particular spatial memories (Dickerson and Eichenbaum 2010). Since the

current task does not involve visual perception induced by visual stimuli, it is highly possible that the perirhinal and entorhinal cortices involved in the task by facilitation of visual imagery process through associating stimulus to stimulus, recognizing item/object and endowing objects with meaning (Murray, Bussey et al. 2007).

According to the source localization results in the upper alpha band, visual imagery processing of both the figurative features and the spatial/contextual scenes might be involved in the NE-IL task. This deduction is justifiable since our stimuli-questions cover both of these two aspects (some questions are related to a specific object, e.g. software, tool, and detailed information on working experience; others are related to the spatial scenes regarding a U.S.A business trip, and the place to receive related job training, etc). Moreover, this is evidenced by the participation of lingual gyrus, posterior cingulate, fusiform gyrus, parahippocampal gyrus and cuneus. According to the previous studies, alpha band has been found positively correlated with the DMN activity (Knyazev 2013) and the regions that represent this positive correlation are mostly located in the frontal and parietal regions. However, the regions identified with increased upper alpha ERS in this study are located dominantly in the occipital and temporal regions. This observation does not violate with the hypothesis of decreased self-referential processing, or rather, it represents an increased regional controlled processing by visual imagery to extract contextual relevant information from memory pools for fabricating non-experienced events. Not surprisingly, longer response time was also observed in the NE-IL condition compared with the NE-IT condition, and the longer time could be spent on the mental imagery process that is necessarily involved to facilitate fabrication of viable lies.

In the comparison of spontaneous and instructed lying and their counterpart truth-telling tasks, it is interesting to observe that the difference between the spontaneous lying and its truth-telling condition presents differently in the first 2s and last 2s of the stimulus presence period. More specifically, the first 2s saw a decreased ERS in multiple regions in the lower alpha band while the last 2s saw an increased ERS in cuneus and precuneus in the same frequency band. The lower alpha ERS during the first 2s is most likely present as an active state of the brain. Among these regions that present decreased ERS in the first 2s, superior parietal gyrus, precentral and postcentral gyrus and precuneus are regions that have been suggested more active during the SL condition compared to the ST condition (Ganis, Kosslyn et al. 2003). Besides, inferior parietal lobule, precentral gyrus/middle frontal gyrus, right and left insula have been supported by a meta-analysis to present stronger activity during the deception condition in general compared with the truth-telling condition (Christ, Van Essen et al. 2009). Although it was inferred that the involvement of these regions might be related to working memory, the results in this study tend to imply their association with selective auditory attention due to the presence of superior temporal gyrus (BA 41,42,22) as well as motor regions (postcentral and precentral gyrus), which are regions closely related to auditory attention (Chapin, Zanto et al. 2010). Moreover, precuneus and inferior parietal lobule have been reported closely related with selective auditory attention (Pugh, offywitz et al. 1996, Behrmann, Geng et al. 2004). The involvement of insula seems to serve the function of selective amplification of salient events, i.e. which question to lie. It is highly possible that the selective attention (sub) network may collaborate with saliency (sub) network to facilitate the decision making on when to lie. On the other hand, during

the last 2s of stimulus presence, increased ERS occurs in the cuneus in the lower alpha band in the SL w.r.t the ST condition. Moreover, although upper alpha band does not show any significant result, there is an increased ERS trend observed in the anterior cingulate cortex (ACC) and cuneus. These observations seem to again point to an increased demand in inhibition control in the SL condition once a prior decision is made that instructs the subjects to take an action to lie.

4.4.3 Comparison between the WE and the NE tasks

To compare the results for the WE and NE tasks, it can be seen that the visual cortex, perirhinal cortex, granular retrosplenial cortex and agranular retrolimbic area have demonstrated increased clustering coefficient in the upper alpha band in both tasks. This result has confirmed the significant role of the occipital cortex and temporal cortex in both instructed lying tasks. The major difference between the results for the WE and the NE task is that the latter task involves less top-down executive control for memory processing compared to the WE task which needs frontal regions to get involved for top-down modulation and executive control on the memory processing circuit. This result implies that the NE-IL condition requires more regional processing and the WE-IL condition requires more global interaction between regions. Commonalities and differences were also found based on the source localization analysis, among which increased ERS in the upper alpha band was observed in occipital region in both the WE-IL and the NE-IL condition. Compared with the WE-IL condition which involves executive control as the core cognitive processing circuit, the NE-IL condition is distinguished by a decreased self-

referential processing accompanied by visual imagery to fabricate lies for non-experienced events.

4.4.4 Comparison between the IL-IT and the SL-ST tasks

The pairs of SL-IL, and ST-IT have been further compared to identify the potential differences lie in these two similar yet distinguished conditions. Fig.19 (a) shows that bilateral inferior frontal gyrus and insula have been observed decreased in ERS in the theta band, and the same unilateral locations have been observed decreased in ERS in the lower alpha band (Fig.19 (b-c)). These two major observations might lead to the deduction that compared with the SL, the early phase of the IL has already involved strong response inhibition activities, which makes the IL and the SL distinguishable from each other. On the other hand, ST has shown increased ERS in cuneus in the upper alpha band, with similar profile of sources as indicated in the IL-IT comparison, therefore it implies that the main difference between the ST and the IT is an early sign of inhibition in the ST condition which prevents the subjects from making instantaneous truthful response to the question.

4.5 Concluding remarks

The results of this study based on frequency domain EEG source localization analysis have provided intuitive evidence for distinguishable features of instructed lying in the WE and NE tasks as well as spontaneous lying compared with their counter-part truth-telling conditions. Distinguishable features have also been achieved for the comparison between the pairs of instructed-spontaneous lying, and instructed-spontaneous truth-telling. Results

show the corresponding neural anatomies, and their spectra information indicating the involvement of a core neuro-psychological process, i.e. executive control in the WE-IL condition, and a decreased self-referential processing accompanied by increased visual imagery activity in the NE-IL condition. Moreover, selective attention and saliency monitoring at earlier phase and inhibition control in the later phase seem to play an important role to distinguish the SL from the ST condition. In addition, the major difference between the SL and the IL lie in response inhibition in the IL, and the ST and the IT conditions can also be differentiated by an early inhibitory control sign. Thus, this study has provided a neuro-psychological insight for various types of deception based on source localization method that offers a chance to identify neural substrates underlying any condition differences.

CHPATER 5

A HUMAN ELECTROENCEPHALOGRAPHY NETWORK AND CONNECTIVITY BASED METHOD TO STUDY INSTRUCTED LYING TASKS

In this chapter, an electroencephalography (EEG) study is presented regarding the cognitive processes of an instructed liar/truth-teller during the time window of stimulus (question) delivery period (SDP) prior to their deceptive/truthful responses towards questions related to authentic (WE: with prior experience) and fictional experience (NE: no prior experience). To investigate deception in non-experienced events, the subjects were given stimuli in a mock interview scenario that induced them to fabricate lies. To analyze the data, frequency domain network and connectivity analysis was performed in the source space in order to provide a more systematic level understanding of deception during SDP. The results achieved can provide complementary and intuitive evidence for the differences between the IL and IT conditions in SDP for two types of deception tasks, thus elucidating

the electrophysiological mechanisms underlying SDP of deception from regional, inter-regional, network, and inter-network scale analyses.

5.1 Introduction

Except a few fMRI studies made attempts to investigate the neural substrates underlying deception, the deception mechanism remains obscure. Unfortunately, no attempt has been taken before to unveil the functional networks underlying deception related processes, given the fact that deception is such a complicated cognitive process. Despite the challenge, in theory, neuronal communication should play an important role in deception related processes which involves coordination between different brain areas that belong to particular functional networks. Hence, it is interesting to take an attempt to investigate the network activities in the same frequency band from which distinct event related synchronization (ERS) was found (i.e., upper alpha band) in our previous study (Wang, Ng Wu et al. 2013).

In contrast to previous studies that focused on the time window during which deceptive response is being generated, this study investigated the window prior to that period (i.e. stimulus delivery period (SDP)). The underlying hypothesis is that before the subjects giving any deceptive/truthful responses, their corresponding neuronal activities may already start to differentiate from each other, which possibly indicates the existence of a prediction sign of deception. Understanding the networks underlying deception during this time window possibly enables us to divide this whole complicated process into more easily

understandable cognitive processes, and to explore the potential earlier deception sign that has never been discussed before.

In this study, commonalities and differences between two types of instructed lying tasks during SDP were investigated. Interestingly, compared with the ‘with prior-experience’ lying task (WE), the ‘non-experience’ lying task (NE) remains largely uninvestigated. Previous deception studies have focused on comparisons between deception types such as instructed/spontaneous lying (Kim, Jung et al. 2012), self-referential/other-referential lying (Ganis, Morris et al. 2009), and memorized/created lying (Ganis, Kosslyn et al. 2003). Limited work has been carried out on comparisons between deception in experienced and non-experienced events. Among the fMRI studies, one study (Abe, Suzuki et al. 2006) instructed subjects to tell lies/the truth concerning 20 old stimuli and 20 new stimuli by answering ‘I know’ and ‘I don’t know’. This fMRI study considered both experienced and non-experienced events in the deception tasks without requiring fabrication of lies to the unfamiliar objects and the neural circuits underlying the processing were dominated by recognition memory and inhibition control. However, real-life deception for non-experienced events often involves fabricating lies while being asked questions that require semantic processing especially in the interview scenario. In general, this fMRI study remains distinct from the NE task that induces subjects to cheat with extra efforts in semantic processing. The motivation to study these two tasks is based on the further hypothesis that, features that can distinguish the IL and IT during the SDP may be different in varying tasks and when features of lying during the SDP is being discussed, it could be task-dependent.

In summary, this study is aimed to develop a new EEG-based methodology to explore the potential neural mechanism of instructed lying during SDP that could potentially provide a basis for future applications. Additionally, previous EEG-based studies did not provide a neuro-anatomy basis for deception, and previous protocol designs for instructed lying may have only considered limited possibilities and therefore were not sufficiently comprehensive to cover possible real-life instructed lying scenarios. To address these issues, this study employed a i) frequency domain network and connectivity analysis in the source space and ii) an original paradigm to induce subjects to fabricate lies about non-experienced events.

5.2 Data analysis

The experimental modulation effects on the inter-regional neural activities were analyzed through frequency domain connectivity analysis (Dressler, Schneider et al. 2004),(Campbell 2009),(Canuet, Ishii et al. 2011),(Shafi, Brandon Westover et al. 2013). The connectivity is a descriptive index that quantifies the correlational/interactive relationship between two cortical brain areas. The higher the interactive activity, the higher the connectivity. In the EEG domain, there are various ways to quantify two nodes' connectivity behavior. Among the various types of connectivity measurements, phase-lagged index (PLI) (Stam, Nolte et al. 2007), coherence (Wang, Wang et al. 2014), phase coherence and imagery component of coherence(Stam, Nolte et al. 2007), lagged-phase synchronization (LPS) (Pascual-Marqui 2007), partial-directed coherence (PDC) (Baccala and Sameshima 2001), and granger causality (GC) (Barrett, Murphy et al. 2012) and lagged

phase synchronization (LPS) (Ramyeed, Kometer et al. 2014) are frequently employed. Among these methods, granger causality and partial-directed coherence provide directional connectivity estimation. Coherence is a frequently employed connectivity estimator, similar to the notion of temporal correlation, coherence provides quantified evaluation of correlation for two time series in the spectral domain. Despite the fact that it is popularly employed, it cannot exclude the contamination issue caused by volume conduction. Phase-lagged index (PLI) is another way that quantifies the correlational interaction between two time series, the PLI is a measure of the asymmetry of the distribution of phase differences between two signals. Compared to phase coherence, imaginary component of coherence, PLI is less susceptible to spurious connection caused by the volume conduction effect (Stam, Nolte et al. 2007). LPS is a similar index to PLI, in this study, LPS was applied for connectivity measurement, this index is similar to the PLI and it provides zero-lag removal connectivity measurement, which solves the contamination issue caused by volume conduction that is intrinsically present in EEG recordings either on the scalp or at the source level.

Moreover, we were only interested in the connectivity changes that were modulated by the experimental effects irrespective of the exact interactive direction. In the connectivity analysis, the absolute and event-related connectivity were calculated for the first 2s time window during the phase of SDP on the cerebral cortex, which is segmented into 84 Brodmann (BA) areas (i.e. 42 BAs each hemisphere). Within the sLORETA framework, ROIs (regions of interest) can be generated with the default 42 BAs (brodmann areas) parcellation for each hemisphere based on the cytoarchitectonics of neurons (LJ. 2006),

leading to 84 BAs created for the whole brain. Previous studies have applied similar parcellation method for network analysis under sLORETA framework (Jancke and Langer 2011). The LPS is defined according to Pascual-Marqui RD et al. (Pascual-Marqui 2007). Additionally, the clustering coefficient was computed based on the definition according to $C_i = \frac{\sum_{k \neq i} \sum_{l \neq i, l \neq k} w_{ik} w_{il} w_{kl}}{\sum_{k \neq i} \sum_{l \neq i, l \neq k} w_{ik} w_{il}}$ proposed by Chu CJ et al. (Chu, Kramer et al. 2012) , which generally characterizes the node's interaction with the rest of the brain. Normalization procedure was performed on connectivity and clustering coefficient measurement with respect to those measured from the baseline window (i.e. the last 2s of the baseline segment) to remove the different baseline effects for different conditions. As such, the connectivity/clustering coefficient derived after normalization is also called event-related connectivity/clustering coefficient. Standardized low-resolution brain electromagnetic tomography (sLORETA) (Pascual-Marqui 2002) was used to compute the connectivity in selected frequency bands (i.e., the upper alpha band) with a source solution space consisting of 6,239 voxels (voxel dimensions 5×5×5 mm) that was restricted to the cortical gray matter and hippocampi as defined according to the MNI atlas (Mazziotta, Toga et al. 2001). As recommended by sLORETA, single voxel at the ROI centroid was selected for connectivity calculation for two reasons: (1) The calculation of source by sLORETA is based on the assumption that the smoothest of all possible activation distributions is the most plausible one, and this is supported by neuro-physiological data demonstrating that neighbouring neuronal populations present highly correlated activity (Christoph M. Michel 2009). Due to this assumption, signals of spatially adjacent voxels of neighbouring ROIs are highly correlated, inducing larger connectivity, which might not be physiological in

nature. By taking this single centre voxel of each ROI, such contamination for connectivity estimation could be minimized, since information of the centroid voxel is an accurate representative for activity within the ROIs (Jancke and Langer 2011). (2) If you define a large ROI, then the average sLORETA activity spanning a large volume might not be very meaningful. Therefore, given the low spatial resolution of sLORETA, the first method was chosen and as a result, the network analysis is not refined but mainly captures the dominant features of connection. The cortical connectivity estimation is then based on the electrical current source time series estimated by sLORETA (Jancke and Langer 2011).

In the network analysis, a dendrogram that consisted of mirrored C-shape lines was employed to classify the 84 ROIs into a hierarchical cluster tree according to their proximity. Based on the distance calculation for all of the paired nodes (ROIs), which is defined as '1-connectivity' and is opposite the trend of connectivity, a dendrogram was created that enables the clustering of nodes into a sub-network sharing a similar connection pattern (Chen, Ros et al. 2013) with respect to the remaining brain regions with the notion that the nodes that share similar connection pattern are thought to perform similar functional roles and therefore can be considered constituting a network/sub-network.

The dendrogram analysis was performed based on the averaged connectivity matrix across the subjects that provides a group-wise connectivity matrix for each condition (Jancke and Langer 2011, Chen, Ros et al. 2013), and the average procedure is assumed to improve the SNR for the estimation of the connectivity matrix and helps facilitating the identification of the most common and stable network patterns across subjects. Possible concerns

regarding the connectivity/functional network analysis are 1) deception is a complicated process which involves multiple known or unknown cognitive/sensory processes, and 2) the analysis window where talking is involved or too significant time variation is involved (i.e. between the offset of stimuli and the onset of the answering) does not provide reliable and consistent EEG signal due to too much EMG artifact. Luckily, the dendrogram analysis was only performed for a narrow window (i.e. the first 2s of stimuli delivery) bearing more or less predictable underlying sub-processes. Finally, behavior data (response time) were extracted based on the filtered EMG signal (band-pass: 1-25 Hz), which was recorded from a separate EMG channel for correlation analysis with network-scale neuronal activities. In this study, multiple comparison permutation tests were widely employed for all the statistical comparisons on the analyzed index between conditions or correlation analysis based on (Blair and Karniski 1993) and (Groppe, Urbach et al. 2011). The multiple comparison permutation paired test employs a 'tmax' method for paired comparisons which adjusts the p-values of each variable for multiple comparisons among all the 84 ROIs (corrected $p < 0.05$). The multiple comparison permutation correlation tests is based on Pearson's linear correlation coefficient (r) or Spearman's rank correlation coefficient (ρ). When applying the test to multiple variables, the 'max statistic' method is used for adjusting the p-values of each variable for multiple comparisons among all the 84 ROIs (corrected $p < 0.05$). Like Bonferroni correction, this method adjusts p-values in a way that controls the family-wise error rate. However, the permutation method will be more powerful than Bonferroni correction when different variables in the test are correlated. Technically, all the multiple comparison corrected t-tests in this study were performed

based on an open-source Matlab code (downloadable from: http://www.mathworks.com/matlabcentral/fileexchange/29782-one-sample-paired-samples-permutation-t-test-with-correction-for-multiple-comparisons/content/mult_comp_perm_t1.m; http://www.mathworks.com/matlabcentral/fileexchange/34920-correlation-permutation-test-with-correction-for-multiple-comparisons/content/mult_comp_perm_corr.m). The steps of analysis from input EEG data to output network have been illustrated in Fig.21. The ‘EEG-signal’ segment deals with band-pass filtering (1-30Hz) as well as artifact (EOG & EMG) removal; the ‘EEG inverse calculation for ROI’ maps the ‘clean’ EEG into source space on centroid voxels of the 84 ROIs to retrieve source time series; the pair-wise connectivity was calculated based on the 84 ROI’s time series into a 84×84 matrix, and then a group-wise connectivity matrix underwent dendrogram analysis that clusters 84 nodes into groups of sources, among which common networks for the IL and IT conditions were identified and mapped onto a generic cortex model.

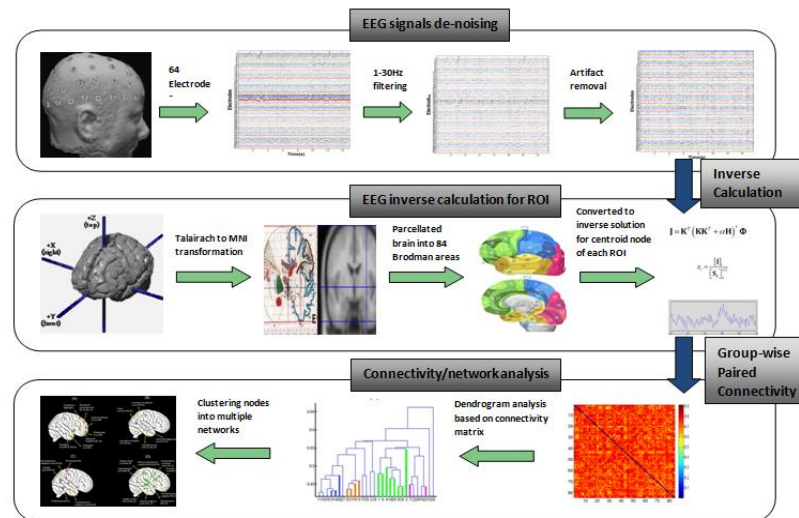


Figure 21 The descriptive steps of analysis from input EEG raw signal to the output network. The major steps are EEG signals de-noising, inverse calculation for ROIs, group-wise paired connectivity computation, dendrogram analysis to cluster nodes into networks.

5.3. Results

5.3.1 Network analysis

In the functional network analysis, the connectivity between regions was calculated based on the un-normalized LPS index because components of the network during the first 2s time window of SDP is independent of the baseline window. A data-driven dendrogram analysis was performed based on the connectivity matrix which represents all nodes' connection pattern with the rest of the brain for both the IL and IT conditions in either task. From these components, four groups were qualitatively selected based on the dendrogram and visual inspection and this method has been applied in a previous study (Chen, Ros et al. 2013); additionally, the sub-networks are required to potentially depict functionally related groups in both the IL and IT conditions.

Interestingly, several sub-networks were identified that were shared by both the IL and IT conditions in both tasks. The dendrogram analysis results are depicted in Fig. 22 and Fig. 23 for the WE and the NE tasks, respectively, where Fig. 22 ((A), (B)) and Fig. 23 ((A), (B)) summarize the information of the connectivity matrix for all of the cortical areas in each condition into a dendrogram by clustering nodes that share similar connection patterns into sub-networks. In Fig. 22 and Fig. 23, different colors are used to indicate different types of sub-networks. Corresponding sources for each sub-network are plotted on a

cortical brain surface (as shown in Fig. 24 and Fig. 25) with the corresponding color used in Fig. 22 and Fig. 23. The detailed sub-network source anatomical information is described in Table 10 and Table 11 for the WE and the NE tasks, respectively.

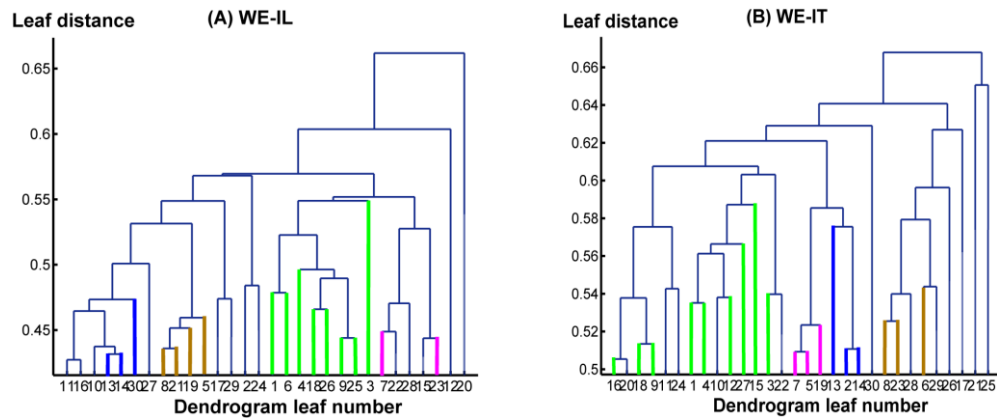


Figure 22 (A) and (B) represent the hierarchy structures based on the dendrogram analysis for the WE-IL and the WE-IT conditions, respectively. The x-axis: leaf number, each leaf represents a cluster of BAs. The y-axis: leaf distance calculated using average linkage clustering based on correlation distance. The yellow color indicates group A, the blue color indicates group B, the pink color indicates group C, and the green color indicates group D.

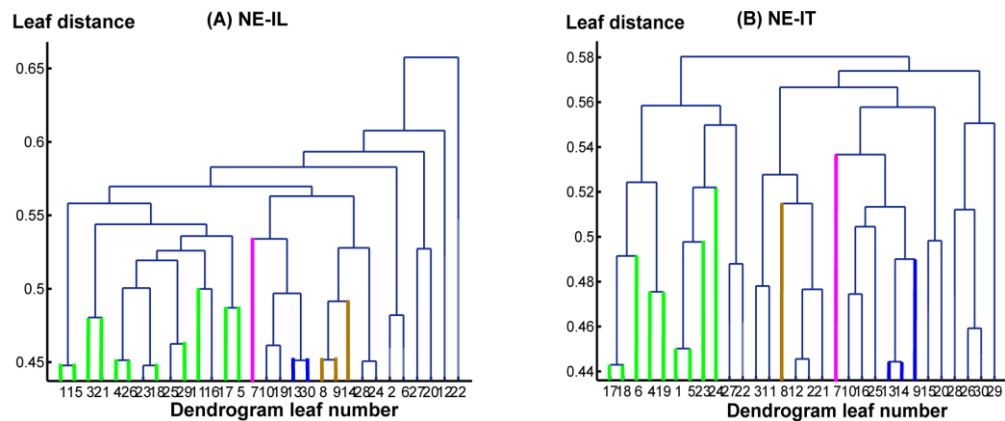


Figure 23 (A) and (B) represent the hierarchy structures based on the dendrogram analysis for the NE-IL and the NE-IT conditions, respectively. The x-axis: leaf number, each leaf represents a cluster of BAs. The y-axis: leaf distance calculated using average linkage clustering based on correlation distance. The yellow color indicates group A, the blue color indicates group B, the pink color indicates group C, and the green color indicates group D.

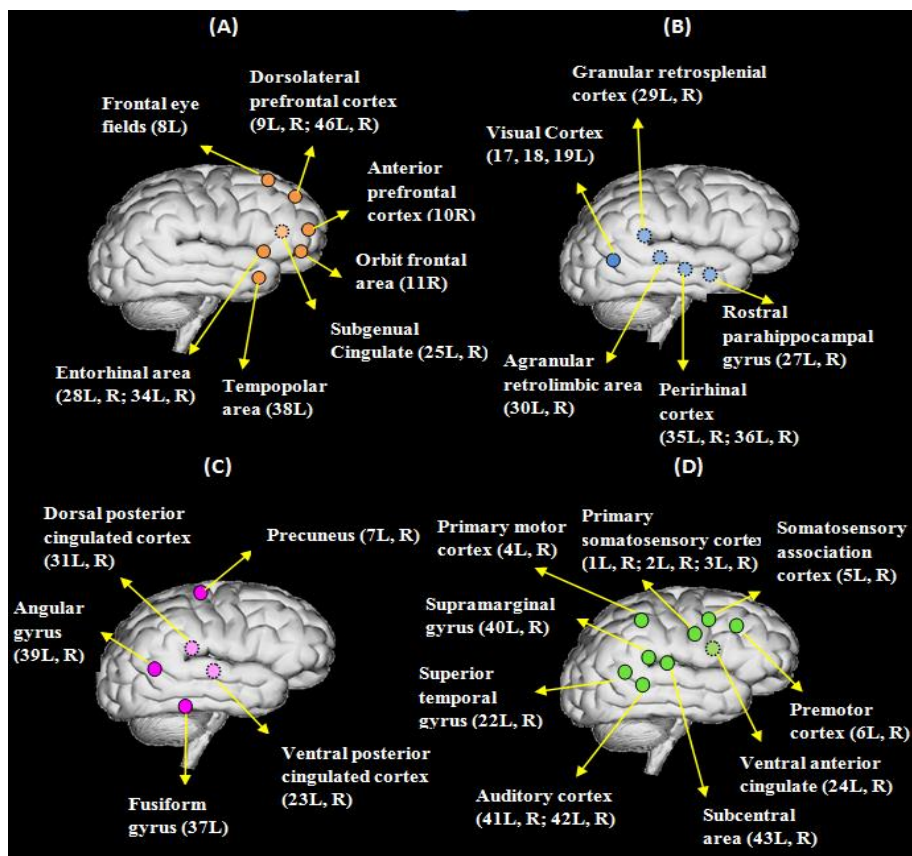


Figure 24 The corresponding cortical sources that functionally cluster into four sub-networks that are common for the WE-IL and the WE-IT conditions: (A), (B), (C) and (D) are hypothetical networks for executing higher-order function, comprehension/memory process processing, and speech perception, respectively. The dotted circle indicates a medial surface source, while the solid circle indicates a lateral surface source. The label for each anatomical region includes the Brodmann area name and the laterality information.

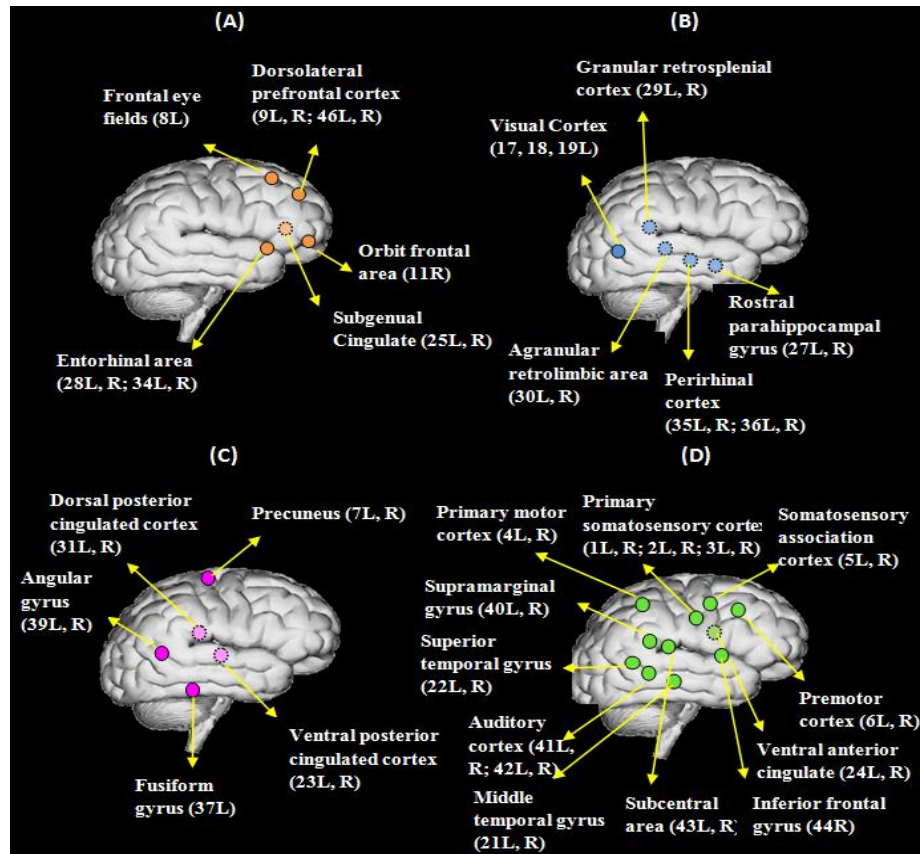


Figure 25 The corresponding cortical sources that functionally cluster into the four sub-networks that are common for the NE-IL and the NE-IT conditions: (A), (B), (C) and (D) are hypothetical networks for executing higher-order function, comprehension/memory processing, and speech perception, respectively. The dotted circle indicates a medial surface source, while the solid circle indicates a lateral surface source. The label for each anatomical region includes the Brodmann area name and the laterality information.

Despite the similarities in sub-network components shared by the two conditions in the WE task, differences were found via further analyses. In Table 12, the inter- and intra-group connectivities were compared between the WE-IL and the WE-IT conditions. The intra-group connectivity/inter-group connectivity was calculated based on the summation of all of the non-repeated paired connectivity values between regions that belonged to the same group/belonged to the two inspected groups, respectively. During the calculation, two

indices that could potentially represent the inter- and intra-group connectivities were calculated for the first two-second window of the auditory stimuli. The first index, $c1$, is a normalized connectivity value that indicates the percentage of change for connectivity in the stimulus period relative to that of the baseline period, i.e., the last two seconds of the ‘fixation’ phase. To some extent, this measurement helps to exclude spurious connection at a statistical level based on how relevant the connection is to the task (i.e. the lower the absolute value, the more irrelevant to the task, and hence less likely to present significant differences between conditions). As a result, the $c1$ index measures the degree of event related modulation on within- and between- network connectivity by the event (tasks during the SDP window). The other index, $c2$, is an un-normalized absolute connectivity value for the first 2s during the SDP window. As referenced in Table 12, the intra-group connectivity does not show any significant difference between the IL and the IT conditions, while the inter-group connectivity shows a significant increase in the IL condition relative to the IT condition in multiple group pairs, i.e., group $A \leftrightarrow B$, group $A \leftrightarrow C$, group $A \leftrightarrow D$, group $B \leftrightarrow D$, and group $C \leftrightarrow D$ by $c1$ index after multiple comparison permutation tests (corrected $p < 0.05$) for inter- and intra- comparisons separately (4 networks’ comparisons vs. 6 pairs’ comparisons). In addition, as predicted, $c1$ is more sensitive than $c2$ for representation of significant differences in inter-group connectivity between the IL and IT conditions.

Correspondingly, in Table 13, the inter- and intra-group connectivities were compared between the NE-IL and the NE-IT conditions with multiple comparison permutation tests (corrected $p < 0.05$) for inter- and intra- comparisons separately (4 networks’ comparisons

vs. 6 pairs' comparisons). Interestingly, group A showed decreased intra-group connectivity by c2 index, while group C showed increased intra-group connectivity by c1 index. The inter-group connectivity also increased in two group pairs, i.e., group A↔D and group B↔C by c1 index.

Table 10 Results from the dendrogram analysis; four groups of sources were found to be common to the WE-IL and the WE-IT conditions in the upper alpha band.

Group A	frontal eye fields (8L), dorsolateral prefrontal cortex (9L, 9R, 46L, 46R), anterior prefrontal cortex (10R), orbitofrontal area (11R), subgenual cingulate (25L, 25R), entorhinal area (28L, 34L), entorhinal area (28R, 34R), temporopolar area (38L)
Group B	visual cortex (17L, 18L, 19L), rostral parahippocampal gyrus (27L, 27R), granular retrosplenial cortex (29L, 29R), agranular retrosplenial area (30L, 30R), perirhinal cortex (35L, 36L, 35R, 36R)
Group C	precuneus (7L, 7R), posterior cingulate cortex (23L, 23R), dorsal posterior cingulate area (31L, 31R), occipitotemporal area (37L), angular area (39L, 39R)
Group D	primary somatosensory cortex (1L, 1R, 2L, 2R, 3L, 3R), primary motor cortex (4L, 4R), somatosensory association cortex (5L, 5R), premotor cortex (6L, 6R), ventral anterior cingulate area (24L, 24R), supramarginal gyrus (40L, 40R), subcentral area (43L, 43R), superior temporal gyrus (22L, 22R), auditory cortex (41L, 41R, 42L, 42R)

Table 11 Results from dendrogram analysis; four groups of sources were found to be common to the NE-IL and the NE-IT conditions in the upper alpha band.

Group A	frontal eye fields (8L), dorsolateral prefrontal cortex (9L, 46L, 9R, 46R), entorhinal area (28L, 34L), entorhinal area (28R, 34R), subgenual cingulate (25L, 25R), orbital area (47L)
Group B	visual cortex (17L, 18L, 19L), rostral parahippocampal gyrus (27L, 27R), granular retrosplenial cortex (29L, 29R), agranular retrosplenial area (30L, 30R), perirhinal cortex (35L, 36L, 35R, 36R)
Group C	precuneus (7L, 7R), ventral posterior cingulate cortex (23L, 23R), dorsal posterior cingulate cortex (31L, 31R), occipitotemporal area (37L), angular gyrus (39L, 39R)
Group D	primary somatosensory cortex (1L, 1R, 2L, 2R), primary motor cortex (4L, 4R), somatosensory association cortex (5L, 5R), premotor cortex (6L, 6R), ventral anterior cingulate cortex (24L, 24R), supramarginal gyrus (40L, 40R), subcentral area (43L, 43R), middle temporal gyrus (21L), superior temporal gyrus (22L, R), auditory cortex (41L, 42L, 41R, 42R), inferior frontal gyrus (44R)

Table 12 The difference in the intra- and inter-group connectivity among sub-networks in the upper alpha band between the WE-IL and the WE-IT conditions. The sources of groups A, B, C, D are depicted in Fig.24.

Intra-Group Connectivity Increase		Inter-Group Connectivity Increase	
Group A	-(p1=0.0657, p2=0.1146)*	Group A ↔ Group B	↑(p1= 0.0177); -(p2=0.1030)
		Group A ↔ Group C	↑(p1= 0.0333); -(p2=0.1304)
		Group A ↔ Group D	↑(p1=0.0150); -(p2=0.1892)
Group B	-(p1=0.1206, p2=0.0989)	Group B ↔ Group C	-(p1=0.3907, p2=0.2204)
		Group B ↔ Group D	↑(p1=0.0262); -(p2=0.2220)
Group C	-(p1=0.2047, p2=0.1436)	Group C ↔ Group D	↑(p1=0.009); -(p2=0.1128)
Group D	-(p1=0.0945, p2=0.2741)		
*p1 and p2 are corrected p-values after multiple comparisons permutation test for c1 and c2 between the IL and IT conditions, respectively			

Table 13 The difference in the intra- and inter-group connectivity among sub-networks in the upper alpha band between the NE-IL and the NE-IT conditions. The sources of groups A, B, C, and D are depicted in Fig.25.

Intra-group Connectivity Increase		Inter-group Connectivity Increase	
Group A	-(p1=0.4870, ↓p2=0.0356)*	Group A ↔ Group B	-(p1=0.1558, p2=0.5137)
		Group A ↔ Group C	-(p1=0.1589, p2=0.6420)
		Group A ↔ Group D	↑(p1=0.0275, p2=0.2209)
Group B	-(p1=0.2464, p2=0.4444)	Group B ↔ Group C	↑(p1=0.0175, p2=0.4732)
		Group B ↔ Group D	-(p1=0.1072, p2=0.5699)
Group C	↑(p1=0.0293, p2=0.3993)	Group C ↔ Group D	-(p1=0.1200, p2=0.4775)
Group D	-(p1=0.4259, p2=0.2972)		
*p1 and p2 are corrected p-values after multiple comparisons permutation test for c1 and c2 between the IL and IT conditions, respectively			

5.3.2 Connectivity analysis

A connectivity analysis was performed for all possible pairs of 84 Brodmann areas which give rise to a connectivity matrix. Based on which, event-related clustering coefficient was derived for each node that characterizes the node's interaction with the rest of the brain under modulation by the stimulus. Table 14 and Table 15 show the ROIs whose event-related clustering coefficients significantly increased in the upper alpha band in the WE-

IL compared with the WE-IT condition (Table 14) and in the NE-IL compared with the NE-IT condition (Table 15) after multiple comparison permutation test among all the 84 ROIs with corrected $p < 0.05$.

Table 14 Source level clustering coefficient increase in the upper alpha band in the WE-IL relative to the WE-IT condition (corrected $p < 0.05$).

Functional Name	BA/hemisphere	Functional Name	BA/hemisphere
dorsolateral prefrontal cortex	9L	pregenual cortex	33L, 33R
retrosplenial cortex	cingulated 29L	perirhinal cortex	35L, 36L
visual cortex	19L	primary motor cortex	4R
parahippocampal gyrus	27L	inferior temporal cortex	20R
entorhinal cortex	28L, 34L		

Table 15 Source level clustering coefficient increase in the upper alpha band in the NE-IL relative to the NE-IT condition (corrected $p < 0.05$).

Functional Name	BA/hemisphere	Functional Name	BA/hemisphere
visual cortex	19 L, 17R	subgenual cingulated	25 L, 25R
posterior insular cortex	13 L, 13R	granular retrolimbic area	30 L, 30R
superior temporal gyrus	22 L	perirhinal area	35 L
entorhinal area	34 L	posterior transverse temporal area	42 L
subgenual area	43 L	postcentral area	3R
premotor cortex, SMA	6R	orbital area	11R
angular gyrus	39R		

5.3.3 Response time (correlation) analysis

Because the response time of the subject's answer to each question is closely related to the overall processing time spent by all of the involved sub-networks and the key processing nodes in the brain, it can be hypothesized that there may be a quantitative relationship (i.e., linear/non-linear) between the response time and the activity of the sub-networks or key

nodes that contributed most to the variation in processing time. To study this possible relationship, a correlation analysis was performed between the response time and the clustering coefficient of each cortical area which characterizes the node's interaction with the rest of the brain (Fig. 26). The rationale for this is two-fold: i) correlation is a method to study linear relation, while nonlinear relation is more sophisticated and less easily clarified, and ii) as mentioned earlier, all nodes in a specific sub-network share a similar connection pattern with the rest of the brain. Therefore, each node can to some degree be representative of its affiliated sub-network's connection pattern. Although the second consideration has not excluded the correlated behavior of all of the nodes affiliated with the same sub-network, it is sufficient to help identify the potential correlation between response time and the underlying sub-network activity. However, the second consideration is not an issue for the key processing node, which may not be affiliated with a specific network.

A correlation analysis was performed via linear regression analysis, which tests the significance of the positive/negative correlation and produces a linear correlation coefficient. Two kinds of data set were used in the linear regression analysis, i.e., the normalized average response time for each subject in each condition and the normalized average clustering coefficient for each subject in each condition. Averaging was performed across the trials in each condition for the response time and the clustering coefficient to minimize the noise level for the correlation analysis. Normalization was performed for the averaged response time and the event-related clustering coefficient to fall in [0,1] which makes the linear correlation coefficients fall between 0 and 1 as a standard range. As

referenced in the results (Fig. 26), several regions were found to be positively/negatively correlated with the normalized response time; the normalized event-related clustering coefficient for the inferior frontal gyrus (44R) was positively correlated with the response time in the WE-IL condition ($p < 0.05$, with multiple comparison correction (Groppe, Urbach et al. 2011)), and the normalized event-related clustering coefficient of the angular gyrus (39R) and precuneus (7L) was found to be correlated with the response time in the WE-IT condition ($p < 0.05$, with multiple comparison correction (Groppe, Urbach et al. 2011)). However, the normalized event-related clustering coefficient of the secondary auditory cortex (42L) was found to be marginally negatively correlated with the response time in the NE-IL condition ($p = 0.058$), while that of the somatosensory association cortex (5L, R) was found to be negatively correlated with the response time in the NE-IT condition ($p < 0.05$, with multiple comparison correction (Groppe, Urbach et al. 2011)).

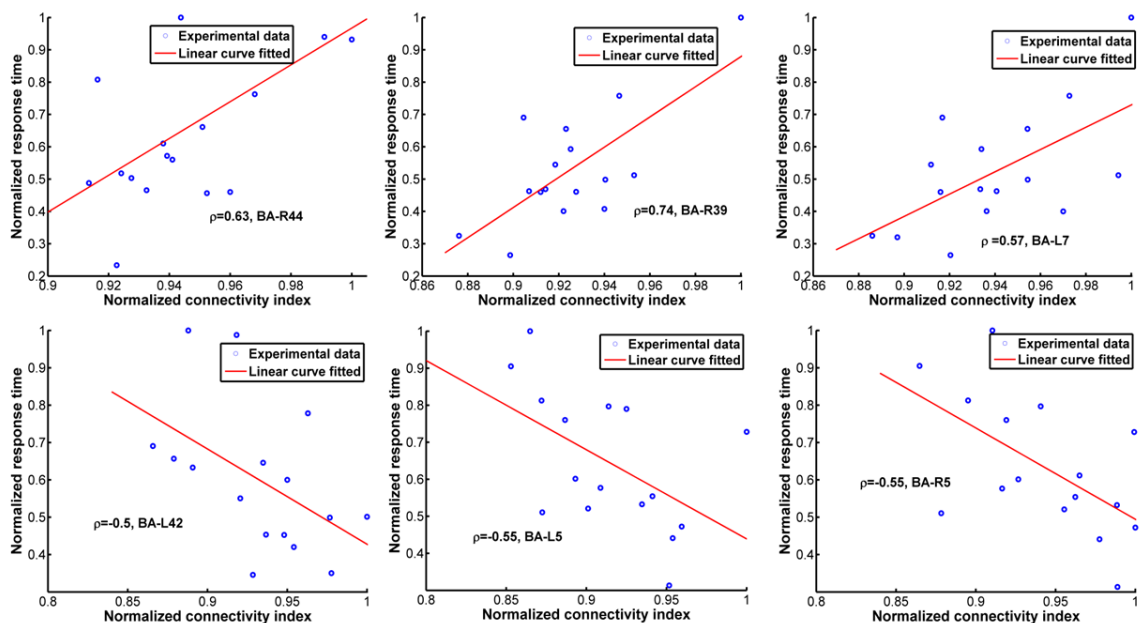


Figure 26 Significant positive correlations were found for between normalized event-related clustering coefficient (NERCC) and normalized response time (NRT) in the WE-IL and the WE-IT conditions. Marginally significant/Significant negative correlations were found for multiple regions between NERCC and NRT in the NE-IL and the NE-IT conditions.

5.4 Discussion

5.4.1 Network analysis

The results of the network analysis are presented in Fig. 22-25 and Table 10-13. It should be noted that the identified sub-networks may be part of a larger hierarchical network. However, because the focus is to identify the common networks shared among the IL and the IT conditions, our discussion may not cover the complete network involved in each condition. Due to the limited length of window analyzed, i.e. the first 2s during SDP, in general, it is most likely that the neuropsychological processes involved are confined to those related with auditory stimulus perception, comprehension of the question, memory recall based on the question being asked, and overall executive control over multiple simultaneous processes. It is no doubt that auditory stimulus perception is a sentinel and must-have component throughout the whole time window. Upon which, comprehension is established through interaction of processing on the perceptual input and retrieval of stored memories, i.e. declarative memory and episodic memory. As such, higher-order executive control unit must be recruited in order to monitor the ongoing processes by integration of input information and navigating the response (i.e. deceptive/truthful) to the question. Most importantly, these are the networks shared by both the IL and the IT conditions. Although

the analyzed window has not covered the deception window directly, this analysis provides a unique perspective from stimulus delivery phase during which there may exist commonalities and differences between conditions as potential features. This narrow window chosen for network analysis bearing more or less predictable underlying sub-processes may potentially initiate an exciting research direction seeking for systematic level of understanding beyond the classic school of thoughts (i.e. inhibition control, saliency detection, risk monitoring) to complement the deception insights.

Among the sub-networks identified for the WE task (Fig 22, 24; Tables 10, 12), it can be postulated that group A may serve as a higher-order executive control network as inferred from the network's neuro-anatomy. Due to the fact that dorsolateral prefrontal cortex (DLPFC), anterior prefrontal cortex (APFC), orbitofrontal area and entorhinal areas are undisputed cortical regions with higher-order functions (Ramnani and Owen 2004, Canto, Wouterlood et al. 2008), it is most likely they synergistically contribute to manage and support other simultaneous cognitive and sensory functions during the time window analyzed. Dorsolateral prefrontal cortex (DLPFC) has been implicated in many higher-order functions, including holding spatial information 'on-line', response selection, verification and evaluation of representations that have been retrieved from long-term memory, monitoring and manipulation with working memory (Ramnani and Owen 2004). In addition, Anterior prefrontal cortex (APFC) has been engaged with a unified role in coordination of information processing and information transfer between multiple operations across supramodal cortex when problems involve more than one discrete cognitive process (Ramnani and Owen 2004). Orbitofrontal area has been implicated in

processes that involve motivational/emotional value of incoming information (Schutter and van Honk 2006), the representation of learnt relationships between arbitrary stimuli and reward/punishment, and integration of these information to guide response, decision making (Ramnani and Owen 2004). Entorhinal area has been considered as a hub functioning in a widespread network for memory and navigation (Hafting, Fyhn et al. 2005). This cortex, in conjunction with the hippocampal formation, appears to specifically deal with the translation of neocortical exteroceptive information into higher order complex representations that, when combined with motivational and interoceptive representations, serves cognitive functions, in particular conscious memory and relational organization of memory (Eichenbaum, Yonelinas et al. 2007). Compared with the above regions, subgenual cingulate has less higher order role but has been demonstrated to play an integral role in both normal and pathological shifts in mood (Gotlib, Sivers et al. 2005) and processing of positively or negatively valenced stimuli (Hamilton, Glover et al. 2011). As such, it can be seen that all the above regions are well postulated to form a network executing 'higher-order' functions to support and manage multiple simultaneous processes during the task.

Given the neuro-anatomy of group B, it can be inferred that this group may contribute to multi-modal contextual association and object recognition in support of comprehension and memory processing. The neuro-anatomy seems to infer the involvement of the ventral stream pathway. This processing pathway usually begins with purely visual information in the primary visual cortex (occipital lobe), and then this information is transferred to the temporal lobe. This pathway is mainly involved in object recognition (i.e. the 'what'

pathway), and is connected to the medial temporal lobe (which is involved in the storage of long-term memories) (Hebart and Hesselmann 2012). Although no visual stimulus has been used in the experiment, visual cortex can be activated by visual imagery of the objects contained in the stimulus (Bridge, Harrold et al. 2012) considering the fact that most of the stimulus tend to induce declarative and episodic memory with requirement to recall specific objects. Not surprisingly, temporal regions such as rostral parahippocampal gyrus and perirhinal cortex involve in this network. Previous studies have shown perirhinal cortex plays an important role in recognition memory by facilitating the recognition and identification of the stimuli through stimulus-stimulus (i.e., word-object) associations (Murray, Bussey et al. 2007). Rostral parahippocampal gyrus as a portion of parahippocampal gyrus, located at the medial temporal lobe, is a key structure in declarative and episodic memory processing (Aminoff, Kveraga et al. , Blaizot, Martinez-Marcos et al. 2004). Recently, a broad synthesis of literature has unified the various functions of this area by the theory of ‘contextual association’, i.e. to define, represent items by bringing meaning to the environment and establish links between these contextual items (Aminoff, Kveraga et al.). The granular retrosplenial cortex and agranular retrolimbic area have also been linked with cross-modal object recognition by observing rats with lesions in these regions performing cross-modal object recognition task (Hindley, Nelson et al. 2014), hence suggesting their role in mediating the integration of information across multiple cue types.

Similar to group B, group C is inferred to be participating as a portion of network to support the comprehension and memory-processing processes. It has been suggested in previous

studies that the anterior medial parietal/posterior cingulate cortex is concerned with linking information with prior knowledge (Lou, Luber et al. 2004), and has repeatedly been associated with episodic memory retrieval (Cabeza and Nyberg 2000). Previous studies have found that precuneus is involved in a wide spectrum of highly integrated tasks, including visuo-spatial imagery, episodic memory retrieval and self-processing operations, namely first-person perspective taking and an experience of agency (Cavanna and Trimble 2006). Studies have also shown that occipitotemporal area plays an important role in constructing scenes from objects by supporting recognition of real-world visual scenes through parallel analysis of within-scene objects (MacEvoy and Epstein 2011). Moreover, the angular gyrus has been considered as a cross-modal hub where converging multisensory information is combined and integrated to comprehend and give sense to events, manipulate mental representations, and reorient attention to relevant information (Seghier 2013). It can be inferred further that these above regions play a central role to facilitate recognition of real-world visual scenes/events and give sense to these scenes/events through a first-person perspective. Compared with group C, group B seems to be more associated with function in establishing contextual association (i.e. word-object) and object recognition, and both contribute as part of a network that support comprehension and memory processing. Nevertheless, group B seems to be associated more with ventral stream pathway, and group C is more associated with dorsal stream pathway.

Different from the former three groups, group D involves mostly perception related regions, and it is most likely a network contributing to auditory and language processing. Auditory cortex is a classic highly organized region that perceives sound, and this cortex area is the

neural crux of hearing for humans in language and music (Purves D 2001). Superior temporal gyrus has been associated with various functions, among which, the most likely function in this experiment is the auditory processing as a key sensory structure contributing to comprehension of language (Friederici, Rüschemeyer et al. 2003, Leff, Schofield et al. 2009). The superior temporal gyrus known as Wernicke's area is one of the human speech areas involved in the understanding of written and spoken language (Wise, Scott et al. 2001). The Wernicke's area in the non-dominant hemisphere is involved in processing and resolution of subordinate meanings of ambiguous words, while the counterpart in the dominant hemisphere is associated with processing dominant word meanings. In addition, previous fMRI study has found subcentral area's involvement in semantic processing, and it is activated when participants are asked to complete tasks which involved the selection of a verbal response from many possible responses (Gabrieli, Poldrack et al. 1998). As an intrinsic and implicit requirement of our experiment, when subjects listen to the questions, their brains are engaged in looking for possible verbal response simultaneously. Involvement of the somatosensory system in the perceptual processing in speech is not clearly known until recent studies have shown that somatosensory input has modulation effect on speech perception (Ito, Tiede et al. 2009, Champoux, Shiller et al. 2011). Similarly, involvement of motor areas such as primary motor cortex and premotor cortex in speech perception can be linked to the concept that perception and production are mediated by common mechanisms originates in the motor theory of speech (Lieberman, Cooper et al. 1967, Lieberman and Mattingly 1985), evidence to date for the link between perception and production comes exclusively from

demonstrations of cortical motor activation in conjunction with speech perception (Fadiga, Craighero et al. 2002, Watkins, Strafella et al. 2003, Meister, Wilson et al. 2007), and is related to articulating speaker's gesture (Meister, Wilson et al. 2007) or mapping articulatory features of speech sounds (Pulvermüller, Huss et al. 2006). According to the neuro-anatomy for language/speech perception, part of parietal region is also involved. Specifically, supramarginal gyrus is thought to be probably involved with language perception and processing (e.g. in phonemic perception and the processing of speech sounds), since lesions in it may cause receptive aphasia (Dehaene-Lambertz, Pallier et al. 2005, Gazzaniga 2009). Primary somatosensory cortex and ventral anterior cingulate area are not typical regions associated with semantic processing; however, ventral anterior cingulate area has been related to self-referential processing of negative stimuli in semantic processing (Yoshimura, Ueda et al. 2009) and primary somatosensory cortex (postcentral gyrus) is involved in attentional and linguistic interactions in speech perception (Sabri, Binder et al. 2008).

Although there is no nominal reference to a specific source and its definitive network category or vice versa, the data-driven functional network results obtained in this study are reasonably justifiable. It is not surprising that the sub-networks identified are neuropsychological processes that appear to be necessarily involved during the analyzed window. Therefore, the top-down perspective of network analysis appears to match well with the data-driven networks.

In within- and between- network analysis, the results from Table 12 show that p1 has a greater significant difference compared with p2 while nearly maintaining the same trend

of p_2 , which means that a normalized connectivity is potentially more sensitive than an unnormalized connectivity in distinguishing the two conditions in the WE task. An increased trend for inter-group connectivities was found for groups A; this increase is marginally significant ($p < 0.1$) and could be interpreted as increased communicative activity within the higher-order executive control group that was induced by the cognitive load of deception. The inter-group connectivity was calculated based on the summation of all non-repeated paired connectivity values between two regions that belonged to the two different groups. Significant increases were found among several pairs of groups; connections significantly increased between i) group A ↔ group B, ii) group A ↔ group C, iii) group A ↔ group D, iv) group B ↔ group D and v) group C ↔ group D. As inferred on each network's most likely functional role, group A as a higher-order executive area represents an extensive increased communicative activity with the parallel memory processing, comprehension, speech perception processes. This further implies the higher-order role of group A in the IL condition, and that the IL condition in the WE task potentially induces enhanced executive control activities, even during the stimulus delivery phase. Furthermore, increased connectivities between B and D, C and D imply that speech perception more closely interacts with comprehension and memory processing to facilitate the deception process.

A functional network analysis was also applied for the NE-IL and NE-IT conditions. The results are shown in Fig. 23, 25 and Table 11, 13. Again, four groups were identified as sub-networks. Interestingly, these functional networks are the exact sub-networks that were identified for the WE task with minor variation in the network component. As shown in

Table 13, a significant decrease of intra-network connectivity has been observed based on the p2 index for group A in the NE-IL condition relative to the NE-IT condition. This is most likely because this group's higher-order function could be less efficiently executed when the subjects had no prior experience related to the questions. But since this index is not normalized, this result is still arguable. In contrast, intra-network connectivity increased in group C for the p1 index possibly due to the increased load in comprehension and memory-recall of questions non-experienced by the subjects. However, significant increases in the inter-network connectivities based on the p1 index have been observed i) between group A ↔ group D and ii) group B ↔ group C. This means the interaction within network possibly responsible for memory processing and relevant comprehension processes increased, since group B and C both partially contribute as sub-network. In addition, connectivity between networks possibly related to executive control and speech perception increased, which implies speech perception for unfamiliar items may need increased cognitive input from executive network in order to make sure the auditory information can be stored well in short-term memory for accurate comprehension.

In summary, the application of dendrogram analysis enables us to understand the most likely fundamental common processing units shared by the WE and NE tasks. It can be observed that the formation of all of the groups in the NE task are very similar to the corresponding groups in the WE task, indicating the potential role of these sub-networks as fundamental building blocks for the instructed lying/truth-telling tasks that involve the processing of auditory questions; the robustness of this result has been cross-validated by the two tasks. However, this result does not exclude the possibility for diversified extra

sub-networks to participate in each of these tasks due to the fact that only the first 2s during stimulus delivery window was analyzed. The network derivation has not yet been cross-validated in other studies; thus, it is important to re-affirm the interpretation of the functional role of these sub-networks via cross-validation with fMRI studies in the future.

5.4.2 Connectivity analysis

In a further analysis as shown in Table 14, multiple memory processing regions were found with an increased overall clustering coefficient in the IL with respect to the IT condition. Because the clustering coefficient summarizes a particular ROI node's overall connection strength to the remaining regions, an increased clustering coefficient for these 'heat nodes' further corroborates the dominant role of higher-order execution and memory processing in the WE deception task. The corresponding result for the NE task is shown in Table 15, significantly increased clustering coefficients were found for several higher-order execution areas, memory processing/comprehension areas and speech perception areas. This increase in higher-order execution areas does not violate the observed decreased intra-network connectivity in the corresponding network. Different from inter-group connectivity; the clustering coefficient for a node is a more general evaluation of connectivity with respect to the rest of the brain. The trend between them does not necessarily correlate. Among all nodes, the visual cortex (19L), dorsolateral prefrontal cortex (9L) and entorhinal cortex (34L) are common heat nodes with increased clustering coefficients for both tasks (WE vs. NE). This finding fits well with the hypothesis that

deception involves executive control over memory processing and can possibly be universally a rule for various types of instructed lying.

5.4.3 Response time (correlation) analysis

Interestingly, the normalized event-related clustering coefficient for the inferior frontal gyrus (44R, Broca's area) is positively correlated with the normalized response time in the WE-IL condition; this implies an increased amount of effort in executive control (as required in the IL condition), which leads to a delayed response time. Recent neuroimaging studies show BA44's involvement in selective response suppression in a go/no-go task; BA44 is therefore believed to play an important role in the suppression of response tendency (Forstmann, van den Wildenberg et al. 2008). The normalized event-related clustering coefficients for precuneus (7L) and angular gyrus (39R), which are associated with comprehension/memory-processing in this study, show positive correlations with the normalized response time in the IT condition, indicating that comprehension/memory-processing could be processes that primarily contribute to the response time in this condition. However, a reverse trend of correlation was found for the NE task. The normalized event-related clustering coefficient of the secondary auditory cortex (42L) was found to be marginally negatively correlated with the response time in the NE-IL condition. Additionally, the normalized event-related clustering coefficients of the somatosensory association cortex (5L, 5R) were found to be negatively correlated with the response time in the NE-IT condition. It is known that both the secondary auditory cortex (42L) and the somatosensory association cortex (5L, 5R) are involved in sensory-level speech perception.

For both regions, increased clustering coefficients in the IL condition imply their role in facilitating the semantic processing of stimuli. This largely explains the variation of response times between the NE-IL and the NE-IT conditions. This dominance by speech perception in both conditions may be due to the subjects' not having experiential knowledge of the stimuli, which requires them to spend even more time on speech perception. This also implies that well-designed probe stimuli (i.e., questions) play an important role in inducing neuronal features regarding the semantic processing during the lying task.

5.5 Concluding Remarks

The results of this study have provided intuitive evidence for distinguishable features of instructed lying with respect to instructed truth-telling conditions in network scale from EEG signals analysis in both the WE and the NE tasks during the stimulus delivery phase. The data analyzed with connectivity analysis/network analysis in the source space indicated contrastive network connection and nodal clustering coefficient patterns between the IL and IT conditions. Importantly, this study identified several fundamental processing units during the SDP that are common to all of the conditions. However, the involvement of these networks should be thoroughly investigated in the future with more instructed lying/truth-telling tasks and imaging modalities. As predicted, the major differences between the IL and IT conditions exist within the intra- and inter- group connectivity patterns. In addition, response time has been correlated with several key nodes' clustering coefficients. As such, this study has provided a systematic level of understanding of the

neural mechanisms underlying the IL and IT tasks based on a unique window of analysis, i.e. SDP with network analysis, and the results may be of great importance for future lie detection related researches and applications.

CHAPTER 6

USE JUDGMENTAL FEEDBACKS TO STUDY EVENT-RELATED ELECTRICAL NEURAL RESPONSE BY LIARS AND INNOCENTS

Despite decades of researches in the neuronal mechanism of deception, this complex neuropsychology phenomenon remains obscure. Most of the previous studies followed the intuitive clue to study deception during the deception process. In contrast to previous studies, this study proposed a novel EEG-based protocol that investigates the subjects' responses to judgmental feedbacks. The hypothesis is that liars and innocents could be differentiated by neural responses towards judgmental feedbacks expressing trust or doubt to their answers. We elicited instructed and spontaneous lying/truth-telling in a virtual custom inspection task. Four types of feedback combinations were investigated by permutations and combinations of lying/truth-telling with trust/doubt feedbacks. An event related potential analysis (ERP) was performed to identify spatial-temporal signatures that distinguish lying from truth-telling. Independent component analysis and source localization were employed to elucidate the neural anatomy basis of the observed (ERP) differences.

6.1 Introduction

Most previous studies focused on the deception execution window for investigation of neural correlates of deception. Few studies have ever looked into other phases of deception. This might be due to the natural belief that deception is more directly manifested during the execution window. However, deception is a complicated process that involves the mentality as a liar from the beginning to the end and could even sustain until the subjects receive the interrogator's judgmental feedback. In this study, a virtual custom inspection role play task has been developed which is adapted from a prior work that successfully elicit deceptive response by mimicking real-life scenarios where lying involves potential financial risk or reward (Seth, Iversen et al. 2006). Unlike the previous studies, this study focuses on brain activity elicited by the judgmental feedback given by the virtual custom officer post lying. The hypothesis for this study is that liars and innocents could be differentiated by their neuro-physiological responses towards judgmental feedbacks expressing either trust or doubt in their answers (i.e. 'trustful' and 'doubtful' feedbacks). The novelty and advantage of this experimental protocol is the relative independency of specific probe questions or item pictures used to induce subjects' lying brain responses; furthermore, it can empower all the other existing EEG-based lie detection protocols by inclusion of an additional 'feedback'/'post feedback' session that might facilitate lie detection. Excitedly, our study has identified an incongruity-sensitive feature that lies in the ERP waveform P400/N400 as well as N500 and can be used as a unique signature to differentiate lying and truth-telling in both instructed and spontaneous conditions. Both of

these ERP waveforms may precisely illustrate the mentality of innocents after receiving ‘doubtful’ feedbacks by reflecting innocents’ emotional/cognitive conflict processing towards incongruous feedbacks. Given these encouraging findings, this attempt can potentially improve the overall detection accuracy and might be helpful for the design of future lie-detection machines.

6.2 Data analysis

The event related potential (ERP) for each subject in each condition was achieved by removing the baseline signal (using average over the time window: -500ms to 0ms) and averaging over all of the baseline-removed trials in corresponding conditions. To extract the components that contribute to the condition difference, Independent component analysis (ICA) was applied to de-compose the combined raw EEG datasets from the corresponding four conditions in each task as a single dataset into sixty-two independent components respectively with the help of Infomax ICA algorithm (Bell and Sejnowski 1995). Spatial components were screened for contribution to the grand averaged ERP signals in time window 200ms-500ms, which is our time of interest. Components that are considered significant contributors to this time window is selected and further analyzed by the Principle component analysis (PCA) algorithm. The output from this two stages ICA-PCA analysis is the several PCs of interest that contribute significantly to the ERP signals. Furthermore, Standardized low-resolution brain electromagnetic tomography (sLORETA) (Pascual-Marqui 2002) was used to localize the neuro-anatomies for the PCs of interest

with a source solution space consisting of 6,239 voxels (voxel dimensions 5×5×5 mm) that was restricted to the cortical gray matter and hippocampi as defined according to the MNI atlas (Mazziotta, Toga et al. 2001). sLORETA is most suitable for calculation of distributed cortical sources or limited amount of focal cortical sources with distinct field, given the low spatial resolution of this technique (Wagner, Fuchs et al. 2004). Therefore, sLORETA is most likely a suitable source localization method for estimating sources when the underlying sources are limited, for example, the sources for each specific PC which produce distinct field.

For statistical analysis, the scalp ERPs for each subject in each condition were grouped into 4 different anatomical sectors, i.e., Frontal: Fp1, Fpz, Fp2, AF7, AF3, AF4, AF8, F7, F5, F3, F1, FZ, F2, F4, F6, F8; Frontal-central: FT7, FC5, FC3, FC1, FCz, FC4, FC6, FT8, T7, C5, C3, C1, Cz, C2, C4, C6, T8; Central-parietal: TP7, CP5, CP3, CP1, CPz, CP2, CP4, CP6, TP8, P7, P5, P4, P1, Pz, P2, P4, P6, P8; Parietal-occipital: PO7, PO5, PO3, POz, PO4, PO6, PO8, O1, O2, Oz. To test the significance of the observed ERP trend, four-way analysis of variance (ANOVA) was at first performed to evaluate factors of lying/truth-telling, electrodes sector, time point, ‘doubted’/‘trusted’ feedbacks and their interaction effects during the time window 260ms-520ms. In the post-hoc analysis, the ‘check’ group and the ‘trust’ group are compared separately with multiple comparison permutation test (correction with a ‘tmax’ method that controls family-wise error rate (Blair and Karniski 1993) with 5000 times permutations, this permutation method is more powerful than Bonferroni correction when different variables in the test are correlated) were performed simultaneously for all the sectors based on mean amplitude of ERPs calculated across time

points from 260ms to 520ms in order to identify the specific scalp sectors that contribute to the significant differences among conditions. For each time point, the averaged ERP data within a narrow forward window of 8ms was calculated and used for multiple comparison permutation test across the four electrode sectors.

6.3 Results

6.3.1 Event Related Potentials (ERP)

As shown in Fig.27, dynamic waveforms for the across-subjects grand mean averaged ERP on sampled frontal and parietal-occipital electrodes are demonstrated. In each sub-figure (Fig. 27(a-f)), post judgmental feedback ERPs on a particular example electrode (i.e., Fz, POz, Oz) are compared within two pairs of conditions (i.e., IL-IT and SL-ST). It can be observed that, IT-check/ST-check show higher negativity in frontal electrodes, and higher positivity in parietal-occipital electrodes compared with the remaining conditions at around 400ms, which corresponds to the P400/N400 peak. It is also noticeable that the SL-trust condition manifests higher positivity in the frontal/frontal-central electrodes, and higher negativity in parietal-occipital electrodes compared with the ST-trust condition. In Fig.28, topographic demonstration of the across-subjects grand mean averaged ERP difference between paired conditions, IL-IT, SL-ST in window 1 (P400/N400 peak) indicate that, frontal/frontal-central and central-parietal/parietal-occipital electrodes are the most sensitive spatial regions to the condition differences.

According to the results in ANOVA analysis, there are significant condition (i.e. lying vs. truth-telling) ($F=5.71$, $p=0.02$), electrode ($F=2457.59$, $p<10^{-5}$), interaction condition \times electrode factor ($F=64.98$, $p<10^{-5}$), interaction feedback \times electrode factor ($F=30.08$, $p<10^{-5}$) and marginally significant feedback (i.e. 'check' vs. 'trust') ($F=2.73$, $p=0.0984$) factors among the four conditions in the spontaneous lying task. There is marginally significant factor of condition ($F=2.64$, $p=0.10$), significant interaction condition \times electrode factor ($F=28.14$, $p<10^{-5}$) and significant interaction feedback \times electrode factor ($F=44.52$, $p<10^{-5}$) in the instructed lying task. In the post-hoc analysis, for each narrow time window, the corresponding electrode sectors that show significance value <0.05 were listed in Table 16-19 for the four groups in the spontaneous-lying task and in Table 20-21 for the two groups in the instructed-lying task. The tables show the corresponding time window, spatial sectors, mean and standard deviation of the electrical potential for the spatial sectors and their p-values for all the paired conditions for the 'check' group and the 'trust' group separately.

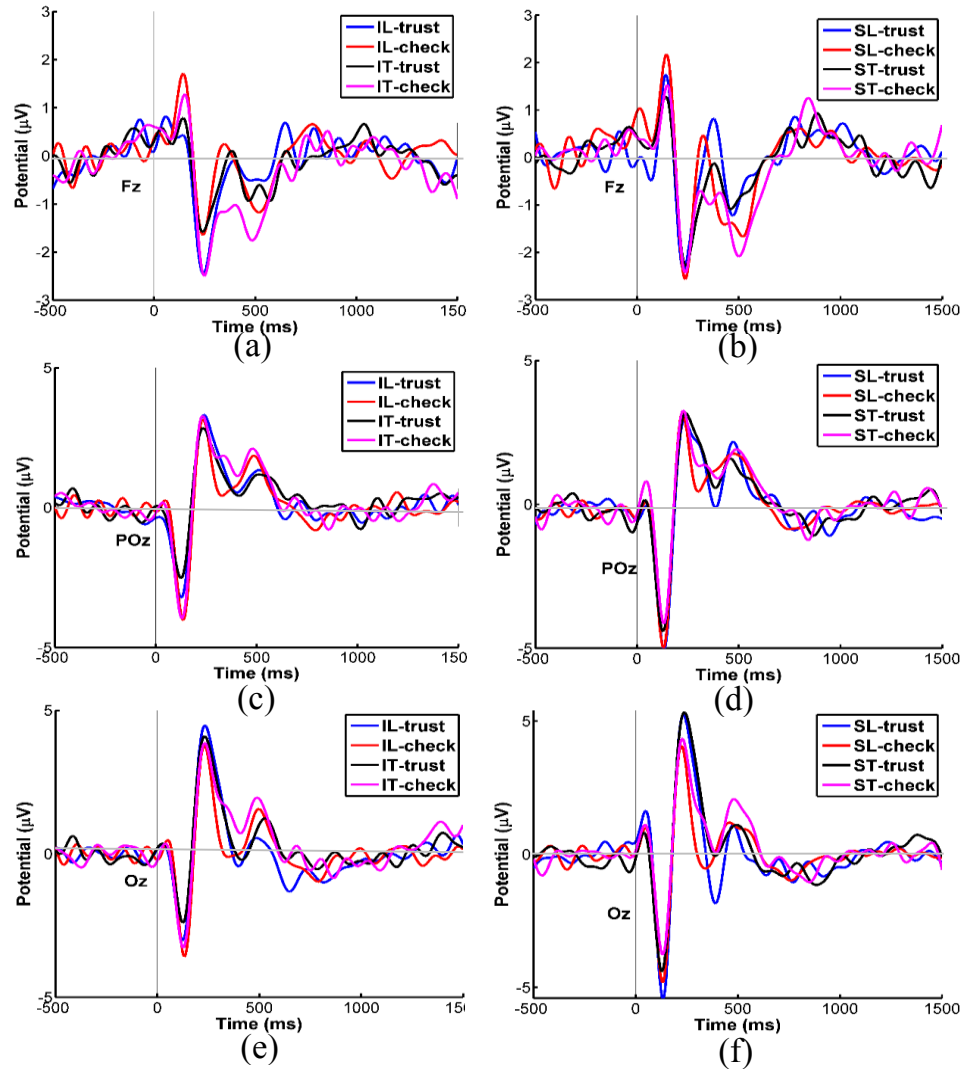


Figure 27 Across-subjects grand mean averaged ERP signals on example frontal electrode Fz and parietal-occipital electrodes POz and Oz in the IL, IT conditions (a,c,e) and in the SL, ST conditions (b,d,f).

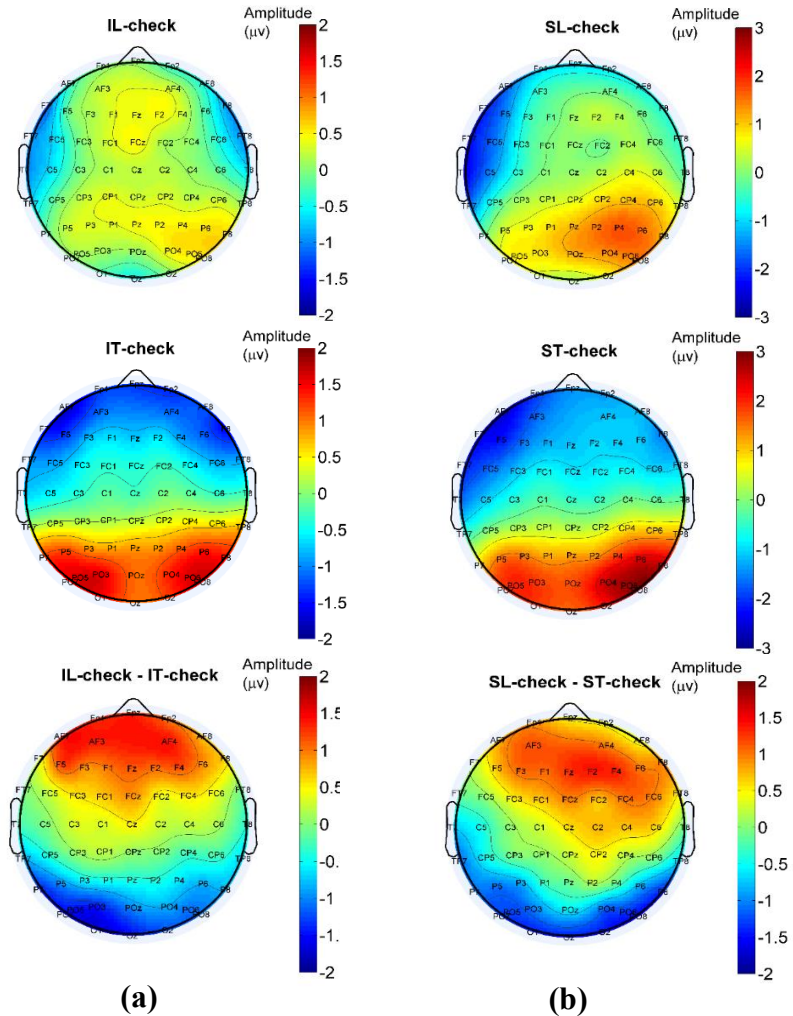


Figure 28 The topographical scalp maps of the across-subject grand mean average voltage in the significant time window for the ‘check’ group in (a).instructed and (b).spontaneous lying/truth-telling task, and the corresponding condition differences.

Table 16 Time point and corresponding electrode sectors that show significant difference between the SL-check and the ST-check conditions.

Time window (ms)	Electrode sector(s)	Electric potential: mean (SD) for the SL-check condition	Electric potential: mean (SD) for the ST-check condition	Significant value (p)
328-336	Frontal	-0.36 (1.27)	-1.49 (1.55)	0.033
	Frontal-central	-0.36 (0.74)	-0.82 (0.58)	0.011
	Parietal-occipital	0.43 (1.65)	2.11 (1.46)	0.002
336-344	Frontal	-0.35 (1.43)	-1.43 (1.42)	0.037
	Frontal-central	-0.37 (0.75)	-0.78 (0.62)	0.012
	Parietal-occipital	0.32 (1.59)	1.98 (1.55)	0.002
344-352	Frontal-central	-0.42 (0.77)	-0.70 (0.72)	0.034
	Parietal-occipital	0.29 (1.58)	1.70 (1.52)	0.005
352-360	Parietal-occipital	0.37 (2.08)	1.43 (2.07)	0.006
360-376	Parietal-occipital	0.51 (2.17)	1.14 (2.15)	0.012

Table 17 Time point and corresponding electrode sectors that show significant difference between the SL-trust and the ST-trust conditions.

Time window (ms)	Electrode sector(s)	Electric potential: mean (SD) for the SL-trust condition	Electric potential: mean (SD) for the ST-trust condition	Significant value (p)
336-344	Frontal	-0.49 (1.90)	-1.52 (1.74)	0.027
344-352	Frontal	-0.29 (1.80)	-1.33 (1.68)	0.036
392-400	Parietal-occipital	0.039 (0.77)	-0.17 (0.92)	0.031
400-408	Parietal-occipital	0.11 (0.69)	-0.25 (0.82)	0.006

408-416	Frontal-central	0.11 (0.68)	-0.32 (0.78)	0.037
	Parietal-occipital	-0.74 (1.78)	0.67 (1.71)	0.005
416-424	Frontal-central	0.01 (0.65)	-0.32 (0.73)	0.044
	Parietal-occipital	-0.37 (1.49)	0.73 (1.60)	0.014

Table 18 Time point and corresponding electrode sectors that show significant difference between the ST-check and the ST-trust conditions.

Time window (ms)	Electrode sector(s)	Electric potential: mean (SD) for the ST-check condition	Electric potential: mean (SD) for the ST-trust condition	Significant value (p)
392-400	Central-parietal	1.09 (0.87)	0.51 (0.67)	0.027
400-408	Central-parietal	1.13 (0.87)	0.61 (0.74)	0.031
440-448	Frontal-central	-0.77 (0.63)	-0.39 (0.54)	0.014
448-456	Frontal-central	-0.78 (0.61)	-0.38 (0.54)	0.007
456-464	Frontal-central	-0.74 (0.56)	-0.35 (0.56)	0.011
	Parietal-occipital	1.77 (1.22)	0.89 (1.03)	0.05
464-472	Frontal-central	-0.75 (0.55)	-0.36 (0.58)	0.021
	Parietal-occipital	1.94 (1.19)	1.03 (1.05)	0.032

Table 19 Time point and corresponding electrode sectors that show significant difference between the SL-check and the SL-trust conditions.

Time window (ms)	Electrode sector(s)	Electric potential: mean (SD) for the SL-check condition	Electric potential: mean (SD) for the SL-trust condition	Significant value (p)
376-384	Frontal-central	-0.57 (0.79)	-0.13 (0.85)	0.023
	Parietal-occipital	0.64 (1.86)	-0.35 (1.86)	0.019
384-392	Frontal-central	-0.53 (0.73)	-0.04 (0.85)	0.023
	Parietal-occipital	0.66 (1.72)	-0.45 (1.87)	0.013
392-400	Frontal-central	-0.54 (0.68)	0.04 (0.77)	0.005
	Parietal-occipital	0.76 (1.59)	-0.63 (1.68)	0.004
400-408	Frontal-central	-0.58 (0.65)	0.11 (0.68)	0.0008
	Parietal-occipital	0.98 (1.43)	-0.82 (1.68)	0.001
408-416	Frontal	-1.46 (1.16)	-0.42 (1.32)	0.041
	Frontal-central	-0.64 (0.68)	0.11(0.68)	0.001
	Parietal-occipital	1.26 (1.37)	-0.74 (1.68)	0.0002
416-424	Frontal	-1.49 (1.13)	-0.66 (1.31)	0.050
	Frontal-central	-0.69 (0.74)	-0.01 (0.65)	0.006
	Parietal-occipital	1.45 (1.46)	-0.37 (1.49)	0.0008
424-432	Frontal-central	-0.74 (0.82)	-0.13 (0.60)	0.013
	Parietal-occipital	1.45 (1.49)	0.034 (1.38)	0.001
432-440	Frontal-central	-0.76 (0.85)	-0.25 (0.54)	0.021
	Parietal-occipital	1.34 (1.53)	0.32 (1.37)	0.004
440-448	Frontal-central	1.27 (1.52)	-0.37 (1.37)	0.015

Table 20 Time point and corresponding electrode sectors that show significant difference between the IL-check and the IT-check conditions.

Time window (ms)	Electrode sector(s)	Electric potential: mean (SD) for the IL-check condition	Electric potential: mean (SD) for the IT-check condition	Significant value (p)
336-344	Frontal-central	-0.55 (0.75)	-1.01 (0.62)	0.016
	Parietal-occipital	0.35 (1.21)	1.10 (0.94)	0.028
344-352	Frontal	-0.11(1.70)	-1.63(1.38)	0.043
	Frontal-central	-0.53(0.63)	-0.94(0.83)	0.026
	Central-parietal	0.32 (1.12)	1.07 (0.90)	0.038
	Parietal-occipital	0.53 (2.15)	2.38 (2.02)	0.030
352-360	Frontal	-0.06 (1.19)	-1.53 (1.36)	0.032
	Central-parietal	0.29 (1.12)	1.01(0.82)	0.028
	Parietal-occipital	0.48 (2.28)	2.18 (2.06)	0.034
360-368	Frontal	-0.12 (1.23)	-1.50 (1.99)	0.034
	Central-parietal	0.34 (0.96)	1.01(0.88)	0.040

Table 21 Time point and corresponding electrode sectors that show significant difference between the IT-check and the IT-trust conditions.

Time window (ms)	Electrode sector(s)	Electric potential: mean (SD) for the IT-check condition	Electric potential: mean (SD) for the IT-trust condition	Significant value (p)
344-360	Frontal	-1.63 (1.38)	-0.41 (1.64)	0.038
	Central-parietal	1.07 (0.90)	0.45 (0.92)	0.050

432-440	Frontal	-1.30 (1.32)	-0.41 (0.92)	0.025
440-448	Frontal	-1.40 (1.36)	-0.35 (1.02)	0.010
	Central-parietal	1.08 (1.00)	0.52 (0.61)	0.050
	Parietal-occipital	1.65 (1.25)	1.07 (1.07)	0.043
448-456	Frontal	-1.49 (1.39)	-0.40 (1.00)	0.015
	Central-parietal	1.12 (0.98)	0.55 (0.65)	0.040
	Parietal-occipital	1.66 (1.32)	0.35 (1.18)	0.032

6.3.2 Independent Component Analysis (ICA) & ERP reconstruction

The baseline-removed data from all the involved conditions after pre-processing were concatenated into a single dataset as input to the independent component analysis (ICA) for the instructed/spontaneous tasks respectively. Through ICA analysis, four major spatial components were found significantly contributing to the P400 components, and eight major spatial components were found significantly contributing to the N400 and meanwhile contributing to the N200 components. The four spatial-temporal components that contribute to the P400 components explain 13% of the variance of the combined ERP datasets, and the eight spatial-temporal components that contribute to the N400 component explain 55% of the variance of the combined ERP datasets. These four P400-related and eight N400-related components were summed up respectively and further analyzed by principle component analysis (PCA), the major PCs contribute to 60% and 58% of the variance of the summed P400-related and N400-related signals respectively. As such, the

two major PCs that represent P400-related and N400-related components contribute to 8% and 32% of the variance of the grand averaged ERP signals.

As shown in Fig.31, the frontal component was found to be a main contributor to both the P400 component, and the central-parietal component was found to be a main contributor to the N400-related component. Meanwhile, these two components both partially contribute to the N500 component. These components were defined as PC-P400 and PC-N400. The confirmation on the contribution of PC-P400 and PC-N400 to the original ERP was achieved by ERP reconstruction of each component to the scalp voltage potential on selected frontal and parietal-occipital electrodes, i.e., Fz, POz and Oz electrodes as shown in Fig.31-32. The reconstruction was done by multiplying the corresponding extracted spatial and temporal components from the factorized spatial- and temporal-coded matrix derived from PCA and mapped onto the scalp electrodes.

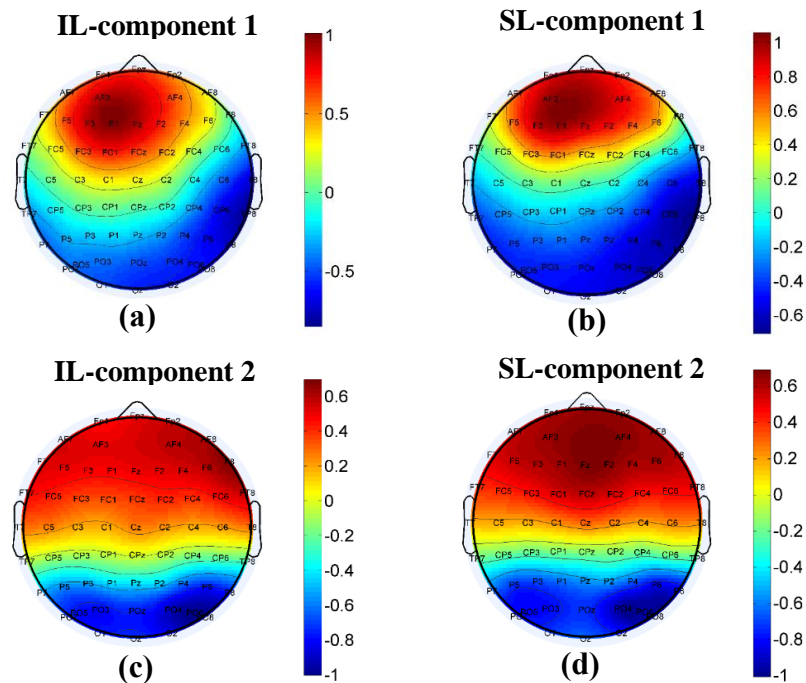


Figure 29 Topography of the major PCs that contribute to the salient ERP signals in instructed/spontaneous tasks. (a) and (b) are major frontal components that contribute to the P400 and partially to the N500 components. (c) and (d) are major central-parietal components that contribute to the N400 and partially to the N500 components.

6.3.3 EEG Source localization (sLORETA) for PC-P400 and PC-N400

The EEG source localization results in Fig.30 show the corresponding neuro-anatomies for each individual PC. Results show that the major contributors to the PC-P400 and PC-N400 for both the IL-IT and SL-ST conditions are frontal sources located primarily in inferior, superior, medial frontal gyrus and anterior cingulate gyrus as well as central sources located in cingulate gyrus. These sources are the nominal PC-P400, which produce peak with positive polarity at around 400ms. In addition, Fig.30 indicates that the major contributors to the PC-N400 for both the IL-IT and SL-ST conditions are central-parietal sources located primarily in precuneus, cingulate gyrus, superior parietal lobe, fusiform gyrus and parahippocampal gyrus. The local maximum sources' coordinates, brodmann areas, and anatomical regions have been listed in Table 22-23 for the instructed and spontaneous tasks respectively. As such, these source localization results provide neuro-anatomical basis for the observed differences that lie in the P400 and N400 components. In addition, the N500 component distributes over larger brain area as it could be contributed by the neuro-generators for the P400 and N400 components simultaneously.

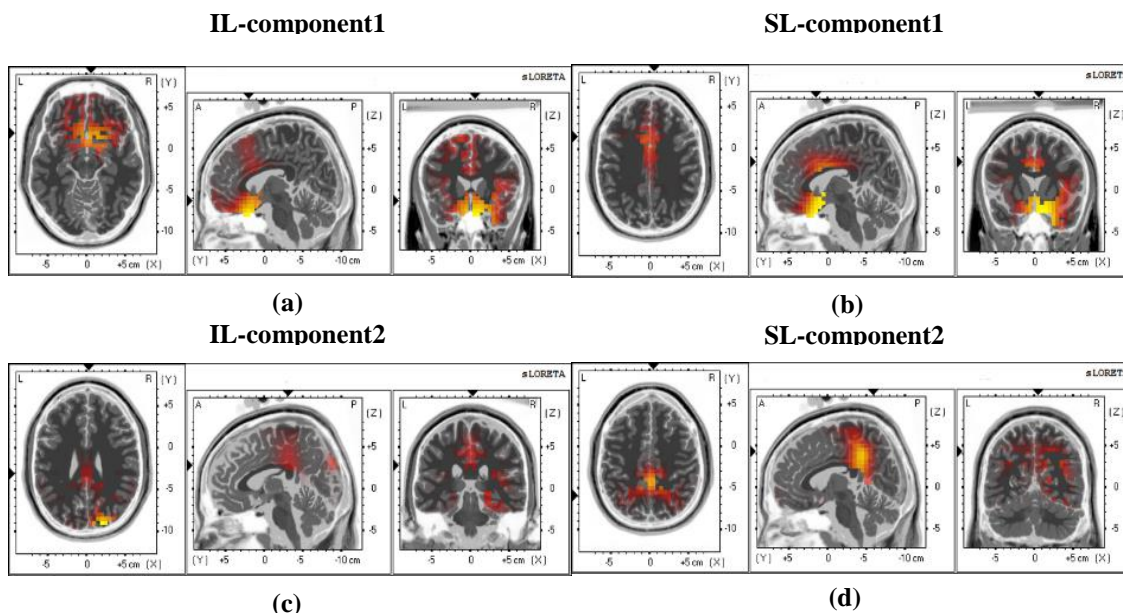


Figure 30 Source localization results for the corresponding PCs identified through ICA-PCA analysis. Frontal sources mainly contribute to the P400 component for (a). the IL-IT conditions and (b). the SL-ST conditions. Central-parietal sources mainly contribute to the N400 component for (c).the IL-IT conditions and (d). the SL-ST conditions.

Table 22 Coordinates, brodmann area, anatomical regions for nodes with biggest local source strength for the identified two major PCs in the instructed lying task.

Condition	X	Y	Z	Brodmann Area	Anatomical Region
Instructed task Component 1	5	26	54	8	(R) Superior frontal gyrus
	-7	26	54		(L) Superior frontal gyrus
Instructed task Component 1	2	15	35	32	(R) Cingulate gyrus
	-9	15	34		(L) Cingulate gyrus
Instructed task Component 1	2	17	30	24	(R) Cingulate gyrus
	-8	14	30		(L) Cingulate gyrus
	4	17	25		(R) Anterior cingulate gyrus
	-10	21	25		(L) Anterior cingulate gyrus
Instructed task Component 1	23	19	-26	47	(R) Inferior frontal gyrus
	-13	28	-23		(L) Inferior frontal gyrus

Instructed task Component 1	2 6 -6	15 27 27	-9 -20 -21	25	(R) Anterior cingulate gyrus (R) Medial frontal gyrus (L) Medial frontal gyrus
Instructed task Component 2	3 -3	-35 -41	37 44	31	(R) Cingulate gyrus (L) Cingulate gyrus
Instructed task Component 2	4 -5	-33 -37	29 29	23	(R) Cingulate gyrus (L) Cingulate gyrus
Instructed task Component 2	23 20	-83 -86	37 28	19	(R) Precuneus (R) Cuneus
Instructed task Component 2	34 32	-40 -42	-10 -13	37	(R) Fusiform gyrus (R) Parahippocampal gyrus
Instructed task Component 2	20	-36	-4	27	(R) Parahippocampal gyrus
Instructed task Component 2	28	-81	46	7	(R) Superior Parietal Lobule

Table 23 Coordinates, brodmann area, anatomical regions for nodes with biggest local source strength for the identified two major PCs in the spontaneous lying task.

Condition	X	Y	Z	Brodmann Area	Anatomical Region
Spontaneous task component 1	4 -7	25 27	54 54	8	(R) Superior frontal gyrus (L) Superior frontal gyrus
Spontaneous task component 1	-7 4	20 16	43 35	32	(R) Cingulate gyrus (L) Cingulate gyrus
Spontaneous task component 1	5 -7 5 -7	14 16 16 11	27 31 25 25	24	(R) Cingulate gyrus (L) Cingulate gyrus (R) Anterior cingulate gyrus (L) Anterior cingulate gyrus
Spontaneous task component 1	3 5 -7	13 22 22	-9 -22 -20	25	(R) Anterior cingulate (R) Medial frontal gyrus (L) Medial frontal gyrus

Spontaneous task component 1	17 -15	24 24	-22 -20	47	(R) Inferior Frontal Gryus (L) Inferior Frontal Gryus
Spontaneous task component 2	4 -7	-44 -41	25 26	23	(R) Posterior cingulate (L) Posterior cingulate
Spontaneous task component 2	13 -6 14 -6	-45 -46 -50 -50	29 39 32 30	31	(R) Cingulate gyrus (L) Cingulate gyrus (R) Precuneus (L) Precuneus
Spontaneous task component 2	15 -12 -26 24	-55 -54 -57 -55	44 44 44 44	7	(R) Precunues (L) Precunues (R) Superior parietal lobule (L) Superior parietal lobule
Spontaneous task component 2	33 28	-40 -40	-10 -10	37	(R) Fusiform gyrus (R) Parahippocampal gyrus
Spontaneous task component 2	18	-36	-4	27	(R) Parahippocampal gyrus

Component 1 temporal profile

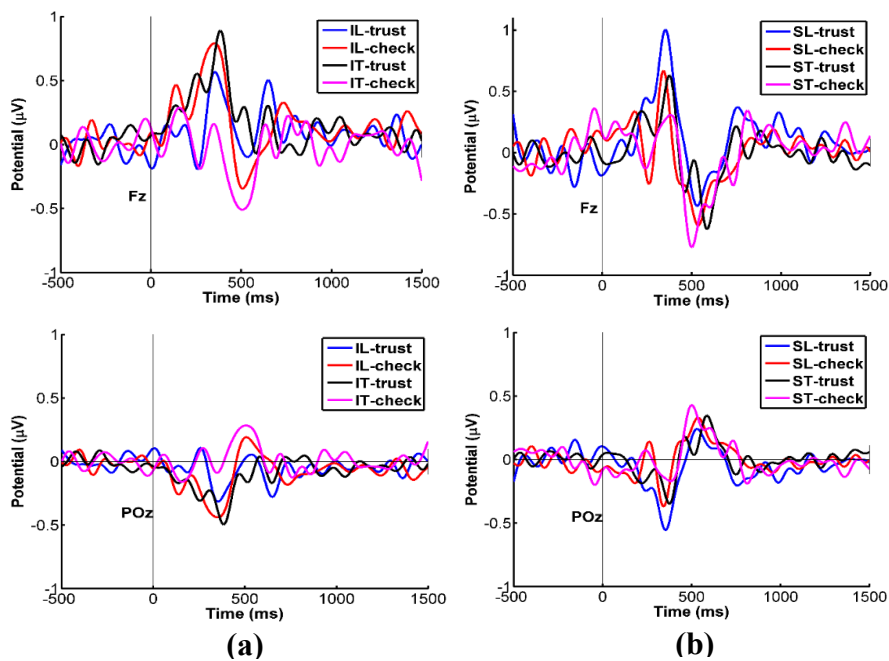


Figure 31 Reconstructed ERP signals on example channels (i.e. Fz and POz) by major PCs. (a) and (b) show the reconstruction of the P400 and partially the N500 peak by its PCs in the IL-IT group and in the SL-ST group respectively.

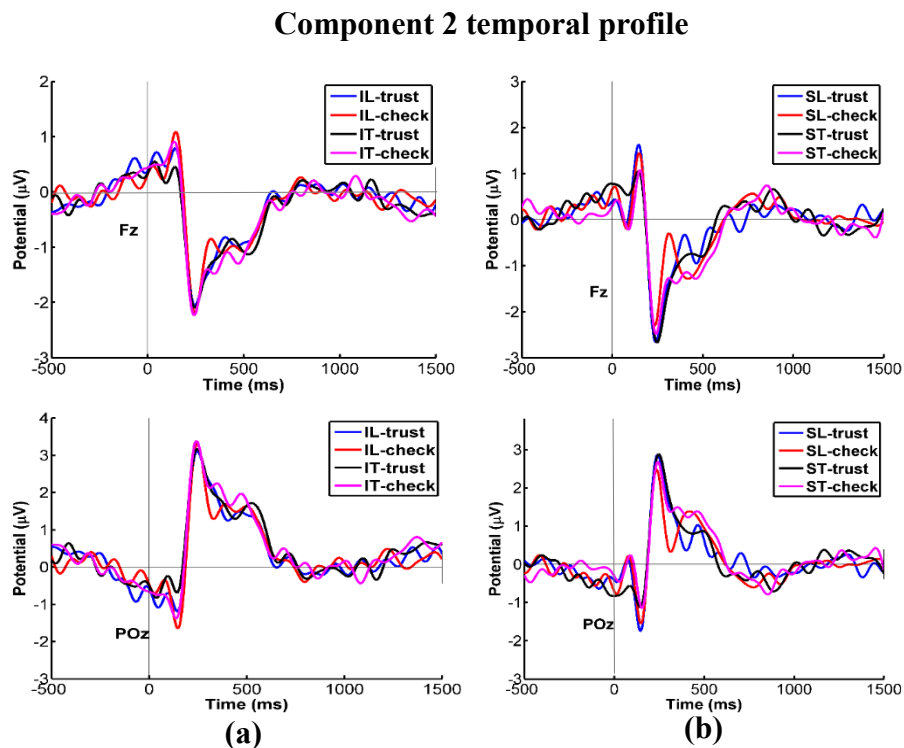


Figure 32 Reconstructed ERP signals on example channels (i.e. Fz and POz) by major PCs. (a) and (b) show the reconstruction of the N400 and partially the N500 peak in the IL-IT group and in the SL-ST group respectively.

6.4 Discussion

The overall ERP difference in the four conditions as shown in Fig.27 might indicate a (mismatch negativity) MMN effect in the visual sequential deviance processing, which manifests deviance response to visual stimulus out of sequential regularity (Czigler, Weisz et al. 2006). However, this difference could be further disentangled by multiple components. As it is shown in Fig.28, there seems to exist a frontal and parietal component

that contribute to the topographic difference. This has been verified by the two stage ICA-PCA analysis in which P400/N400 are identified major components that contribute to the topographic difference. According to the ERP reconstruction results as shown in Fig.31-32, both the P400 and the N400 components distinguish the IT-check/ST-check conditions from the counterpart IL-check/SL-check conditions under the ‘doubtful’ feedback, and as verified by the significant test (Table 16,20), their combined effects contribute to the overall difference between these conditions under the ‘doubtful’ feedback. This also indicates that by using the ‘doubtful’ feedback alone might be effective enough to directly differentiate lying from truth-telling in both tasks.

As is known, the P400 is a positive-going wave that peaks around 400ms post-stimulus and is a component modulated by attention (Nasr 2010), object perception(Kornmeier and Bach 2009) and congruity of semantic stimulus (Dien, Michelson et al. 2010). In our study, the IT-check and ST-check are the two conditions associated with incongruity in semantic processing for the ‘doubtful’ feedback, and therefore the P400/N400 component may precisely illustrate the mentality of innocents after receiving ‘doubtful’ feedbacks by reflecting innocents’ emotional/cognitive conflict processing towards incongruous feedbacks.

Moreover, according to Table 16-17,20, different from the instructed lying versus truth-telling pair which only shows significant difference in the ‘check’ group, the spontaneous lying versus truth-telling pair shows significant differences in both the ‘check’ and the ‘trust’ groups at the P400/N400 peak. The ST-trust shows lower amplitude compared with

the SL-trust condition at the P400/N400 peak. This might be due to the ‘deception intention inhibition’ effect that sustains after spontaneous truth-telling response which has suppressed the P400 amplitude for the ST-trust condition. Different from the P400 suppression in the IT-check/ST-check conditions, this P400 suppression is more likely to be caused by attention suppression to the feedback instead of incongruity effect. Moreover, the attention effect could have been amplified in the SL-trust condition, hence increasing its amplitude at around 400 ms. Since this phenomenon does not happen to the IL-trust and IT-trust pair, using ‘trust’ feedback might only specifically work for the SL-trust and ST-trust pair comparison. However, if the P400 modulation is dominant by attention, it might be more susceptible to variation and inconsistency compared with the modulation caused by incongruity effect. Although it is an interesting observation that the SL and ST pair can be distinguished by both the ‘doubtful’ and the ‘trustful’ feedbacks, the mechanism of the P400 suppression and its robustness in real-life scenario is less clearly known in the ‘trust’ group compared with the ‘check’ group. Therefore, in this study, we focus on the results for the ‘check’ group which happens to both the spontaneous and instructed lying/truth-telling tasks.

According to the literature (Dien, Michelson et al. 2010), P400 reflects an integration of the word into the ongoing sequential representation of events, and the integration process is larger for congruous compared with incongruous endings because the subjects presumably recognize that the incongruous endings are largely nonsense and therefore decline to integrate them into sentence representation. In our scenario, ‘doubtful’ checks always came together with incongruous endings for innocents, e.g. ‘cheat/smuggling/liar’.

Moreover, the P400 peak can also be understood as a component that reflects an expectancy updating process for sequential probabilities, in which scenario the lack of P400 to the nonsense endings would reflect an active avoidance of learning them (Dien, Michelson et al. 2010), just as the P300 is thought to reflect global probabilities (Donchin and Coles 1988). In this particular setting, lack of P400 in both the IT-check and the ST-check means when the subjects realized they are telling-truth but nonetheless receive ‘doubtful’ feedback that negates their honesty, they would experience reluctance to learn or understand the negative feedback since it is incongruous to their expectations for the ongoing sequential events based on the preceding context. But if lying subjects (i.e., IL-check/SL-check) receive ‘doubtful’ feedback, they may not feel strongly the incongruity compared with the IT-check/ST-check since strong doubt followed by checking should be one of the expected consequences by running the risk to lie. It is worth mentioning that the ‘doubtful’ feedbacks may only take effect when expressed in a strong way that leads the innocents to feel incongruous. Although there might be some variation in reaction among population towards a ‘doubtful’ feedback, the judgmental sentences used in this protocol expressing doubt (Table 3) were proved to be effective and this effect was further verified by the post-experiment interview on subjects’ incongruous feeling when encountered any doubt during the experiment. From the ERP results, it is shown that the P400 has differentiated amplitude in both the frontal/frontal-central and central-parietal/occipital-parietal electrodes towards the incongruous feedback stimulus compared with the congruous feedback stimulus (Fig.27). Fig.27 depicts that the P400 peak value has a negative trend at the frontal/central-frontal electrodes and positive trend at the central-

parietal/occipital-parietal electrodes, which could be due to a possibility that there is a simultaneously ongoing negative component that pulls the overall peak down towards negative voltage potential while maintaining the positive polarity. This spatially reverse trend between the frontal/central-frontal and the central-parietal/occipital-parietal electrodes can also be seen from topographic scalp maps as shown in Fig.28. From the ICA-PCA result, it is inferred that the negative component likely reflects an effect of N400, which is considered a component associated with semantic processing. In the ERP reconstruction result, this component is temporally linked with a N200 component, and this might be because they share similar spatial source generators and non-separable by the ICA algorithm. According to the serial and cascaded model of psycholinguistic information access in word recognition (Pulvermuller and Shtyrov 2006), the semantic processing component occurs at around 400ms post stimulus. Previous studies suggested that the N400 with main topographic location over central-posterior scalp regions could be elicited by grammatically possible, but semantically unexpected stimuli and one of its defining characteristics is that it is amplified for sentence completions that are semantically unexpected or incongruous with the preceding context (Kutas and Hillyard 1980, Pulvermuller and Shtyrov 2006), termed as a 'senseless sentence' scenario (Pulvermuller and Shtyrov 2006). However, even if the N400 and the P400 components occur almost at the same time window, they might play different functional roles. It has been clarified by one previous study (Dien, Michelson et al. 2010) that the N400 has more visual sentence effect whereas the P400 has more general sequential expectancy effect. It has also been further justified by the ICA-PCA analysis in this study (Fig.31-32) that both the P400 and

N400 contribute to the condition difference in ERP around 400 ms, with the P400 located in frontal anatomical regions generating more prominent voltage difference among conditions than the N400 that is located in the central-parietal regions. This implies that the sequential expectancy related P400 might have played a more significant role to the condition differences compared with the N400.

Interestingly, another ERP component at around 500 ms can be observed from the across-subjects grand mean averaged ERP curves. This N500 component was reported to be evoked by the cognitive and emotional conflicts faced by subjects in counter-conformity scenario (Chen, Ma et al. 2010). In our study, this waveform is more likely to be related to the ‘feedback differences’ (‘trustful’ v.s. ‘doubtful’ feedbacks) than the ‘condition differences’ (lying v.s. truth-telling) as observed from the ERP waveform in Fig.27. This phenomenon can be further verified from Table 17 and 18 that the N500 component does not present any significant difference between the lying and truth-telling conditions in the spontaneous task. Nevertheless, the ‘check’ and the ‘trust’ pair demonstrates significant differences in the IT, SL and ST tasks. The insensitivity of the late component N500 to the condition differences might be because that different from the P400/N400 which is an incongruity-specific component, the N500 might be a more general component reflecting cognitive and emotional conflicts faced by the subjects. As such, the sensitivity of the N500 to the ‘doubtful’ feedback could be due to the possibility that we applied feedback expressing strong doubt statements to the subjects which seem to be counter-conformity in the regular social settings. Different from the instructed lying task, the N500 shows significant difference between the ‘check’ and the ‘trust’ condition in both the SL and the

ST tasks. This might be possibly due to the larger cognitive/emotional conflict encountered by the SL-check condition compared with the IL-check condition as the spontaneous lying task is considered to involve more self-generated deception intention which incurs extra cognitive conflict by the need to keep other's mental states in mind while deceiving them (Carrion, Keenan et al. 2010). It also explains why the 'check' and the 'trust' pair only demonstrates significant differences in the SL but not the IL task. Therefore, it implies that the N500 maybe a task-dependent component in differentiating lying and truth-telling condition, as in this study, this component can only be used to distinguish the IL and the IT condition but not the SL and ST condition since the IT-check and IT-trust pair shows significant difference at the N500 component which differs from the IL-check and IL-trust pair, and this difference does not exist for the corresponding SL-ST pairs.

To further elucidate the neuro-anatomies underlying the observed differences, two stage ICA-PCA analysis and source localization were performed to identify the major spatial-temporal components of salient ERPs that could also be the main contributors to the observed ERP differences. Task independent components P400/N400 and one task dependent component N500 has been identified. It was reported by previous study that the source generator of the P400 are mainly located in frontal, parietal and temporal cortex (Frishkoff, Tucker et al. 2004, Dien, Michelson et al. 2010) with major contributor located in the frontal cortex (Frishkoff, Tucker et al. 2004), and this location accords with our findings. Moreover, these frontal and cingulated zone neural generators have been proved to process the validity and valence of the given feedback (Mies, van der Molen et al. 2011). In addition, previous studies have found sources that contribute to the N400 component are

located in central-parietal cortex (Pulvermuller and Shtyrov 2006, Schulz, Maurer et al. 2008, Dien, Michelson et al. 2010), this further justifies our findings for the anatomy of the N400 component. In our scenario, both cognitive and affective processing might be involved simultaneously in response to incongruous feedback expressing doubt towards innocents. Besides, although the N500 and P400/N400 component share different temporal features and may have slightly different physiological implication, they seem to share common spatial neural-anatomy given the ERP reconstruction result as shown in Fig.31-32. This implies that the P400/N400 and the late N500 components are neuro-psychologically closely related via cognitive/emotional conflict processing incurred in incongruous scenarios and therefore they could be associated with the same neuronal generators.

This study has proposed a novel ERP protocol for lie detection. It is known that the P300 is frequently used as lie detection tool, the principle of using P300 for lie detection is detection of liars' saliency in response to target items (to be denied/hidden) compared to non-target items (to tell the truth) and irrelevant items. The previous P300 studies mainly focus on subjects' responses to probe items that are intended to induce their differential responses to the lying and the truth-telling items. The focus of this study is to trigger liars' and innocents' differential responses towards 'trusted' and 'doubted' feedbacks that are independent of items used during lying/truth-telling trials. The difference between the P400/N400 and the P300 component is that the P400/N400 component is more of a feedback related component manifesting subjects' incongruity processing of the incongruent feedback stimulus, while the P300 component reflects subjects' saliency

processing towards the target items. Both of these two components provide indirect cue for lying and have some values in application as complementary methods for lie detection. Therefore, it is highly possible that the combination of these two components can increase the overall lie detection accuracy. However, this study only focused on investigating the feedback related neural responses.

In summary, the unique signature of the task-independent P400/N400 and the task-dependent N500 components that effectively distinguish innocents from liars through the incongruity processing component are important findings in this study. Moreover, since these features as a detection reference are derived from innocents' intrinsic responses towards the feedbacks, they are less likely to be susceptible to liars' neuronal responses that could involve unpredictable variations. Finally, it could be difficult for liars to pretend to be a truth teller by consciously 'mimicking' the incongruity processing towards the 'doubtful'/'trustful' feedbacks. However, postulated as such, future studies may still be necessary to further verify this postulation and excludes out potential counteracts. Based on the above results, several suggestions are proposed for potential application, 1) By simply showing 'doubtful' feedback to the subjects, the lying and truth-telling conditions could be differentiated based on the ERP amplitude at the 400ms window. 2) The identified ICA components can potentially be used as a spatial filter for a single trial/single subject to extract the local P400/N400 and N500 phenomenon that can manifest the condition difference. 3) This protocol can be integrated into the P300 GKT test protocol and use both the P300 and the feedback related components to distinguish the lying from the truth-telling condition. The limitation of this study is also worth-mentioning. It is considered that the

P400/N400 reflects sequential expectancy processing while the P300 reflects global expectancy processing. This study has employed equal number of trials in each condition in order to retrieve feedback related evoked potential, therefore, the results in this study have shown feedback related ERP and precluded the occurrence of the P300 component that might occur to trials with global expectancy processing which only happens to trials that involve salient processing to the feedbacks. In future studies, the protocol design can be adapted to observe the role of the P300 component in ‘doubtful’ feedback processing. In addition, the effect of the feedback stimuli used should be further analyzed for determination on what type of feedback stimuli are effective in maximizing the difference between the lying and truth-telling conditions.

6.5 Concluding remarks

The results from this study have provided intuitive evidence for distinguishable features of truth-telling from lying based on EEG signal with the proposed novel protocol. Feedback related evoked potential has been analyzed, from which P400/N400 and N500 have been shown to be the most significant ERP peaks that provide intrinsic self-labeling features for innocents in the IT-check/ST-check conditions. The features that effectively identify the ‘doubt honesty’ conditions are most likely related to semantic incongruity processing, as ‘strong doubt’ in honesty appears to be an incongruous and illogical situation. These generic findings could be applied in extensive scenarios besides the custom inspection setting, where the IT-check/ST-check conditions can be easily established. This new protocol may not only bring up new directions for deception research community but also

could potentially empower all the existing deception detection protocols by incorporating this new protocol to achieve a more comprehensive detection tool. The work might also contribute to inspire the EEG community for inventing and enhancing closely related methods.

CHAPTER 7

CONCLUSIONS AND RECOMMENDATIONS

7.1 Conclusions

In this thesis, four EEG-based methodologies (two novel analysis methods and two novel protocols) have been developed for investigation of neural correlates of deception. Corresponding experiments on human subjects have been conducted to verify the effectiveness of the new methods and protocols. These new methods also enable exploration and identification neural correlates of deception. Specific contributions and achievements are listed as highlight points shown below:

- This thesis has developed a source localization based deception study method with power-spectrum analysis in the source space, as described in Chapter 4, based on which, underlying neural anatomies that lie differences between deception and truth-telling associated brain activities were identified in two types of lying conditions (instructed vs. spontaneous lying). These specific source findings suggest that selective attention and saliency monitoring at earlier phase and inhibition control in the later phase seem to play an important role in distinguishing the SL from the ST condition. In addition, the major difference between the SL and

the IL conditions lie in response inhibition in the IL, and the ST and the IT conditions can also be differentiated by an early inhibitory control sign.

- This thesis has investigated two instructed lying tasks that are differentiated by subjects' own prior experience and fictional experience via EEG recordings (described in Chapter 4). One was to deceive on autobiographic information for which subjects had prior experience (WE: with prior experience) and the other was to deceive on their working experience by pretending to possess prolific knowledge and experience in a target field where they in fact had little prior experience (NE: no prior experience). The second task is a novel deception task that has scarcely been discussed in previous studies. Specific findings in this study are, with the application of source localization method proposed in the first study, a dominant role of executive control has been found in the first lying task that is consistent with previous studies. Moreover, deception condition in the second lying task can be distinguished by a decreased self-referential processing which may be accompanied by a mental imagery processing involved to fabricate viable lies for non-experienced events as evidenced by a network of neural anatomies that present significant differences in delta and upper alpha band ERS neural activities in lying compared with truth-telling conditions.
- This thesis has developed a network and connectivity analysis method for deception study (described in Chapter 5). The analysis method has been applied to the two deception tasks developed in Chapter 4. This study reveals several groups of neuronal generators underlying both the instructed lying (IL) and the instructed

truth-telling (IT) conditions for both tasks during the Stimulus Delivery Period (SDP), they are inferred as functional networks underlying auditory stimulus perception process, comprehension and memory retrieval process, as well an overall executive control over multiple simultaneous processes. Despite the similarities existed in these group components, significant differences were found in the intra- and inter-group connectivity between the IL and IT conditions in either task.

- This thesis has developed a novel ERP-based deception paradigm that investigates human subjects' responses towards judgmental feedbacks (either 'trustful' or 'doubtful' feedbacks) with respect to their deceptive or truthful responses (described in Chapter 6). This study has identified unique signatures based on the P400/N400 and the N500 waveforms that allow identification for the presence of the conflict/incongruity processing that is specifically underlying innocents' neural responses towards 'doubtful' feedbacks.

In summary, new methodologies developed for this thesis have provided intuitive evidence for distinguishable features of several deception types from their counterpart truth-telling conditions based on recorded EEG signals. A better and more comprehensive understanding of neural mechanism underlying deception is of great significance in generating deception specific neural correlates/features which play the core role in real-life application of lie detection.

7.2 Recommendations for future deception researches and applications

This thesis has developed several novel EEG-based methods to study deception and the neural correlates of deception have been suggested by the corresponding studies. However, there still remain directions worthy of being further explored based on the work proposed in this thesis, recommendations for future deception researches and applications are listed below:

- It is important to be aware that the neural correlates identified have been derived from single signal modality, i.e. EEG, it may not be able to be directly generalized as generic neural correlates underlying deception, the interpretation of the neuropsychological mechanism indicated by these neural correlates needs to be further justified by other signal modalities, such as fMRI and fNIR. In other words, more cross-validation studies might be necessary before these findings can be exploited in real-life applications.
- Studies in this thesis have performed an extensive comparison between multiple deception and the counterpart truth-telling conditions, from the perspectives of neural substrates (sources), functional network / connectivity pattern, ERP waveforms, and significant differences have been found from each of these perspectives. Yet, findings from this thesis may not be straight forward to be employed as feature sets in application of lie detection. In order to translate the relevant information into applicable feature sets, follow-up feature selection studies

might be required to further test and optimize the feature sets that can offer best detection/classification accuracy. Moreover, combination of some of these feature sets might be valuable to be explored which can potentially provide a more comprehensive detection algorithm.

- In addition, each study has reported results based on limited number of subjects and population. Despite the significant results among this group of population, a wider population needs to be tested to ensure that results found in this study have the generalizability to be applied in a wider population that might have diverse population characteristics. Future work should expand the testing scale to a larger population.
- In this thesis, connectivity analysis, network analysis and source localization analysis have been applied to time window prior to and posterior to the deception execution phase, in the future studies, it is of great interest to investigate the liars' and innocents' neural response during the deception execution phase with refined experimental design and more advanced artifact removal technique.

PUBLICATIONS FROM THE PRESENT

STUDY

International Journal Articles

- **Yue Wang**, Wu Chun Ng, Khoon Siong Ng, Ke Yu, Tiecheng Wu, Xiaoping Li. An electroencephalography network and connectivity analysis for deception in instructed lying tasks. *PLoS ONE*. In press.
- **Yue Wang**, Mohamed Syazwan b Mohamed S, Wu Chun Ng, Ke Yu, Khoon Siong Ng, Xiaoping Li. Liars and innocents' neuronal response to judgmental feedbacks can be differentiated with Electroencephalography: the role of judgmental feedbacks in deception. *PLoS ONE*. Major revision.
- **Yue Wang**, Wu Chun Ng, Khoon Siong Ng, Ke Yu, Xiaoping Li. A human electroencephalography investigation on instructed lying tasks for experienced and non-experienced events. International journal of neuroscience. Submitted for Publication.
- Ke Yu, **Yue Wang**, Kaiquan Shen, Xiaoping Li (2013). The Synergy between Complex Channel-Specific FIR Filter and Spatial Filter for Single-Trial EEG Classification. *PLoS ONE* 8(10): e76923. doi:10.1371/journal.pone.0076923.

International Conference Papers

- **Wang Y**, Ng Wu C, Ng Khoon S, Wu T, Li X. An EEG source localization and connectivity study on deception of autobiography memories; 2013 6-8 Nov. 2013. pp. 468-471.

- Ye Yan, **Wang Yue**, Fan Jie, Li Xiaoping; Evaluation of a human head phantom system for visual event-related potential studies, International Forum on Systems and Mechatronics, Guilin, China, 2013
- W.C. Ng, W.L. Khoa, **Y.Wang**, Y. Ye, X.P.Li, In-vivo measurement of the effect of compression on the human skin impedance, International Forum on Systems and Mechatronics, Singapore, 2010

BIBLIOGRAPHY

(2009). Quantitative EEG Analysis Methods and Clinical Applications. N. V. T. Shanbao Tong, Artech House.

Abe, N., M. Suzuki, E. Mori, M. Itoh and T. Fujii (2007). "Deceiving others: distinct neural responses of the prefrontal cortex and amygdala in simple fabrication and deception with social interactions." J Cogn Neurosci **19**(2): 287-295.

Abe, N., M. Suzuki, T. Tsukiura, E. Mori, K. Yamaguchi, M. Itoh and T. Fujii (2006). "Dissociable Roles of Prefrontal and Anterior Cingulate Cortices in Deception." Cerebral Cortex **16**(2): 192-199.

Abootalebi, V., M. H. Moradi and M. A. Khalilzadeh (2009). "A new approach for EEG feature extraction in P300-based lie detection." Computer Methods and Programs in Biomedicine **94**(1): 48-57.

Ahlfors, S. P., G. V. Simpson, A. M. Dale, J. W. Belliveau, A. K. Liu, A. Korvenoja, J. Virtanen, M. Huotilainen, R. B. Tootell, H. J. Aronen and R. J. Ilmoniemi (1999). "Spatiotemporal activity of a cortical network for processing visual motion revealed by MEG and fMRI." J Neurophysiol **82**(5): 2545-2555.

Aleman, A., L. van Lee, M. H. Mantione, I. G. Verkoijen and E. H. de Haan (2001). "Visual imagery without visual experience: evidence from congenitally totally blind people." Neuroreport **12**(11): 2601-2604.

Aminoff, E. M., K. Kveraga and M. Bar "The role of the parahippocampal cortex in cognition." Trends in Cognitive Sciences **17**(8): 379-390.

Asma, L. (2008). Emotional pain modulation : an effect of emotion, attention or empathy for pain.

Astolfi, L., F. Cincotti, D. Mattia, M. G. Marciani, L. A. Baccala, F. de Vico Fallani, S. Salinari, M. Ursino, M. Zavaglia, L. Ding, J. C. Edgar, G. A. Miller, B. He and F. Babiloni (2007). "Comparison of different cortical connectivity estimators for high-resolution EEG recordings." Hum Brain Mapp **28**(2): 143-157.

Baccala, L. A. and K. Sameshima (2001). "Partial directed coherence: a new concept in neural structure determination." Biol Cybern **84**(6): 463-474.

Baizer, J. S., L. G. Ungerleider and R. Desimone (1991). "Organization of visual inputs to the inferior temporal and posterior parietal cortex in macaques." J Neurosci **11**(1): 168-190.

Barkoukis, T. J., A. Y. Avidan and ScienceDirect (2007). Review of sleep medicine, Butterworth-Heinemann.

Barrett, A. B., M. Murphy, M.-A. Bruno, Q. Noirhomme, M. Boly, S. Laureys and A. K. Seth (2012). "Granger Causality Analysis of Steady-State Electroencephalographic Signals during Propofol-Induced Anaesthesia." PLoS ONE **7**(1): e29072.

Barth, M. "Functional MRI, Edited by C.T.W. Moonen and P.A. Bandettini, Springer-Verlag, 1999, 575 pp. ISBN 3-540-64263-3." European Journal of Radiology **36**(1): 58.

Behrmann, M., J. J. Geng and S. Shomstein (2004). "Parietal cortex and attention." Curr Opin Neurobiol **14**(2): 212-217.

Bell, A. J. and T. J. Sejnowski (1995). "An Information-Maximization Approach to Blind Separation and Blind Deconvolution." Neural Computation **7**(6): 1129-1159.

Bentin, S., T. Allison, A. Puce, E. Perez and G. McCarthy (1996). "Electrophysiological Studies of Face Perception in Humans." Journal of cognitive neuroscience **8**(6): 551-565.

Berg, P. and M. Scherg (1991). "Dipole modelling of eye activity and its application to the removal of eye artefacts from the EEG and MEG." Clin Phys Physiol Meas **12 Suppl A**: 49-54.

Blair, R. C. and W. Karniski (1993). "An alternative method for significance testing of waveform difference potentials." Psychophysiology **30**(5): 518-524.

Blaizot, X., A. Martinez-Marcos, M. Arroyo-Jimenez Md Mdel, P. Marcos, E. Artacho-Perula, M. Munoz, C. Chavoix and R. Insausti (2004). "The parahippocampal gyrus in the baboon: anatomical, cytoarchitectonic and magnetic resonance imaging (MRI) studies." Cereb Cortex **14**(3): 231-246.

Bridge, H., S. Harrold, E. A. Holmes, M. Stokes and C. Kennard (2012). "Vivid visual mental imagery in the absence of the primary visual cortex." J Neurol **259**(6): 1062-1070.

Brodbeck, V., L. Spinelli, A. M. Lascano, M. Wissmeier, M.-I. Vargas, S. Vulliemoz, C. Pollo, K. Schaller, C. M. Michel and M. Seeck (2011). "Electroencephalographic source imaging: a prospective study of 152 operated epileptic patients." Brain **134**(10): 2887-2897.

Buckner, R. L., J. R. Andrews-Hanna and D. L. Schacter (2008). "The brain's default network: anatomy, function, and relevance to disease." Ann N Y Acad Sci **1124**: 1-38.

Bull, P. (2006). "Detecting lies and deceit: the psychology of lying and the implications for professional practice. Aldert Vrij. (2000) Wiley: Chichester. xv + 254 pp. ISBN 0-471-85316-X." Journal of Community & Applied Social Psychology **16**(2): 166-167.

Cabeza, R. and L. Nyberg (2000). "Imaging cognition II: An empirical review of 275 PET and fMRI studies." J Cogn Neurosci **12**(1): 1-47.

Campbell, I. G. (2009). "EEG recording and analysis for sleep research." Curr Protoc Neurosci **Chapter 10**: Unit10 12.

Canto, C. B., F. G. Wouterlood and M. P. Witter (2008). "What Does the Anatomical Organization of the Entorhinal Cortex Tell Us?" Neural Plasticity **2008**: 18.

Canuet, L., R. Ishii, R. D. Pascual-Marqui, M. Iwase, R. Kurimoto, Y. Aoki, S. Ikeda, H. Takahashi, T. Nakahachi and M. Takeda (2011). "Resting-State EEG Source Localization and Functional Connectivity in Schizophrenia-Like Psychosis of Epilepsy." PLoS ONE **6**(11): e27863.

Carmel, D., E. Dayan, A. Naveh, O. Raveh and G. Ben-Shakhar (2003). "Estimating the validity of the guilty knowledge test from simulated experiments: the external validity of mock crime studies." J Exp Psychol Appl **9**(4): 261-269.

Carrion, R. E., J. P. Keenan and N. Sebanz (2010). "A truth that's told with bad intent: an ERP study of deception." Cognition **114**(1): 105-110.

Cavanna, A. E. and M. R. Trimble (2006). "The precuneus: a review of its functional anatomy and behavioural correlates." Brain **129**(Pt 3): 564-583.

Champoux, F., D. M. Shiller and R. J. Zatorre (2011). "Feel What You Say: An Auditory Effect on Somatosensory Perception." PLoS ONE **6**(8): e22829.

Chapin, H. L., T. Zanto, K. J. Jantzen, S. J. A. Kelso, F. Steinberg and E. W. Large (2010). "Neural Responses to Complex Auditory Rhythms: The Role of Attending." Frontiers in Psychology **1**: 224.

Chen, J. L., T. Ros and J. H. Gruzelier (2013). "Dynamic changes of ICA-derived EEG functional connectivity in the resting state." Hum Brain Mapp **34**(4): 852-868.

Chen, M., Q. Ma, M. Li, H. Lai, X. Wang and L. Shu (2010). "Cognitive and emotional conflicts of counter-conformity choice in purchasing books online: an event-related potentials study." Biol Psychol **85**(3): 437-445.

Christ, S. E., D. C. Van Essen, J. M. Watson, L. E. Brubaker and K. B. McDermott (2009). "The contributions of prefrontal cortex and executive control to deception: evidence from activation likelihood estimate meta-analyses." Cereb Cortex **19**(7): 1557-1566.

Christoph M. Michel, T. K., Daniel Brandeis , Lorena R. R. Gianotti , Jiří Wackermann, Ed. (2009). Electrical Neuroimaging, Cambridge: Cambridge University Press.

Chu, C. J., M. A. Kramer, J. Pathmanathan, M. T. Bianchi, M. B. Westover, L. Wison and S. S. Cash (2012). "Emergence of Stable Functional Networks in Long-Term Human Electroencephalography." The Journal of Neuroscience **32**(8): 2703-2713.

Council, N. R. (2003). The Polygraph and Lie Detection, The National Academies Press.

Cuong, N. K., V. Ha, N. M. Huong, T. Khoa, N. Tam, H. Linh and V. Van Toi (2010). Removing Noise and Artifacts from EEG Using Adaptive Noise Cancelator and Blind Source Separation. The Third International Conference on the Development of Biomedical Engineering in Vietnam. V. Van Toi and T. Khoa, Springer Berlin Heidelberg. **27**: 282-286.

Curran, T., D. M. Tucker, M. Kutas and M. I. Posner (1993). "Topography of the N400: brain electrical activity reflecting semantic expectancy." Electroencephalogr Clin Neurophysiol **88**(3): 188-209.

Customs, S. (2013). "“Customs Clearance Procedure” ”.

Czigler, I., J. Weisz and I. Winkler (2006). "ERPs and deviance detection: visual mismatch negativity to repeated visual stimuli." Neurosci Lett **401**(1-2): 178-182.

Davatzikos, C., K. Ruparel, Y. Fan, D. G. Shen, M. Acharyya, J. W. Loughhead, R. C. Gur and D. D. Langleben (2005). "Classifying spatial patterns of brain activity with machine learning methods: application to lie detection." Neuroimage **28**(3): 663-668.

De Clercq, W., A. Vergult, B. Vanrumste, J. Van Hees, A. Palmi, W. Van Paesschen and S. Van Huffel (2005). "A new muscle artifact removal technique to improve the interpretation of the ictal scalp electroencephalogram." Conf Proc IEEE Eng Med Biol Soc **1**: 944-947.

De Clercq, W., A. Vergult, B. Vanrumste, W. Van Paesschen and S. Van Huffel (2006). "Canonical correlation analysis applied to remove muscle artifacts from the electroencephalogram." IEEE Trans Biomed Eng **53**(12 Pt 1): 2583-2587.

De Volder, A. G., H. Toyama, Y. Kimura, M. Kiyosawa, H. Nakano, A. Vanlierde, M. C. Wanet-Defalque, M. Mishina, K. Oda, K. Ishiwata and M. Senda (2001). "Auditory triggered mental imagery of shape involves visual association areas in early blind humans." Neuroimage **14**(1 Pt 1): 129-139.

Dehaene-Lambertz, G., C. Pallier, W. Serniclaes, L. Sprenger-Charolles, A. Jobert and S. Dehaene (2005). "Neural correlates of switching from auditory to speech perception." Neuroimage **24**(1): 21-33.

Di Russo, F., A. Martinez and S. A. Hillyard (2003). "Source analysis of event-related cortical activity during visuo-spatial attention." Cereb Cortex **13**(5): 486-499.

Dickerson, B. C. and H. Eichenbaum (2010). "The episodic memory system: neurocircuitry and disorders." Neuropsychopharmacology **35**(1): 86-104.

Dien, J., C. A. Michelson and M. S. Franklin (2010). "Separating the visual sentence N400 effect from the P400 sequential expectancy effect: cognitive and neuroanatomical implications." Brain Res **1355**: 126-140.

Ding, X. P., X. Gao, G. Fu and K. Lee (2013). "Neural correlates of spontaneous deception: A functional near-infrared spectroscopy (fNIRS) study." Neuropsychologia **51**(4): 704-712.

Donchin, E. and M. G. H. Coles (1988). "Is the P300 component a manifestation of context updating?" Behavioral and Brain Sciences **11**(03): 357-374.

Dressler, O., G. Schneider, G. Stockmanns and E. F. Kochs (2004). "Awareness and the EEG power spectrum: analysis of frequencies." Br J Anaesth **93**(6): 806-809.

Eichenbaum, H., A. P. Yonelinas and C. Ranganath (2007). "The medial temporal lobe and recognition memory." Annu Rev Neurosci **30**: 123-152.

Fadiga, L., L. Craighero, G. Buccino and G. Rizzolatti (2002). "Speech listening specifically modulates the excitability of tongue muscles: a TMS study." Eur J Neurosci **15**(2): 399-402.

Forstmann, B. U., W. P. van den Wildenberg and K. R. Ridderinkhof (2008). "Neural mechanisms, temporal dynamics, and individual differences in interference control." J Cogn Neurosci **20**(10): 1854-1865.

Fransson, P. and G. Marrelec (2008). "The precuneus/posterior cingulate cortex plays a pivotal role in the default mode network: Evidence from a partial correlation network analysis." NeuroImage **42**(3): 1178-1184.

Friederici, A. D., S.-A. Rüschemeyer, A. Hahne and C. J. Fiebach (2003). "The Role of Left Inferior Frontal and Superior Temporal Cortex in Sentence Comprehension: Localizing Syntactic and Semantic Processes." Cerebral Cortex **13**(2): 170-177.

Frishkoff, G. A., D. M. Tucker, C. Davey and M. Scherg (2004). "Frontal and posterior sources of event-related potentials in semantic comprehension." Cognitive Brain Research **20**(3): 329-354.

Gabrieli, J. D., R. A. Poldrack and J. E. Desmond (1998). "The role of left prefrontal cortex in language and memory." Proc Natl Acad Sci U S A **95**(3): 906-913.

Ganapati M. Tarase, P. D. H., M. S. Ramadurg (2013). "Scientific and legal procedure of polygraph test." Journal of Bio Innovation **2**(1): 12.

Ganis, G., S. M. Kosslyn, S. Stose, W. L. Thompson and D. A. Yurgelun-Todd (2003). "Neural Correlates of Different Types of Deception: An fMRI Investigation." Cerebral Cortex **13**(8): 830-836.

Ganis, G., R. R. Morris and S. M. Kosslyn (2009). "Neural processes underlying self- and other-related lies: an individual difference approach using fMRI." Soc Neurosci **4**(6): 539-553.

Ganis, G., W. L. Thompson and S. M. Kosslyn (2004). "Brain areas underlying visual mental imagery and visual perception: an fMRI study." Brain Res Cogn Brain Res **20**(2): 226-241.

Gazzaniga, M. S. I., Richard B. Mangun, G. R. (2009). *Cognitive neuroscience the biology of the mind*, W.W. Norton: 395–401.

Gilbert, C. D. and W. Li (2013). "Top-down influences on visual processing." Nat Rev Neurosci **14**(5): 350-363.

Gloor, P. (1985). "Neuronal generators and the problem of localization in electroencephalography: application of volume conductor theory to electroencephalography." J Clin Neurophysiol **2**(4): 327-354.

Gobbini, M. I., A. C. Koralek, R. E. Bryan, K. J. Montgomery and J. V. Haxby (2007). "Two takes on the social brain: A comparison of theory of mind tasks." J. Cognitive Neuroscience **19**(11): 1803-1814.

Gomez-Herrero, G. (2006). Automatic Removal of Ocular Artifacts in the EEG without an EOG Reference Channel. Proceedings of the 7th Nordic Signal Processing Symposium.

Gómez-Herrero, G. (2008). "Automatic Artifact Removal (AAR) toolbox for MATLAB." from <http://kasku.org/projects/eeg/aar.htm>.

Goncharova, II, D. J. McFarland, T. M. Vaughan and J. R. Wolpaw (2003). "EMG contamination of EEG: spectral and topographical characteristics." Clin Neurophysiol **114**(9): 1580-1593.

Gotlib, I. H., H. Sivers, J. D. Gabrieli, S. Whitfield-Gabrieli, P. Goldin, K. L. Minor and T. Canli (2005). "Subgenual anterior cingulate activation to valenced emotional stimuli in major depression." Neuroreport **16**(16): 1731-1734.

Gratton, G., M. G. Coles and E. Donchin (1983). "A new method for off-line removal of ocular artifact." Electroencephalogr Clin Neurophysiol **55**(4): 468-484.

Greene, J. D. and J. M. Paxton (2009). "Patterns of neural activity associated with honest and dishonest moral decisions." Proceedings of the National Academy of Sciences **106**(30): 12506-12511.

Groppe, D. M., T. P. Urbach and M. Kutas (2011). "Mass univariate analysis of event-related brain potentials/fields I: A critical tutorial review." Psychophysiology **48**(12): 1711-1725.

Grubin, D. (2010). "The Polygraph and Forensic Psychiatry." Journal of the American Academy of Psychiatry and the Law Online **38**(4): 446-451.

Hafting, T., M. Fyhn, S. Molden, M.-B. Moser and E. I. Moser (2005). "Microstructure of a spatial map in the entorhinal cortex." Nature **436**(7052): 801-806.

Hämäläinen, M., R. Hari, R. J. Ilmoniemi, J. Knuutila and O. V. Lounasmaa (1993). "Magnetoencephalography—theory, instrumentation, and applications to noninvasive studies of the working human brain." Reviews of Modern Physics **65**(2): 413-497.

Hamilton, J. P., G. H. Glover, J. J. Hsu, R. F. Johnson and I. H. Gotlib (2011). "Modulation of subgenual anterior cingulate cortex activity with real-time neurofeedback." Hum Brain Mapp **32**(1): 22-31.

Hebart, M. N. and G. Hesselmann (2012). "What Visual Information Is Processed in the Human Dorsal Stream?" The Journal of Neuroscience **32**(24): 8107-8109.

Hindley, E. L., A. J. D. Nelson, J. P. Aggleton and S. D. Vann (2014). "Dysgranular retrosplenial cortex lesions in rats disrupt cross-modal object recognition." Learning & Memory **21**(3): 171-179.

Hinterberger, T., S. Schmidt, T. Kamei and H. Walach (2014). "Decreased electrophysiological activity represents the conscious state of emptiness in meditation." Front Psychol **5**: 99.

Hlinka, J., C. Alexakis, A. Diukova, P. F. Liddle and D. P. Auer (2010). "Slow EEG pattern predicts reduced intrinsic functional connectivity in the default mode network: an inter-subject analysis." Neuroimage **53**(1): 239-246.

Ito, T., M. Tiede and D. J. Ostry (2009). "Somatosensory function in speech perception." Proceedings of the National Academy of Sciences **106**(4): 1245-1248.

Jancke, L. and N. Langer (2011). "A strong parietal hub in the small-world network of coloured-hearing synaesthetes during resting state EEG." J Neuropsychol **5**(2): 178-202.

Jeon, Y., C. S. Nam, Y.-J. Kim and M. C. Whang (2011). "Event-related (De)synchronization (ERD/ERS) during motor imagery tasks: Implications for brain-computer interfaces." International Journal of Industrial Ergonomics **41**(5): 428-436.

Jung, K.-H. and J.-H. Lee (2012). "Cognitive and Emotional Correlates of Different Types of Deception." Social Behavior and Personality: an international journal **40**(4): 575-584.

Jung, T. P., S. Makeig, C. Humphries, T. W. Lee, M. J. McKeown, V. Iragui and T. J. Sejnowski (2000). "Removing electroencephalographic artifacts by blind source separation." Psychophysiology **37**(2): 163-178.

Kathner, I., S. C. Wriessneger, G. R. Muller-Putz, A. Kubler and S. Halder (2014). "Effects of mental workload and fatigue on the P300, alpha and theta band power during operation of an ERP (P300) brain-computer interface." Biol Psychol **102**: 118-129.

Kenemans, J. L., P. C. Molenaar, M. N. Verbaten and J. L. Slangen (1991). "Removal of the ocular artifact from the EEG: a comparison of time and frequency domain methods with simulated and real data." Psychophysiology **28**(1): 114-121.

Kim, S., K. H. Jung and J. H. Lee (2012). "Characteristics of alpha power event-related desynchronization in the discrimination of spontaneous deceptive responses." Int J Psychophysiol **85**(2): 230-235.

Klimesch, W. (2012). "alpha-band oscillations, attention, and controlled access to stored information." Trends Cogn Sci **16**(12): 606-617.

Knyazev, G. (2013). "EEG correlates of self-referential processing." Frontiers in Human Neuroscience **7**.

Kornmeier, J. and M. Bach (2009). "Object perception: When our brain is impressed but we do not notice it." Journal of Vision **9**(1).

Kosslyn, S. M. and K. N. Ochsner (1994). "In search of occipital activation during visual mental imagery." Trends in Neurosciences **17**(7): 290-292.

Krause, C. M., L. Sillanmaki, M. Koivisto, C. Saarela, A. Haggqvist, M. Laine and H. Hamalainen (2000). "The effects of memory load on event-related EEG desynchronization and synchronization." Clin Neurophysiol **111**(11): 2071-2078.

Kutas, M. and K. D. Federmeier (2000). "Electrophysiology reveals semantic memory use in language comprehension." Trends Cogn Sci **4**(12): 463-470.

Kutas, M. and S. Hillyard (1980). "Reading senseless sentences: brain potentials reflect semantic incongruity." Science **207**(4427): 203-205.

Lambert, S., E. Sampaio, Y. Mauss and C. Scheiber (2004). "Blindness and brain plasticity: contribution of mental imagery? An fMRI study." Brain Res Cogn Brain Res **20**(1): 1-11.

Langleben, D. D. (2008). "Detection of deception with fMRI: Are we there yet?" Legal and Criminological Psychology **13**(1): 1-9.

Langleben, D. D., L. Schroeder, J. A. Maldjian, R. C. Gur, S. McDonald, J. D. Ragland, C. P. O'Brien and A. R. Childress (2002). "Brain Activity during Simulated Deception: An Event-Related Functional Magnetic Resonance Study." NeuroImage **15**(3): 727-732.

Lawrence A. Farwell, D. C. R., Graham M. Richardson (2013). "Brain fingerprinting field studies comparing P300-MERMER and P300 brainwave responses in the detection of concealed information." Cognitive Neurodynamics **7**: 37.

Lee, T. M., H. L. Liu, L. H. Tan, C. C. Chan, S. Mahankali, C. M. Feng, J. Hou, P. T. Fox and J. H. Gao (2002). "Lie detection by functional magnetic resonance imaging." Hum Brain Mapp **15**(3): 157-164.

Leff, A. P., T. M. Schofield, J. T. Crinion, M. L. Seghier, A. Grogan, D. W. Green and C. J. Price (2009). "The left superior temporal gyrus is a shared substrate for auditory short-term memory and speech comprehension: evidence from 210 patients with stroke." Brain **132**(Pt 12): 3401-3410.

Lieberman, A. M., F. S. Cooper, D. P. Shankweiler and M. Studdert-Kennedy (1967). "Perception of the speech code." Psychol Rev **74**(6): 431-461.

Lieberman, A. M. and I. G. Mattingly (1985). "The motor theory of speech perception revised." Cognition **21**(1): 1-36.

Limpiti, T., B. D. Van Veen, H. T. Attias and S. S. Nagarajan (2009). "A Spatio-Temporal Framework for Estimating Trial-to-Trial Amplitude Variation in Event-Related MEG/EEG." IEEE transactions on bio-medical engineering **56**(3): 633-645.

LJ., G. (2006). Brodmann's Localisation in the Cerebral Cortex, New York: Springer.

Lou, H. C., B. Luber, M. Crupain, J. P. Keenan, M. Nowak, T. W. Kjaer, H. A. Sackeim and S. H. Lisanby (2004). "Parietal cortex and representation of the mental Self." Proceedings of the National Academy of Sciences of the United States of America **101**(17): 6827-6832.

Luck, S. J., H. J. Heinze, G. R. Mangun and S. A. Hillyard (1990). "Visual event-related potentials index focused attention within bilateral stimulus arrays. II. Functional dissociation of P1 and N1 components." Electroencephalogr Clin Neurophysiol **75**(6): 528-542.

Ludwig, K. A., R. M. Miriani, N. B. Langhals, M. D. Joseph, D. J. Anderson and D. R. Kipke (2009). "Using a common average reference to improve cortical neuron recordings from microelectrode arrays." J Neurophysiol **101**(3): 1679-1689.

Lutz, A., L. L. Greischar, N. B. Rawlings, M. Ricard and R. J. Davidson (2004). "Long-term meditators self-induce high-amplitude gamma synchrony during mental practice." Proceedings of the National Academy of Sciences of the United States of America **101**(46): 16369-16373.

MacEvoy, S. P. and R. A. Epstein (2011). "Constructing scenes from objects in human occipitotemporal cortex." Nat Neurosci **14**(10): 1323-1329.

Magliero, A., T. R. Bashore, M. G. Coles and E. Donchin (1984). "On the dependence of P300 latency on stimulus evaluation processes." Psychophysiology **21**(2): 171-186.

Makeig, S., M. Westerfield, J. Townsend, T. P. Jung, E. Courchesne and T. J. Sejnowski (1999). "Functionally independent components of early event-related potentials in a visual spatial attention task." Philosophical Transactions of the Royal Society B: Biological Sciences **354**(1387): 1135-1144.

Marshall, L., R. Kirov, J. Brade, M. Molle and J. Born (2011). "Transcranial electrical currents to probe EEG brain rhythms and memory consolidation during sleep in humans." PLoS One **6**(2): e16905.

Matsubara, M., S. Yamaguchi, J. Xu and S. Kobayashi (2004). "Neural correlates for the suppression of habitual behavior: a functional MRI study." J Cogn Neurosci **16**(6): 944-954.

Matte, J. A. (2007). "Psychological Structure and Theoretical Concept of the Backster Zone Comparison Technique." Polygraph, Journal of the American Polygraph Association **36**(2).

Mazziotta, J., A. Toga, A. Evans, P. Fox, J. Lancaster, K. Zilles, R. Woods, T. Paus, G. Simpson, B. Pike, C. Holmes, L. Collins, P. Thompson, D. MacDonald, M. Iacoboni, T. Schormann, K. Amunts, N. Palomero-Gallagher, S. Geyer, L. Parsons, K. Narr, N. Kabani, G. Le Goualher, D. Boomsma, T. Cannon, R. Kawashima and B. Mazoyer (2001). "A probabilistic atlas and reference system for the human brain: International Consortium for Brain Mapping (ICBM)." Philos Trans R Soc Lond B Biol Sci **356**(1412): 1293-1322.

McMenamin, B. W., A. J. Shackman, J. S. Maxwell, L. L. Greischar and R. J. Davidson (2009). "Validation of regression-based myogenic correction techniques for scalp and source-localized EEG." Psychophysiology **46**(3): 578-592.

Meister, I. G., S. M. Wilson, C. Deblieck, A. D. Wu and M. Iacoboni (2007). "The essential role of premotor cortex in speech perception." Curr Biol **17**(19): 1692-1696.

Mellet, E., N. Tzourio, F. Crivello, M. Joliot, M. Denis and B. Mazoyer (1996). "Functional Anatomy of Spatial Mental Imagery Generated from Verbal Instructions." The Journal of Neuroscience **16**(20): 6504-6512.

Michael, A. J., S. Krishnaswamy and J. Mohamed (2005). "An open label study of the use of EEG biofeedback using beta training to reduce anxiety for patients with cardiac events." Neuropsychiatr Dis Treat **1**(4): 357-363.

Michels, L., K. Bucher, R. Lüchinger, P. Klaver, E. Martin, D. Jeanmonod and D. Brandeis (2010). "Simultaneous EEG-fMRI during a Working Memory Task: Modulations in Low and High Frequency Bands." PLoS ONE **5**(4): e10298.

Michels, L., M. Moazami-Goudarzi, D. Jeanmonod and J. Sarnthein (2008). "EEG alpha distinguishes between cuneal and precuneal activation in working memory." Neuroimage **40**(3): 1296-1310.

Mies, G. W., M. W. van der Molen, M. Smits, M. W. Hengeveld and F. M. van der Veen (2011). "The anterior cingulate cortex responds differently to the validity and valence of feedback in a time-estimation task." Neuroimage **56**(4): 2321-2328.

Mitchell, J. P. (2006). "Mentalizing and Marr: an information processing approach to the study of social cognition." Brain Res **1079**(1): 66-75.

Mulert, C., L. Jager, R. Schmitt, P. Bussfeld, O. Pogarell, H. J. Moller, G. Juckel and U. Hegerl (2004). "Integration of fMRI and simultaneous EEG: towards a comprehensive understanding of localization and time-course of brain activity in target detection." Neuroimage **22**(1): 83-94.

Mullally, S. L. and E. A. Maguire (2011). "A New Role for the Parahippocampal Cortex in Representing Space." The Journal of Neuroscience **31**(20): 7441-7449.

Müller, V. and A. P. Anokhin (2012). "Neural Synchrony during Response Production and Inhibition." PLoS ONE **7**(6): e38931.

Murray, E. A., T. J. Bussey and L. M. Saksida (2007). "Visual perception and memory: a new view of medial temporal lobe function in primates and rodents." Annu Rev Neurosci **30**: 99-122.

N Sethi, P. S., J Torgovnick, E Arsura (2006). "Physiological and non-physiological EEG artifacts." The Internet Journal of Neuromonitoring **5**(2).

Nasr, S. (2010). "Differential impact of attention on the early and late categorization related human brain potentials." J Vis **10**(11): 18.

Nichols, T. E. and A. P. Holmes (2002). "Nonparametric permutation tests for functional neuroimaging: a primer with examples." Hum Brain Mapp **15**(1): 1-25.

Nunez, P. L., and Srinivasan, R. (2006). Electric Fields of the Brain: the neurophysics of EEG, 2nd Ed. New York, Oxford University Press.

Pascual-Marqui, R. D. (2002). "Standardized low-resolution brain electromagnetic tomography (sLORETA): technical details." Methods Find Exp Clin Pharmacol **24 Suppl D**: 5-12.

Pascual-Marqui, R. D. (2007). "Instantaneous and lagged measurements of linear and nonlinear dependence between groups of multivariate time series: frequency decomposition."

Pfurtscheller, G. (1992). "Event-related synchronization (ERS): an electrophysiological correlate of cortical areas at rest." Electroencephalogr Clin Neurophysiol **83**(1): 62-69.

Pfurtscheller, G. and F. H. Lopes da Silva (1999). "Event-related EEG/MEG synchronization and desynchronization: basic principles." Clin Neurophysiol **110**(11): 1842-1857.

Polich, J. and C. Margala (1997). "P300 and probability: comparison of oddball and single-stimulus paradigms." Int J Psychophysiol **25**(2): 169-176.

Poupard, L., R. Sartene and J. C. Wallet (2001). "Scaling behavior in beta-wave amplitude modulation and its relationship to alertness." Biol Cybern **85**(1): 19-26.

Prisciandaro, J. J., J. E. Joseph, H. Myrick, A. L. McRae-Clark, S. Henderson, J. Pfeifer and K. T. Brady (2014). "The relationship between years of cocaine use and brain activation to cocaine and response inhibition cues." Addiction **109**(12): 2062-2070.

Pugh, K. R., B. A. offywitz, S. E. Shaywitz, R. K. Fulbright, D. Byrd, P. Skudlarski, D. P. Shankweiler, L. Katz, R. T. Constable, J. Fletcher, C. Lacadie, K. Marchione and J. C. Gore (1996). "Auditory selective attention: an fMRI investigation." Neuroimage **4**(3 Pt 1): 159-173.

Pulvermüller, F., M. Huss, F. Kherif, F. Moscoso del Prado Martin, O. Hauk and Y. Shtyrov (2006). "Motor cortex maps articulatory features of speech sounds." Proceedings of the National Academy of Sciences **103**(20): 7865-7870.

Pulvermuller, F. and Y. Shtyrov (2006). "Language outside the focus of attention: the mismatch negativity as a tool for studying higher cognitive processes." Prog Neurobiol **79**(1): 49-71.

Purves D, A. G., Fitzpatrick D, et al., editors. (2001). Neuroscience. The Auditory Cortex. Sunderland (MA), Sinauer Associates;.

Ramnani, N. and A. M. Owen (2004). "Anterior prefrontal cortex: insights into function from anatomy and neuroimaging." Nat Rev Neurosci **5**(3): 184-194.

Ramyead, A., M. Komater, E. Studerus, S. Koranyi, S. Ittig, U. Gschwandtner, P. Fuhr and A. Riecher-Rossler (2014). "Aberrant Current Source-Density and Lagged Phase Synchronization of Neural Oscillations as Markers for Emerging Psychosis." Schizophr Bull.

Roth, T. (2009). "Slow wave sleep: does it matter?" J Clin Sleep Med **5**(2 Suppl): S4-5.

Rugg, M. D., A. D. Milner, C. R. Lines and R. Phalp (1987). "Modulation of visual event-related potentials by spatial and non-spatial visual selective attention." Neuropsychologia **25**(1A): 85-96.

Sabri, M., J. R. Binder, R. Desai, D. A. Medler, M. D. Leitm and E. Liebenthal (2008). "Attentional and linguistic interactions in speech perception." Neuroimage **39**(3): 1444-1456.

Sartori, G., S. Agosta, C. Zogmaister, S. D. Ferrara and U. Castiello (2008). "How to accurately detect autobiographical events." Psychol Sci **19**(8): 772-780.

Saxe, L. B.-S., Gershon (1999). "Admissibility of polygraph tests: The application of scientific standards post- Daubert." Psychology, Public Policy, and Law **5**(1): 21.

Schulz, E., U. Maurer, S. van der Mark, K. Bucher, S. Brem, E. Martin and D. Brandeis (2008). "Impaired semantic processing during sentence reading in children with dyslexia: combined fMRI and ERP evidence." Neuroimage **41**(1): 153-168.

Schutter, D. J. and J. van Honk (2006). "Increased positive emotional memory after repetitive transcranial magnetic stimulation over the orbitofrontal cortex." J Psychiatry Neurosci **31**(2): 101-104.

Seghier, M. L. (2013). "The angular gyrus: multiple functions and multiple subdivisions." Neuroscientist **19**(1): 43-61.

Seth, A. K., J. R. Iversen and G. M. Edelman (2006). "Single-trial discrimination of truthful from deceptive responses during a game of financial risk using alpha-band MEG signals." Neuroimage **32**(1): 465-476.

Shackman, A. J., B. W. McMenamin, H. A. Slagter, J. S. Maxwell, L. L. Greischar and R. J. Davidson (2009). "Electromyogenic artifacts and electroencephalographic inferences." Brain Topogr **22**(1): 7-12.

Shafi, M. M., M. Brandon Westover, L. Oberman, S. S. Cash and A. Pascual-Leone (2013). "Modulation of EEG Functional Connectivity Networks in Subjects Undergoing Repetitive Transcranial Magnetic Stimulation." Brain Topogr.

Shao, S., K. Shen, K. Yu, E. P. V. Wilder-Smith and X. Li (2012). "Frequency-domain EEG source analysis for acute tonic cold pain perception." Clinical Neurophysiology **123**(10): 2042-2049.

Shi-Yue, S. and L. Yue-Jia (2010). The cognitive processes related to deceptive responding. Natural Computation (ICNC), 2010 Sixth International Conference on.

Simpson, J. R. (2008). "Functional MRI lie detection: too good to be true?" J Am Acad Psychiatry Law **36**(4): 491-498.

Solomon, G. E. (1983). "Electroencephalography: Basic principles, clinical applications and related fields edited by ernst niedermeyer and fernando lopes da silva urban &schwarzenberg, baltimore, md, 1982 752 pp, illustrated, \$88.00." Annals of Neurology **14**(1): 96-96.

Sridharan, D., D. J. Levitin and V. Menon (2008). "A critical role for the right fronto-insular cortex in switching between central-executive and default-mode networks." Proceedings of the National Academy of Sciences **105**(34): 12569-12574.

Stam, C. J., G. Nolte and A. Daffertshofer (2007). "Phase lag index: assessment of functional connectivity from multi channel EEG and MEG with diminished bias from common sources." Hum Brain Mapp **28**(11): 1178-1193.

Stolarova, M., A. Keil and S. Moratti (2006). "Modulation of the C1 visual event-related component by conditioned stimuli: evidence for sensory plasticity in early affective perception." Cereb Cortex **16**(6): 876-887.

Swick, D., V. Ashley and A. U. Turken (2008). "Left inferior frontal gyrus is critical for response inhibition." BMC Neurosci **9**: 102.

Tatum, W. O. (2008). Handbook of EEG Interpretation. New York, Demos Medical Pub.

Varela, F., J.-P. Lachaux, E. Rodriguez and J. Martinerie (2001). "The brainweb: Phase synchronization and large-scale integration." Nat Rev Neurosci **2**(4): 229-239.

Vendemia, J. M., R. F. Buzan and E. P. Green (2005). "Practice effects, workload, and reaction time in deception." Am J Psychol **118**(3): 413-429.

Vrij, A. (2000). Detecting lies and deceit: the psychology of lying and implications for professional practice. Chichester, John Wiley & Sons.

Wagner, M., M. Fuchs and J. Kastner (2004). "Evaluation of sLORETA in the presence of noise and multiple sources." Brain Topogr **16**(4): 277-280.

Wang, R., J. Wang, H. Yu, X. Wei, C. Yang and B. Deng (2014). "Power spectral density and coherence analysis of Alzheimer's EEG." Cognitive Neurodynamics: 1-14.

Wang, Y., C. Ng Wu, S. Ng Khoon, T. Wu and X. Li (2013). An EEG source localization and connectivity study on deception of autobiography memories. Neural Engineering (NER), 2013 6th International IEEE/EMBS Conference on.

Watkins, K. E., A. P. Strafella and T. Paus (2003). "Seeing and hearing speech excites the motor system involved in speech production." Neuropsychologia **41**(8): 989-994.

Wise, R. J. S., S. K. Scott, S. C. Blank, C. J. Mummery, K. Murphy and E. A. Warburton (2001). Separate neural subsystems within 'Wernicke's area'.

Woestenburg, J. C., M. N. Verbaten and J. L. Slangen (1983). "The removal of the eye-movement artifact from the EEG by regression analysis in the frequency domain." Biol Psychol **16**(1-2): 127-147.

Woodman, G. F. (2010). "A brief introduction to the use of event-related potentials in studies of perception and attention." Atten Percept Psychophys **72**(8): 2031-2046.

Yonelinas, A. P., J. B. Hopfinger, M. H. Buonocore, N. E. Kroll and K. Baynes (2001). "Hippocampal, parahippocampal and occipital-temporal contributions to associative and item recognition memory: an fMRI study." Neuroreport **12**(2): 359-363.

Yoshimura, S., K. Ueda, S. Suzuki, K. Onoda, Y. Okamoto and S. Yamawaki (2009). "Self-referential processing of negative stimuli within the ventral anterior cingulate gyrus and right amygdala." Brain Cogn **69**(1): 218-225.

Zaehle, T., I. Frund, J. Schadow, S. Tharig, M. A. Schoenfeld and C. S. Herrmann (2009). "Inter- and intra-individual covariations of hemodynamic and oscillatory gamma responses in the human cortex." Front Hum Neurosci **3**: 8.

Zickar, M. J. and F. Drasgow (1996). "Detecting Faking on a Personality Instrument Using Appropriateness Measurement." Applied Psychological Measurement **20**(1): 71-87.

APPENDIX

QUESTIONNAIRE LIST

Instructed lying questions in the WE (with prior experience) task

1. In which year did you enter the university?
2. What is your major in your university?
3. What is your favorite type of movie?
4. Which country's food do you like most?
5. What kind of weather do you like most?
6. How do you travel to school every day?
7. Who do you admire most in your life?
8. How many books do you read per year?
9. What kind of sports do you like most?
10. How often do you go for travelling?
11. How many countries have you been to?
12. How long do you work every day?
13. How many brothers/sisters do you have?
14. Which university are you studying in?
15. Where did you buy your laptop?
16. What's the brand of your laptop?

17. What's the brand of your cellphone?
18. How long do you surf internet every day?
19. What is your bank account login password?
20. Which Professor's course do you like most?
21. What's the last number of your student ID?
22. Which tourist place do you like most?
23. Where is your place of birth?
24. Have you received any scholarship?
25. Do you have any credit card/master card?

Instructed truth-telling questions in the WE (with prior experience) task

1. How much is your living cost per month?
2. How often do you go to the supermarket?
3. How long does it take to travel to school?
4. What drink is your favorite type of drink?
5. When do you usually go to sleep at night?
6. When do you usually get up in the morning?
7. Have you ever lost your money before?
8. How much does your cellphone cost?
9. Where do you usually have your lunch?
10. What do you usually do during holidays?
11. How many email addresses do you have?
12. Have you ever been to the eastern of China?

13. Have you ever won any lottery before?
14. How many cellphones have you ever had?
15. What do you usually do with friends?
16. Where did you buy your cellphone?
17. Have you taken any part-time job before?
18. Have you ever failed any exam before?
19. Have you ever achieved any prize before?
20. Which book impresses you most?
21. Have you ever had any white wine before?
22. Which country are your parents living in?
23. Have you ever been hospitalized before?
24. What do you usually do on the airplane?
25. What kind of exercise do you like most?

Instructed lying questions in the NE (without prior experience) task

1. What is your position in your previous company?
2. When did you start to learn TANK software?
3. What is your salary in your previous company?
4. How long have you worked in oil digging?
5. What course have you learned for this area?
6. When did you go to U.S for an internship?
7. Do you have any certificate for this area?
8. Which state did you stay in U.S as an intern?

9. How many companies have you ever worked for?
10. Do you do more simulations or experiments?
11. Which drawing program do you use most?
12. What's the name of your previous company?
13. How long did you usually work every day?
14. Do you often go to the oil tank site before?
15. Which division did you stay in the company?
16. How often did you go for business travel?
17. Did you have any client in Singapore and China?
18. Did you do any related projects in school?
19. What's name of your previous company?
20. Was your work individual or teamwork based?
21. Did you get along well with your colleagues?
22. How did you get to know our job openings?
23. Where did you receive your Ph.D degree?
24. How many projects could you finish per year?
25. Have you ever been to the north of U.S?

Instructed truth-telling questions in the NE (without prior experience) task

1. Have you been to Germany to receive any training?
2. Have you received any certificate for oil digging?
3. Do you have any friend working in our company?
4. Can you use any software such as TANK DESIGN?

5. Have you once worked in Saudi Arabic before?
6. Are you are member of our Design association?
7. Have you published any paper in this area?
8. Do you have a patent during your previous job?
9. Have you done any project management before?
10. Did you attend any conference in oil digging?
11. Have you ever worked in China before?
12. Have you undergone any health check recently?
13. Are you familiar with other design software?
14. Where do you get your bachelor degree?
15. Have you ever been to any oil site in China?
16. Have you ever worked with western colleagues?
17. Have you received 'Permanent Residence' here?
18. Which countries have you been to for business?
19. Have you ever worked for any start-up company?
20. What's your grade average point in university?
21. Have you ever organized any event before?
22. Which country are you most familiar with?
23. Do you have any skill in algorithm development?
24. Have you get married or remains still single?
25. Did you ever receive any scholarship?

Spontaneous lying questions in the WE (with prior experience) task

1. When did you graduate from the high school?
2. What is the degree you're pursuing now?
3. What is your favorite type of book?
4. Which country's food do you dislike most?
5. Do you prefer sunny or rainy day?
6. How long do you travel to school every day?
7. What kind of job do you like most?
8. How many books do you read per month?
9. What kind of sports do you do most?
10. Do you prefer domestic or overseas travelling?
11. Have you ever been to U.S.A?
12. How long do you sleep every day?
13. How many children are there in your family?
14. Which high school did you study in?
15. How long have you used your newest laptop?
16. Do you prefer Apple or Samsung cellphone?
17. How many cellphones are you using now?
18. How long do you read book every day?
19. What is your laptop login password?
20. Which course do you dislike most?
21. What's the first character of your student ID?
22. Which country do you like most?

23. Where is your issue country of your passport?
24. Do you usually do online shopping?
25. How many credit cards do you have?

Spontaneous truth-telling questions in the WE (with prior experience) task

1. How much is your monthly cost on housing?
2. How often do you go to the library?
3. How long does it take to travel to school?
4. Do you prefer to drink tea or coffee?
5. What do you usually do before sleeping?
6. Where do you usually have your breakfast?
7. Have you ever lost your wallet before?
8. Who bought the cellphone for you?
9. Which social interaction tool do you use most?
10. How many bank accounts do you have?
11. How many cellphone number do you have?
12. Have you ever been to Africa or middle-east?
13. Have you ever started up a company before?
14. Have you ever had any intern experience?
15. Do you dine or Karaoke more with your friends?
16. Do you have a driving license?
17. Do you use tablet or notebook to take note?
18. When is your expected graduation year?

19. Which department are you studying in?
20. Do you like KFC or Macdonalds?
21. Which airline do you most often fly with?
22. Do you have personal healthcare insurance?
23. Have you undergone any surgery before?
24. What kind of TV programs do you often watch?
25. What color do you like most?